

# Lawrence Berkeley National Laboratory

## Recent Work

### Title

AN X-RAY CRYSTALLOGRAPHIC STUDY OF CHLOROPHYLL ANALOGUES AND OTHER BIO-ORGANIC COMPOUNDS

### Permalink

<https://escholarship.org/uc/item/19t6v31g>

### Author

Fischer, Mark Samuel.

### Publication Date

1969-12-01

*c.2*

RECEIVED  
RADIATION LABORATORY

JAN 23 1970

LIBRARY AND  
DOCUMENTS SECTION

AN X-RAY CRYSTALLOGRAPHIC STUDY OF CHLOROPHYLL  
ANALOGUES AND OTHER BIO-ORGANIC COMPOUNDS

Mark S. Fischer  
(Ph. D. Thesis)

December 1969

AEC Contract No. W-7405-eng-48

TWO-WEEK LOAN COPY

*This is a Library Circulating Copy  
which may be borrowed for two weeks.  
For a personal retention copy, call  
Tech. Info. Division, Ext. 5545*

LAWRENCE RADIATION LABORATORY  
UNIVERSITY of CALIFORNIA BERKELEY

*cy. 2*  
UCRL-19524

## **DISCLAIMER**

This document was prepared as an account of work sponsored by the United States Government. While this document is believed to contain correct information, neither the United States Government nor any agency thereof, nor the Regents of the University of California, nor any of their employees, makes any warranty, express or implied, or assumes any legal responsibility for the accuracy, completeness, or usefulness of any information, apparatus, product, or process disclosed, or represents that its use would not infringe privately owned rights. Reference herein to any specific commercial product, process, or service by its trade name, trademark, manufacturer, or otherwise, does not necessarily constitute or imply its endorsement, recommendation, or favoring by the United States Government or any agency thereof, or the Regents of the University of California. The views and opinions of authors expressed herein do not necessarily state or reflect those of the United States Government or any agency thereof or the Regents of the University of California.

An X-Ray Crystallographic Study of Chlorophyll Analogues  
and Other Bio-organic Compounds

By

Mark Samuel Fischer

A.B. (Brandeis University) 1965

DISSERTATION

Submitted in partial satisfaction of the requirements for the degree of

DOCTOR OF PHILOSOPHY

in

Chemistry

in the

GRADUATE DIVISION

of the

UNIVERSITY OF CALIFORNIA, BERKELEY

An X-ray Crystallographic Study of Chlorophyll Analogues  
and Other Bio-organic Compounds

By

Mark Samuel Fischer

A.B. (Brandeis University) 1965

DISSERTATION

Submitted in partial satisfaction of the requirements for the degree of

DOCTOR OF PHILOSOPHY

in

Chemistry

in the

GRADUATE DIVISION

of the

UNIVERSITY OF CALIFORNIA, BERKELEY

Approved:

..... David H. Templeton .....

..... Melvin Calvin .....

..... Samuel S. Kistler, Jr. ....

Committee in Charge

Degree conferred.....

Date

To my wife, Lucy, and our parents.

An X-Ray Crystallographic Study of Chlorophyll Analogues and  
Other Bio-organic Compounds

Contents

Abstract . . . . .	v
INTRODUCTION . . . . .	1
THE CHLOROPHYLLS . . . . .	5
Monohydrated Dipyridinated Magnesium Phthalocyanin Complex . . . . .	17
Experimental Procedure . . . . .	21
Solution and Refinement . . . . .	25
Results and Discussion . . . . .	29
Methyl Pheophorbide <u>a</u> . . . . .	59
Experimental Procedure . . . . .	59
Solution of the Structure . . . . .	62
Molecular Structure . . . . .	78
Molecular Dimensions . . . . .	82
Packing . . . . .	87
Powder Pattern . . . . .	90
Packing of Chlorophyll in Photosynthetic Lamellae . . . . .	91
Anhydrous Chlorophyll Dimers . . . . .	98
Effects of Ring Geometry on Triplet Energies in Metalloporphyrins . . . . .	104

THE CHOLINES . . . . .	121
Betaine Hydrochloride . . . . .	125
Experimental . . . . .	126
Structure Determination and Refinement . . . . .	130
Results and Discussion . . . . .	132
Choline Iodide . . . . .	143
Solution and Refinement of the Structure . . . . .	145
Results and Discussion . . . . .	148
Choline Bromide . . . . .	156
Phosphonium Analogue . . . . .	160
Mechanism for the Decomposition of Choline Chloride . . . . .	161
OTHER BIO-ORGANIC COMPOUNDS . . . . .	168
7-Chloromercurinaphthalene-1-sulfonyl Fluoride . . . . .	169
Experimental . . . . .	170
Structure Determination . . . . .	174
Results and Discussion . . . . .	179
Oxaziridines . . . . .	192
Acknowledgements . . . . .	194
APPENDIX - Glossary . . . . .	195



AN X-RAY CRYSTALLOGRAPHIC STUDY OF CHLOROPHYLL ANALOGUES  
AND OTHER BIO-ORGANIC COMPOUNDS

Mark S. Fischer

Lawrence Radiation Laboratory and

Chemistry Department

University of California

Berkeley, California

December 1969

Abstract

The crystal and molecular structures of two analogues of chlorophyll have been determined by x-ray diffraction. The monohydrated dipyridinated magnesium phthalocyanin crystallizes in space group  $P2_1/n$  with cell dimensions  $a = 17.098 \text{ \AA}$ ,  $b = 16.951 \text{ \AA}$ ,  $c = 12.449 \text{ \AA}$  and  $\beta = 105.88^\circ$ . All hydrogen atoms were located, and the final R-value is 0.050 for the 3323 independent non-zero reflections which were peak-counted on a diffractometer. The asymmetric unit contains one magnesium phthalocyanin molecule in which the magnesium atom is also coordinated to the oxygen atom of a water molecule. The hydrogens of the water molecule are hydrogen-bonded to two pyridine molecules of crystallization. The phthalocyanin ring deviates significantly from a plane, and the magnesium atom is  $0.496 \text{ \AA}$  out of the plane of the inner nitrogen atoms and towards the water

molecule. The biosynthesis and possible non-planarity of chlorophyll are discussed.

The chlorophyll derivative methyl pheophorbide a crystallizes in space group  $P2_1$  with cell dimensions  $a = 8.035 \text{ \AA}$ ,  $b = 28.531 \text{ \AA}$ ,  $c = 7.320 \text{ \AA}$  and  $\beta = 110.96^\circ$  and with two molecules in the unit cell. The final R-value is 0.051 for the 1616 independent non-zero reflections collected on a diffractometer. The inner hydrogen atoms are disordered. The Ring I vinyl and Ring V carbonyl groups are in conjugation with the nearly flat chlorin ring. There are no chlorin-chlorin intermolecular contacts less than  $3.5 \text{ \AA}$ . We propose a detailed model for the arrangement of chlorophyll in photosynthetic lamellae, in which non-parallel chlorophyll molecules are related by a  $2_1$  screw axis and are linked by water molecules.

With the use of molecular orbital calculations, we predict a correlation between the phosphorescence energy of metalloporphyrins and the ionic radius of the central metal atom. This prediction is in agreement with data in the literature. Since the metallic ionic radius depends on its coordination geometry, we suggest that phosphorescence spectra of metalloporphyrins be used to infer the environment of the central metal atom.

Unsuccessful attempts to crystallize chlorophyll and a successful synthesis of zinc methyl chlorophyllide are described.

We have determined the structures of two choline chloride analogues in detail as well as listed space group information on the

phosphonium analogue of choline chloride and on choline bromide. Betaine hydrochloride crystallizes in space group  $P2_1/c$  with cell parameters  $a = 7.428 \text{ \AA}$ ,  $b = 9.108 \text{ \AA}$ ,  $c = 11.550 \text{ \AA}$  and  $\beta = 96.71^\circ$  and with four molecules in the unit cell. The final R-value has been reduced to 0.026. The cation assumes a completely staggered conformation with the acidic hydrogen atom as far away as possible from the nitrogen atom. Because of space group difficulties, we present only an approximate structure of choline iodide. Iodide-choline interactions determine the packing arrangement. The configuration of the choline cation is nearly identical for choline chloride and choline iodide. The mechanism for the unique radiation sensitivity of choline chloride is discussed.

We have determined the crystal structure of 7-chloromercurinaphthalene-1-sulfonyl fluoride, a possible protein label, by x-ray diffraction. It crystallizes in space group  $P2_1/m$  with the molecule lying in the mirror plane. The unit cell dimensions are  $a = 9.725 \text{ \AA}$ ,  $b = 6.836 \text{ \AA}$ ,  $c = 8.351 \text{ \AA}$  and  $\beta = 90.99^\circ$ , and there are two molecules in the unit cell. The conventional R-value is 0.027 for the 1055 independent data collected on a scanning counter diffractometer and corrected for acute absorption effects. The fluorine atom always lies near a hydrogen atom of the naphthalene ring.

We present space group data for triphenyl oxaziridine and N-(p-bromophenyl)-C,C-diphenyloxaziridine. A glossary of crystallographic terms is attached in the Appendix.

INTRODUCTION

This study is an attempt to apply the physical tool of x-ray crystallography to a few problems of biological interest. The technique of x-ray diffraction is employed to determine the structures of molecular crystals and the structural knowledge is used, in turn, to help us understand biological problems.

X-Ray crystallography is one of the most powerful techniques for the investigation of molecular structure. Through the use of the hundreds or even thousands of independent data which we obtain as a result of the diffraction process, we can obtain an extraordinarily detailed description of the crystal structure. Interatomic distances for the molecules in the crystals often are determined to a precision of better than  $0.01 \text{ \AA} = 10^{-8} \text{ cm}$ . Furthermore, because commercial equipment is available and because much of the mathematics of the diffraction process has been derived previously, we are able to concentrate much of our effort on the applications of the technique.

One problem associated with the x-ray crystallographic technique is the difficulty of obtaining single crystals of sufficient size and quality for a detailed analysis. Moreover, the x-ray technique is expensive in terms not only of the cost of equipment and the time involved but also of the enormous amounts of computer time (in the range of hours) needed for the calculations which involve large amounts of data and large numbers of molecular parameters. An additional problem is the necessity to extrapolate from molecular structures in crystals to molecular structures in solutions and in biological systems.

The difficulty of obtaining crystals proved to be insurmountable for chlorophyll itself, and we were forced to crystallize model compounds. Crystals of some of the other compounds studied were donated to us by other people. (See Acknowledgements) The cost problem was overcome through the generosity of the Atomic Energy Commission as well as the National Institutes of Health and the National Science Foundation. In order to reduce the computing time, we chose molecules with less than a hundred independent atoms as the subjects for this study.

The major part of this study is devoted to a discussion of chlorophyll, its analogues and derivatives. Chlorophyll is a relatively rigid molecule so that an analysis of the structure of its rigid analogues is likely to be relevant to the structure of chlorophyll in various environments. We describe first our attempts to isolate and crystallize chlorophyll and its derivatives. This is followed by a description of the x-ray crystallographic analyses of monohydrated dipyridinized magnesium phthalocyanin, which is a chlorophyll analogue, and methyl pheophorbide, which is a chlorophyll derivative. An effort is made to extrapolate from these model compounds to the structure of photosynthetic lamellae. We have also included an analysis of the results of several other crystal structure analyses of porphyrins and we have applied these results to a discussion of the determination of coordination numbers by spectroscopic techniques.

In the next section of this study we present an analysis of structural aspects of the radiation sensitivity of choline chloride analogues in the solid state. We have studied the structures of two of these compounds in detail -- betaine hydrochloride and choline iodide. There is also a shorter description of preliminary x-ray characterization work of a few other analogues. We have suggested a mechanism for the radiation decomposition of choline chloride.

We have also studied the structure of the protein label 7-chloromercurinaphthalene-1-sulfonyl fluoride. In addition, we have some preliminary work on an isomer of that mercury compound and on two oxaziridine compounds.

The highly specialized vocabulary of x-ray crystallography is often a barrier to the understanding of the non-specialist. Elementary but systematic explanations of the techniques of x-ray crystallography may be found in many books, but the following two books are especially recommended: "Crystal Structure Analysis" by Martin J. Buerger published by John Wiley and Sons in New York in 1960 and "X-Ray Structure Determination. A Practical Guide" by George H. Stout and Lyle H. Jensen published by the Macmillan Company in Toronto in 1968. Attached to this study is an Appendix which contains our glossary of crystallographic terms.

THE CHLOROPHYLLS

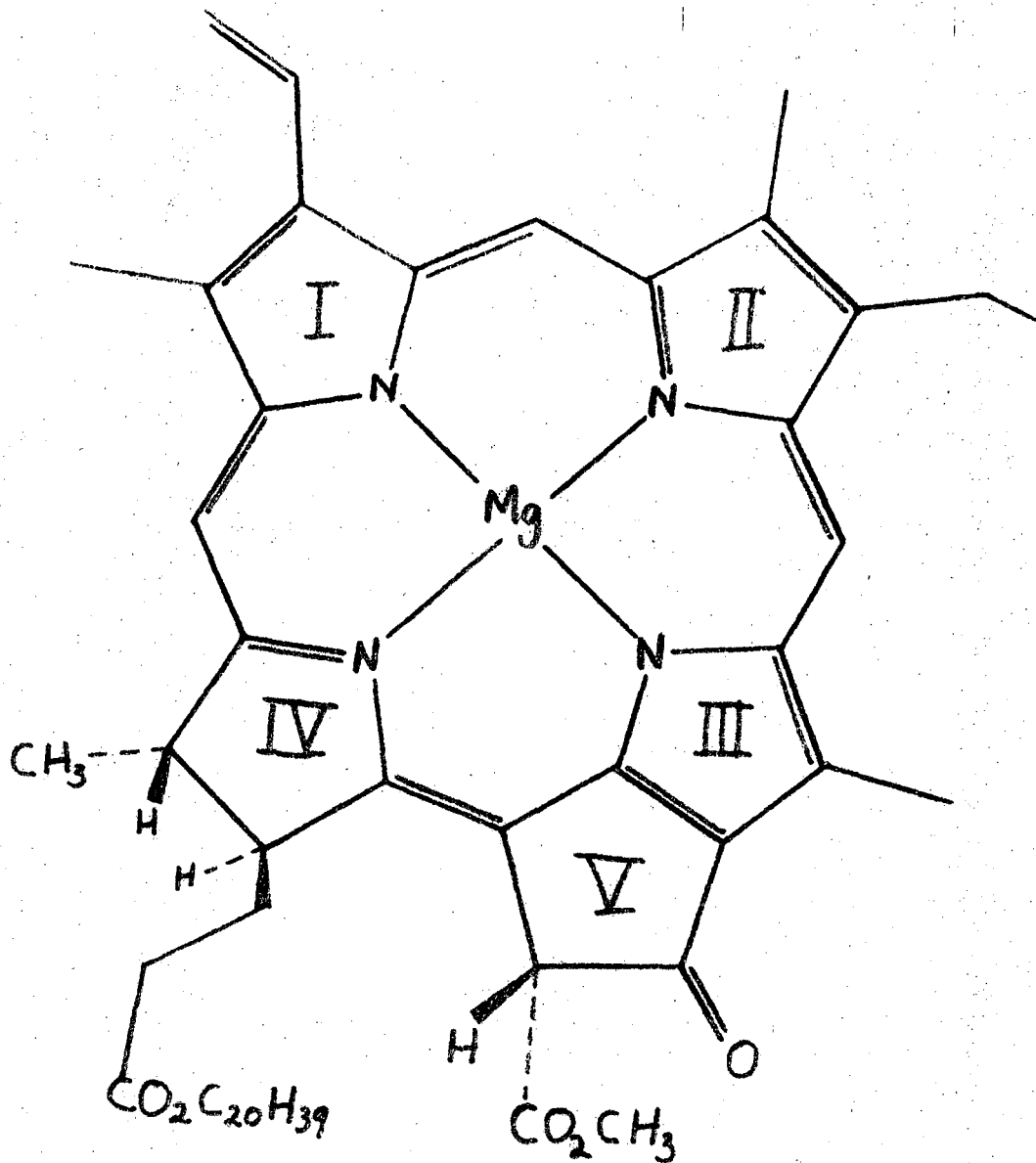


In green plants, photosynthesis occurs in the lamellae, which are membranes composed half of proteins and half of lipids (by weight) (Park, 1966). Chlorophyll, whose structure is shown in Figure 1, comprises approximately fifteen percent of the lipid fraction. It is widely believed that chlorophyll molecules participate in the first steps of photosynthesis by capturing the initial photons and transmitting the energy to some form of chemical trap. The chemical formula of chlorophyll was first determined by H. Fischer (1942). The total synthesis of chlorophyll was accomplished by R. B. Woodward in 1960. Yet the structure of aggregated chlorophyll in vivo remains unclear.

We were interested in determining the crystal structure of chlorophyll not only to derive a highly precise geometry but also to investigate its packing and to extrapolate to the in vivo situation. Several workers (Hanson, 1939; Mackinney, 1940; Jacobs, Vatter and Holt, 1953; Zill, Colmans and Trurnit, 1958; Anderson and Calvin, 1962) have succeeded previously in obtaining crystals of chlorophyll, but these have always been microcrystals, too small for a single crystal study. Zill supplied microcrystals to G. Donnay (1959) who obtained a highly precise powder diffraction pattern. However, she was not able to deduce chlorophyll's packing arrangement from the pattern.

Our first efforts were spent on isolating pure chlorophyll compounds and trying to crystallize them. The red photosynthetic bacterium Rhodospirillum rubrum contains the chlorophyll pigment

Figure 1. Chemical formula of chlorophyll a.



bacteriochlorophyll, which has saturated bonds in both Rings II and IV. Its isolation procedure is more straightforward than chlorophyll a's isolation because the former isolation involves one less column separation. Our isolation procedure was similar to that of Lindsay-Smith and Sauer (1965). We concentrated 22 liters of two day old R. rubrum to a 50 g mass with a Sharples continuous flow centrifuge. The bacteriochlorophyll was extracted from the bacteria with 200 ml of acetone with the use of a Waring blender. Water was added to the solution to make a 3:1 acetone/water mixture. The solution was filtered through cheesecloth and added to a polyethylene column which had been previously washed with a 3:2 acetone/water solvent. The bacteriochlorophyll was eluted with a 3:1 mixture of acetone/water, and pink and orange colored pigments remained at the top of the column. The bacteriochlorophyll was transferred to petroleum ether and the solvent was evaporated. The resulting 31 mg of bacteriochlorophyll had peaks in its absorption spectrum at 771, 358, 393, 575 and 700-710 nm. Both the peak heights and wavelength of absorption maxima were nearly identical to those in the bacteriochlorophyll absorption spectrum obtained by Holt and Jacobs (1954).

We attempted to crystallize the bacteriochlorophyll from five different solvent systems: 1) water, 2) methanol, 3) 6:1 n-hexane/ether, 4) 3:1 iso-octane/ether and 5) 3:2 iso-octane/methanol. Each of the solutions was evaporated over anhydrous  $\text{CaSO}_4$  in the dark.

In all cases, we obtained two phases, a green oil and dark green shiny solid, which produced either no diffraction pattern or a poor powder pattern when exposed to x-rays.

We tried to crystallize bacteriochlorophyll from a low melting point wax and from an aluminum stearate soap. Our hope was that the nonpolar solvent system would help the chlorophyll to aggregate. However, both solvents were opaque when solidified and their use was discontinued. We considered two other solvent systems -- agar and gelatin. We prepared a solution of bacteriochlorophyll in a 1:1 acetone-water agar by adding water to the agar, heating to 95° C, dissolving the bacteriochlorophyll in acetone, bringing both to a temperature of ~35° and mixing. As the mixture cooled, it solidified. We hoped that the agar matrix would retard the acetone evaporation. As the acetone would evaporate, the bacteriochlorophyll presumably would aggregate, since it is insoluble in water. We found that the volume of agar had decreased to about one fifth of its previous volume after five months. The chlorophyll was aggregated into small lumps, but the x-ray photographs showed poor powder patterns.

A gelatin diffusion experiment was tried. We found that when more than 0.5 g gelatin was dissolved in 100 ml of water and placed in an ice-water bath, the solution became extremely viscous. We dissolved 0.95 g of gelatin in 100 ml of water, put the material in an ice-water bath, placed a drop of a concentrated solution of

bacteriochlorophyll in acetone on top of the gelatin, and sealed the container with paraffin. Two weeks later drops of acetone containing very concentrated solutions of bacteriochlorophyll were present, but there was no solid material present.

We isolated a large quantity of chlorophyll a and b according to the method of Anderson and Calvin (1962) with the modifications of Vogt et al. (1965). We washed 320 g of spinach and dissolved the pigments in 500 ml of acetone with the help of the Waring blender. We added 110 ml of water and filtered the solution through cheesecloth. The filtered solution was added to a polyethylene column. The xanthophylls were collected first and then the chlorophylls were eluted with an 85% aqueous acetone solvent. The chlorophylls were transferred to isooctane and dried with  $\text{NaSO}_4$ . A sugar column was used to separate chlorophyll a from chlorophyll b by varying the amount of n-propanol mixed with the isooctane eluting solvent. Two main bands appeared, with the chlorophyll a on the bottom and the chlorophyll b farther up the column.

Slow evaporation and slow cooling experiments of the chlorophylls in isooctane yielded microcrystals of chlorophyll but no single crystals large enough for a single crystal diffraction experiment.

We turned our attention to the crystallization of chlorophyll derivatives and analogues. Related structures which had been determined by single crystal x-ray diffraction included those of the porphyrins and phthalocyanins, e.g. porphin (Webb and Fleischer,

1965), two modifications of tetraphenylporphin (TPP) (Silvers and Tulinsky, 1967; Hamor, Hamor and Hoard, 1964) and phthalocyanin ( $H_2Pc$ ) (Robertson, 1936). Three additional and more closely related structures were determined by other workers while this study was in progress: aquo MgTPP (Tinkovitch and Tulinsky, 1969), a phyllochlorin ester (in a low resolution study) (Hoppe et al., 1969) and vandyl deoxophylloerythroetioporphyrin (VO-DPEP) (Pettersen, 1969). The phyllochlorin ester has the chlorin moiety of chlorophyll, i.e. a saturated bond in Ring IV, but it lacks the fifth isocyclic ring. The porphyrin VO-DPEP has the isocyclic ring but is unsaturated in Ring IV. Neither of the last two mentioned derivatives has the phytyl chain of chlorophyll. Several successful attempts at crystallizing the methyl and ethyl chlorophyllides are reported in the literature, e.g. Borodin (1882), Ketelaar and Hansen (1937) and Holt and Jacobs (1954).

We obtained methyl pheophorbide a from R. B. Woodward. The red-violet flakes appeared highly crystalline under the polarizing microscope but they were too small for a single crystal x-ray study. They were successfully recrystallized from a 1:1 benzene-methanol solvent system by evaporation to dryness in the dark during a two-week period. The resultant crystals were opaque to visible light and resembled soft lumps of coal with dimensions as great as 2 mm. X-Ray photographs indicated that the macrocrystals were composed of many crystals, some of which might be of suitable size for a single crystal analysis. A small fragment was sliced from a macrocrystal and used in the single crystal study described below.

Since methyl pheophorbide a contains no heavy atom, the solution of the phase problem is greatly complicated. We decided to prepare a heavy atom derivative of methyl pheophorbide. Accordingly 52 mg of methyl pheophorbide was dissolved in 30 ml of methanol. The solution was deoxygenated by repeated freezing in a nitrogen environment and evacuating. A solution composed of 33 mg of  $\text{Zn}(\text{Ac})_2 \cdot \text{H}_2\text{O}$  crystals in 30 ml methanol similarly was degassed. Within minutes after the  $\text{Zn}(\text{Ac})_2$  solution was added, the purple flakes of MePPb dissolved and the solution turned green. The reaction was monitored by syringing samples, dissolving them in benzene and taking an absorption spectrum. After one and a half hours the reaction was not complete. However, after 19 hours the peak at 538 nm disappeared entirely, and a peak at 658 nm grew from a shoulder at 655 nm of the MePPb spectrum. The solution was evacuated to eliminate both the solvent and the acetic acid reaction product. The excess zinc acetate was removed by dissolving the solid in a water-ether mixture and discarding the water layer. We obtained a 95% yield of zinc methyl chlorophyllide (Zn Chlide).

After our initial, unsuccessful attempts to crystallize the material by the evaporation from a pyridine solution, we used silica~~gel~~ thin layer chromatography (TLC) to check the purity of product. There was no more than 1% starting material present, but there were three spots corresponding to reaction products. When a 6:1 benzene/methanol solvent was used, the  $R_F$  of MePPb and the three products are 0.63, 0.39, 0.29 and 0.22, respectively, where

$R_F$  is defined as the ratio of the height of the spot above the origin to the height of the solvent front. We used multiple elutions with a 5:1 methanol/benzene solvent of preparative TLC to separate the main products of the reaction mixture. The pigments were applied in methylene chloride solutions. The peak heights and wavelength of the absorption maxima for three of the resulting pigment bands are given in Table I. Two other bands were present as minor products. We attempted to crystallize the two main products corresponding to bands III and IV, in the following solvents: pyridine; tetrahydrofuran; a 7:1 mixture of ether and acetone; a 1:1 mixture of ether and acetone; chloroform; carbon tetrachloride; and toluene. Because all of these crystallization attempts were unsuccessful, we abandoned work on the ZnChlide.

In order to investigate the environment of magnesium in porphyrins, we obtained crystals of magnesium phthalocyanin (MgPc) from E. I. duPont Co., duPont Code No. DD 1383. Although the bottle was labeled "Magnesium Phthalocyanin," the analysis of nitrogen written on the bottle ( $N_{\text{calc}} = 20.88\%$ ,  $N_{\text{obs}} = 19.5\%$ ) and an independent assay of the hydrogen present ( $H_{\text{calc}} = 2.98\%$ ,  $H_{\text{obs}} = 3.53\%$ ) implied that two water molecules of hydration were present per MgPc molecule. The violet colored powder was recrystallized from an air-exposed solution in pyridine by slow evaporation to dryness. The deep violet crystals which remained were well formed. The most prominent crystal faces are the (011), (110), (101), ( $10\bar{1}$ ) and (210) forms.



Table I. Absorption maxima of three main products in the reaction  $\text{MePPb} + \text{Zn}(\text{Ac})_2 \longrightarrow \text{ZnChlide} + 2\text{HAc}$ .

<u>Band III</u>		<u>Band IV</u>		<u>Band V</u>	
$\lambda(\text{nm})$	<u>Height</u>	$\lambda(\text{nm})$	<u>Height</u>	$\lambda(\text{nm})$	<u>Height</u>
655	35	657	81	658	46
647	50			648	46
603	9	610	17	608	14
558	7	567	10	565	9
517	4	525	7	520	6
		426	100		
414	100	410 <sup>a</sup>	88	414	100
358	27	373	57	365 <sup>a</sup>	49
318	15	334	42	330 <sup>a</sup>	29
288	14			260 <sup>a</sup>	25
at 200	22	at 200	0	at 200	51

<sup>a</sup> Shoulder

References

- A. F. H. Anderson and M. Calvin, Nature, 194, 285 (1962).
- J. Borodin, Bot. Zeitung, 40, 608 (1882).
- G. Donnay, Arch. Biochem. Biophys., 80, 80 (1959).
- H. Fischer and H. Gibian, Justus Liebigs Ann. Chem., 552, 153 (1942).
- M. J. Hamor, T. A. Hamor and J. L. Hoard, J. Amer. Chem. Soc., 86, 1938 (1964).
- E. A. Hanson, Nederlandisch botanische vereeniging, 36, 180 (1939).
- A. S. Holt and E. E. Jacobs, Am. J. Botany, 41, 710 (1954).
- W. Hoppe, G. Will, J. Gassmann and H. Weichselgartner, Z. Kristalogr., 128, 18 (1969).
- E. E. Jacobs, A. E. Vatter and A. S. Holt, J. Chem. Phys., 21, 2246 (1953).
- J. A. A. Ketelaar and E. A. Hansen, Nature, 140, 196 (1937).
- J. R. Lindsay-Smith and K. Sauer, LCB Quarterly Report 7-72, Lawrence Radiation Laboratory, Berkeley, California, June, 1965.
- G. Mackinney, J. Biol. Chem., 132, 91 (1940).
- R. B. Park, Int. Rev. of Cytology, 20, 67 (1966).
- R. C. Pettersen, Acta Cryst., in press.
- J. M. Robertson, J. Chem. Soc., 1195 (1936).
- S. J. Silvers and A. Tulinsky, J. Amer. Chem. Soc., 89, 3331 (1967).
- R. Timkovitch and A. Tulinsky, J. Amer. Chem. Soc., 91, 4430 (1969).

L. H. Vogt, Jr., M. Byrn, K. Sauer and P. Walson, LCB Quarterly  
Report 6-133, Lawrence Radiation Laboratory, Berkeley,  
California, March 1965.

L. E. Webb and E. B. Fleischer, J. Chem. Phys., 43, 3100 (1965).

R. B. Woodward, Angew. Chem., 72, 651 (1960).

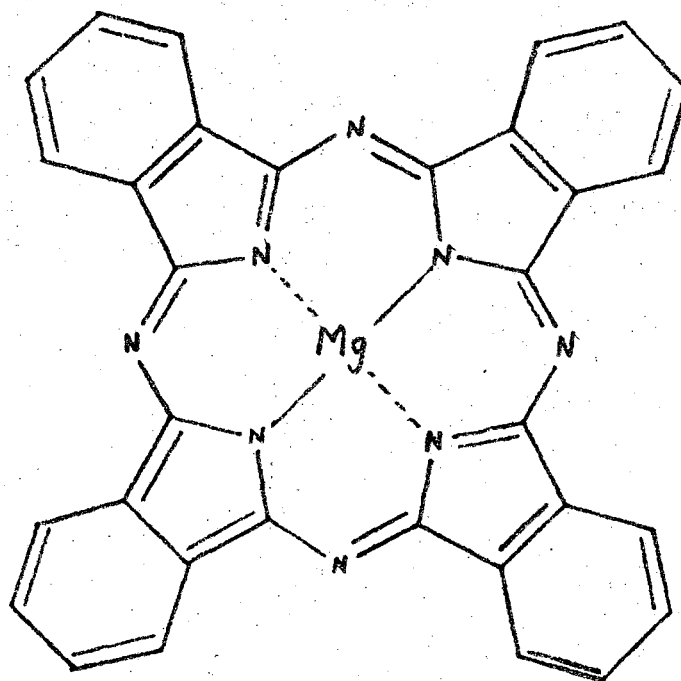
L. P. Zill, G. Colmans, H. J. Trurnit, Science, 128, 478 (1958).

The Crystal and Molecular Structure of the Monohydrated Dipyrrolylated Magnesium Phthalocyanin Complex

Phthalocyanin ( $H_2Pc$ ) was first synthesized (accidentally) by Braun and Tcherniac (1907) and first characterized by Linstead and Lowe (1936).  $MgPc$  is depicted in Figure 1. Because of their intense light absorption, the metallophthalocyanins have been used commercially as dyes. Theoretical chemists have studied their highly resonating bond system in order to test quantum mechanical models, and inorganic chemists have studied the effect of metal atoms on their geometry and spectra. Although the phthalocyanins do not occur in nature, their structural similarity to the hemes, chlorins and corrins have caused them to be of interest to biologically oriented chemists.

Through single crystal x-ray analysis, Robertson et al. (1935, 1936a, 1936b, 1937, 1940) showed that phthalocyanin and its Mn, Fe, Co, Ni, Cu and anhydrous Be and Mg derivatives are isomorphous. The  $PtPc$  was shown to be nearly but not exactly isomorphous. The structures of  $H_2Pc$ ,  $NiPc$  and  $PtPc$  were determined in detail. They were each found to be planar within  $0.02 \text{ \AA}$  and the metal atom always lay in the  $Pc$  ring. It was on the basis of the structures of these flat molecules that chemists have assumed that porphyrin molecules are flat. Only in the 1960's when other porphyrin molecules were studied was it shown that porphyrins with that degree of planarity are the exception.

Figure 1. Chemical formula of magnesium phthalocyanin.



More recently Brown (1968a, 1968b) has determined the structure of CuPc and redetermined the PtPc structure. The structure of  $C_5H_5N \cdot MnPc \cdot O \cdot MnPc \cdot C_5H_5N$  was determined by Vogt, Zalkin and Templeton (1967). In this structure the Pc rings show deviations from planarity which are as large as 0.7 Å.

Our intent in determining the MgPc structure was to study the environment of magnesium atom in porphyrins. We hoped to be able to extrapolate to the environment of the magnesium atom in chlorophyll. We discovered that when MgPc is crystallized in the non-anhydrous environment of an uncovered pyridine solution, the MgPc is not isomorphous with those phthalocyanins studied by Robertson (1936b).

The solution of the MgPc structure was made difficult by the absence of any atom appreciably heavier than carbon. The magnesium atom contains only twice as many electrons as do carbon atoms, and the Mg-Mg or Mg-C vectors do not stand out in a Patterson map calculation. However, the absence of a heavy atom meant that if high quality data were obtained and if there were no complications such as disorder, crystal twinning or very high thermal motion, then the structure which would be obtained would be of very high precision. A structure of high precision would be of help in understanding bonding schemes, molecular orbitals and the related chemical ground and excited state properties (Weiss, 1970).

References

- A. Braun and J. Tcherniac, Ber., 40, 2709 (1907).
- C. J. Brown, ibid., A, 2488 (1968a).
- C. J. Brown, ibid., A, 2494 (1968b).
- R. P. Linstead and A. R. Lowe, J. Chem. Soc., 1031 (1934).
- J. M. Robertson, J. Chem. Soc., 615 (1935).
- J. M. Robertson, ibid., 1195 (1936a).
- J. M. Robertson and R. P. Linstead, ibid., 1736 (1936b).
- J. M. Robertson and I. Woodward, ibid., 219 (1937).
- J. M. Robertson and I. Woodward, ibid., 36 (1940).
- L. H. Vogt, A. Zalkin and D. H. Templeton, Inorg. Chem., 6, 1725 (1967).
- C. Weiss, in preparation (1970).

### Experimental Procedure

Weissenberg photographs of the  $0kl$ ,  $1kl$ ,  $2kl$ ,  $3kl$ , and  $4kl$  levels indicated Laue symmetry  $2/m$ . The observed systematic absences ( $0k0$ , for  $k \neq 2n$ ;  $h0l$ , for  $h + l \neq 2n$ ) correspond to the monoclinic space group  $P2_1/n$ , with the four general equivalent positions:  $x, y, z$ ;  $-x, -y, -z$ ;  $\frac{1}{2}+x, \frac{1}{2}-y, \frac{1}{2}+z$ ;  $\frac{1}{2}-x, \frac{1}{2}+y, \frac{1}{2}-z$ . A General Electric XRD-5 x-ray diffractometer equipped with a copper x-ray tube, a manual quarter-circle Eulerian-cradle goniostat, and a 0.0003 inch thick Ni-filter at the receiving slit were used to measure both the cell dimensions and the intensity data. The unit cell dimensions were determined from the d-spacings of the  $h00$ ,  $00l$ ,  $0k0$ ,  $h0h$ , and  $h0\bar{h}$  reflections. The alpha doublet ( $\lambda = 1.5405 \text{ \AA}$  for  $\text{CuK}\alpha_1$ ) was resolved for those reflections of highest order. The cell dimensions are  $a = 17.098 \pm 0.003 \text{ \AA}$ ,



$b = 16.951 \pm 0.003 \text{ \AA}$ ,  $c = 12.449 \pm 0.003 \text{ \AA}$ , and  $\beta = 105.88 \pm 0.03^\circ$ . The observed density of  $1.368 \pm 0.015 \text{ g cm}^{-3}$ , which was determined by flotation in an aqueous  $\text{ZnBr}_2$  solution, agrees well with the calculated density of 1.364 for a formula weight of 713.1 of one MgPc, one water, and two pyridine molecules, for  $Z = 4$ , and for a unit cell volume of  $3470 \text{ \AA}^3$ . The calculated densities for one MgPc,  $1\frac{1}{2}$  MgPc, and one MgPc and two pyridine molecules are 1.025, 1.539, and  $1.329 \text{ g cm}^{-3}$ , respectively.

The data were taken on a crystal of approximate dimensions  $0.1 \times 0.1 \times 0.15 \text{ mm}$  so aligned that the reciprocal  $a$  axis coincided with the instrument  $\varphi$  axis. The distances from the source and from the receiving slit to the crystal were 14.5 and 17.8 cm respectively. All of the independent reflections (excluding space group absences) lying within one quadrant of a sphere in reciprocal space corresponding to spacings  $\cong 1.006 \text{ \AA}$  ( $2\theta \cong 100^\circ$ ) were counted for ten seconds with both crystal and counter stationary and at a takeoff angle of  $4^\circ$ . Individual backgrounds were measured for those reflections seriously affected by streaking from lower orders; for the rest, backgrounds were taken from a plot of the background counts as a function of the Bragg scattering angle for various values of  $\varphi$  and  $\chi$ . Of the 3558 reflections measured, the intensities of 3323 were above background. Periodic checks of four standard reflections showed only small ( $\pm 2\%$ ) random variations in intensity. Variations of only 5% in the intensities of the  $h00$  reflections were observed as a function of the crystal orientation, and no absorption correction ( $\mu = 9.1 \text{ cm}^{-1}$ ) was

applied. The reflections were corrected for Lorentz and polarization effects, and a set of  $|F_o|^2$  and  $|F_c|$  values on a relative scale thus was obtained.

The atomic scattering factors used during this analysis were those of Cromer and Mann<sup>14</sup> for the non-hydrogen atoms and those of Stewart, Davidson, and Simpson<sup>15</sup> for the hydrogen atoms. The anomalous dispersion corrections, both real ( $\Delta f' = 0.15$  e) and imaginary ( $\Delta f'' = 0.19$  e) parts, which were applied to the magnesium scattering factors, were those given by Cromer<sup>16</sup>. The function minimized during the least-squares refinements was  $(R_2)^2 = \frac{\sum_w (|kF_o| - |F_c|)^2}{\sum_w |kF_o|^2}$ , where  $|F_o|$  and  $|F_c|$  are the observed and calculated structure amplitudes, respectively,  $k$  is the scale factor, and  $w$  is the weighting factor for that reflection. In the early stages of refinement,  $w$  was set equal to one, but in the later stages  $w = 1/\sigma^2(F)$  for the non-zero data and  $w = 0$  if  $I = 0$ .  $\sigma(F)$  was calculated from  $\sigma^2(I) = I + 2I_b + (cI)^2$  by using the relationships:  $\sigma(F^2) = (LP)^{1/2} \sigma(I)$ ,  $\sigma(F) = [\sigma(F^2)]^{1/2}$  if  $I \leq \sigma(I)$ , and  $\sigma(F) = F - [F^2 - \sigma(F^2)]^{1/2}$  if  $I > \sigma(I)$ . In these expressions,  $I$  is the net count,  $I_b$  is the background count,  $(LP)$  is the Lorentz-polarization factor and  $c$  is a constant chosen to decrease the weights of the highest intensity data and represents our attempt to compensate for such systematic errors as extinction, absorption, and non-linearity of the counter and was originally fixed at 0.07.

The following programs for the CDC 6600 computer were used in this structure analysis and interpretation: GONIO, a goniometric settings program; INCOR, a general data reduction program; FORDAP,

a Fourier analysis program; DISTAN, a crystallographic bond distance and bond angle program; LIST, a data presentation program; WILSON, an unpublished Wilson-plot program by Maddox and Maddox; R.E. Long's phase determination program<sup>17</sup>; LS200, our unpublished modified version of the Ganzel-Sparks-Trueblood least squares program; DATLOK, D.J. St.Clair's unpublished weighting scheme analysis program; and ORTEP, Johnson's molecular crystallographic plotting program.<sup>18</sup>

### Solution and Refinement of the Structure

Normalized structure factors,  $E_{\underline{h}}$ , were calculated using Wilson's Method<sup>19</sup>. The phases of the highest 181 E values  $\geq 2.0$  were determined from Long's sign determination program<sup>17</sup> which iteratively applies the equation:  $\text{sign}(E_{\underline{h}}) = \text{sign}(\sum_{\underline{k}} E_{\underline{k}} E_{\underline{h}-\underline{k}})$ . The fixed positive phases of the  $135$ ,  $014$ , and  $132$  reflections defined the origin, and the phases of an additional four reflections  $024$ ,  $381$ ,  $192$ , and  $115$  were held fixed for each of the sixteen computer runs in which they were allowed to have all combinations of positive and negative phases. A consistency index defined as  $C = \frac{\sum_{\underline{h}} \sum_{\underline{k}} E_{\underline{h}} E_{\underline{k}} E_{\underline{h}-\underline{k}}}{\sum_{\underline{h}} \sum_{\underline{k}} |E_{\underline{h}} E_{\underline{k}} E_{\underline{h}-\underline{k}}|}$  was calculated for each combination. Two of the sixteen possibilities had  $C = 0.68$ , whereas  $C = 0.47-0.55$  for the other fourteen.

Fourier maps were calculated from the  $E$  values phased from the two most consistent sets. One map showed a half molecule adjacent to a center of symmetry while the other showed a full molecule with the same orientation but translated to a general position with the magnesium atom at the fractional coordinates  $(.30, .00, .55)$ . We checked the orientation obtained from the statistical approach in two ways. First, we found that the plane through the highest peaks of each  $E$  map agreed well with the plane of highest density calculated from a three-dimensional Patterson map. Second, an optical transform of a single molecule was made by shining a laser beam through a photoreduced image of the molecule. The orientation of the molecule on the plane was determined by rotating the image of the molecule and comparing resultant rotated optical

transforms with the  $\underline{E}$ -values (i.e. the normalized transform of the electron density) for the  $h0l$  data. This technique suggested that the orientation of the molecule in the plane agreed with the  $\underline{E}$  map orientation to within five degrees.

Conventional least squares and Fourier calculations were used to distinguish between the two possibilities. The positions of the twenty-two highest peaks on the  $\underline{E}$  map with the molecule in the special position were refined to a discrepancy index of  $R_1 = \Sigma(|kF_o| - |F_c|) / \Sigma |kF_o| = 0.62$ . A Fourier synthesis using  $F_o$  with the phases of  $F_c$  revealed no additional atoms in reasonable locations, and the use of this trial structure was terminated. Thirty-six of the highest peaks on the other  $\underline{E}$  map with the high consistency index refined to  $R_1 = 0.45$ . The remaining six atoms in the MgPc ring were among the highest peaks of a difference Fourier synthesis, and  $R_1$  with the 42 atoms refined to 0.37. Another difference Fourier was calculated using all of the data. The twelve highest peaks, in the form of two pyridine rings, were added to the previous 42 to bring the number of atoms up to 54 and the  $R_1$  value down to 0.18. Subsequently it was determined that 52 of the 56 highest peaks in the correct  $\underline{E}$  map corresponded to atoms in the asymmetric unit. The remaining two atoms appeared only as shoulders on two other peaks.

After several mispunched data were corrected,  $R_1$  dropped to 0.13. Anisotropic temperature factors of the form  $\exp(-h^2\beta_{11} - k^2\beta_{22} - l^2\beta_{33} - 2hk\beta_{12} - 2kl\beta_{23} - 2hl\beta_{13})$  were used for the 54 atoms. A

diagonal least squares refinement of the 487 parameters including the scale factor  $k$  reduced  $R_1$  to 0.101. The positions of the hydrogen atoms were found in a difference Fourier map calculated from all non-zero reflections. They were given isotropic temperature factors which were allowed to vary, and the discrepancy index dropped to 0.070. To economize on computing time the 82 atoms were split into three groups: the water and two pyridine molecules as one group and the two halves of the MgPc molecule as the other two groups. Full-matrix least squares refinements were run on one group at a time keeping the atomic coordinates of the other two groups fixed. Each group was refined for only one cycle before refining the coordinates of another group. Three cycles for each group reduced  $R_1$  to 0.054. At this point it was noticed that the values of  $|F_o/F_c|$  for the reflections of highest intensity were all less than 1.0. Remeasurement of the intensities of these strong reflections at lower x-ray flux proved that non-linearity of the scintillation counter was not responsible. Therefore an extinction correction of the form  $F'_o = F_o (1 + (EF)(I))$ , where the extinction factor  $EF$  is a constant  $= 5 \times 10^{-7}$ , was applied to give a maximum correction of 14% for the strongest reflection. The most intense reflections were now given a higher weight by changing  $c$  in the weighting equation from 0.07 to 0.05.  $R_1$  was reduced to 0.052. The atoms were now divided into two groups: the 57 atoms in the MgPc ring and the remaining 25 atoms. Three full-matrix least squares cycles run on one

group at a time were sufficient to reduce the maximum shift of any atomic parameter to less than one-tenth of its standard deviation.

The final discrepancy values are  $R_1 = 0.050$  for 3323 non-zero data,  $R_1 = 0.056$  for all 3558 data, and the weighted  $R_2 = 0.050$ .

The standard deviation of an observation of unit weight equals 1.02.  
systematic

There is no  $\Delta$  trend in either  $|F_o/F_c|$  or  $w^{1/2}|\Delta F|$  as a function of intensity or Bragg scattering angle of the reflections. No peaks on a difference Fourier which was based on the final structure were higher than  $0.18 \text{ e } \text{\AA}^{-3}$ .

## Results and Discussion

The asymmetric unit contains one MgPc, one water and two pyridine molecules. Figure 1 shows the atoms in the asymmetric unit projected on the bc plane and indicates the numbering system. The final atomic parameters for the non-hydrogen atoms are listed in Table I, while those for the hydrogen atoms are presented in Table II. Hydrogen atoms are numbered by the atom to which they are attached. The observed and calculated structure factor amplitudes  $|F_o|$  and  $|F_c|$  are listed in Table III.

The MgPc molecule itself is non-planar, and the magnesium atom is 0.496 Å out of the plane of the central nitrogen atoms directed towards the water molecule. The two hydrogen atoms of the water molecule are hydrogen-bonded to the two pyridine molecules of crystallization, and the planes through the pyridine molecules make angles of 8.6° and 30.8° with the plane through the four central nitrogen atoms of MgPc. The intramolecular bond distances and bond angles, which are presented in Tables IV and V respectively, are the same as those in other Pc's<sup>2-9</sup> to within the respective standard deviations. The precision, however, is greater by at least a factor of two for the MgPc<sup>A</sup> than for the other Pc's.

The environment around the central magnesium atom is depicted in Figure 2. The 2.022 ± 0.003 Å Mg-O(1) distance is increased to 2.028 if corrected for thermal motion according to the model with the water molecule riding on the Mg atom. This distance is only slightly shorter than the average Mg-OH<sub>2</sub> distances for the six-



Figure 1. The molecular structure projected on the *bc* plane.

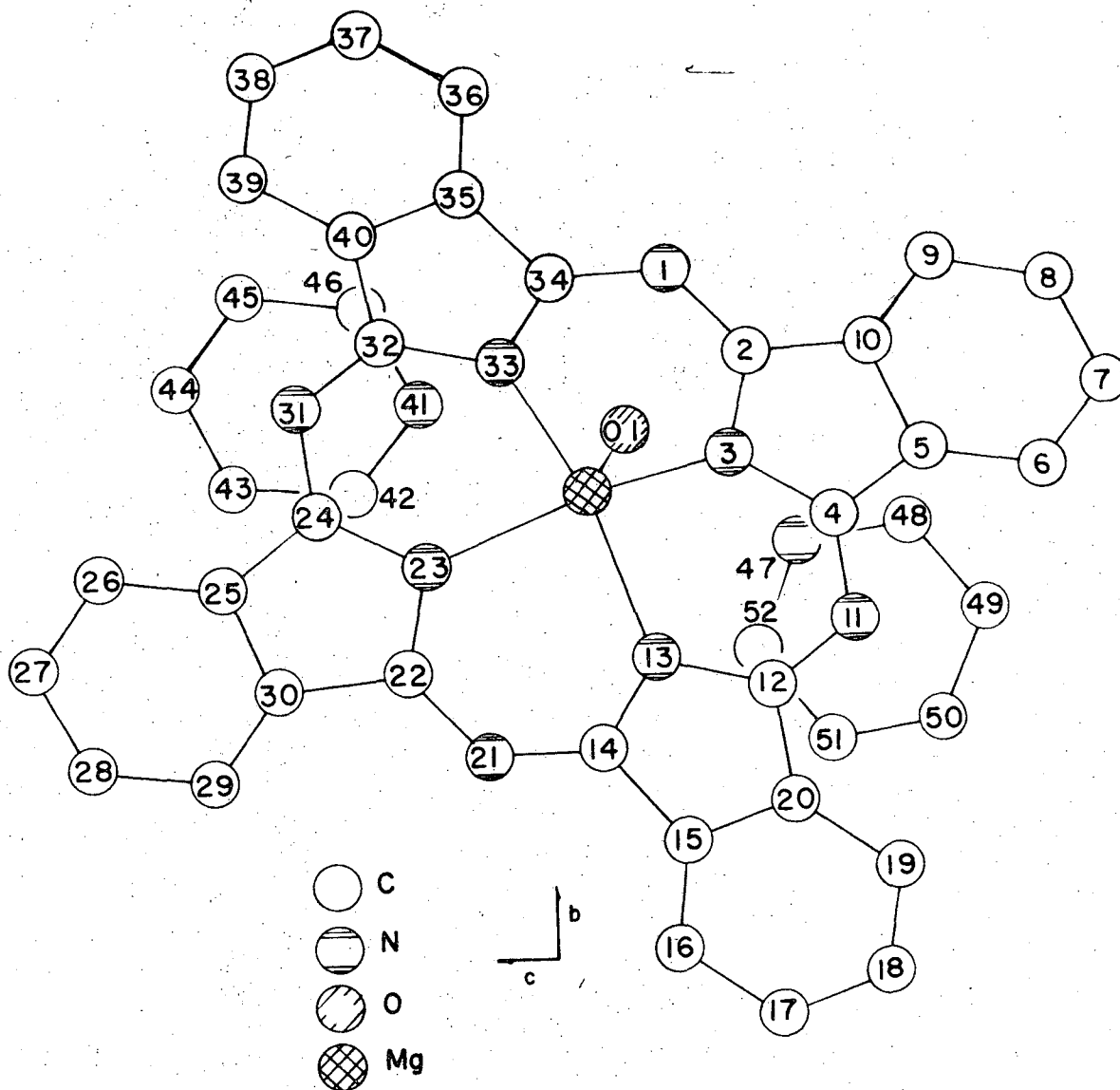
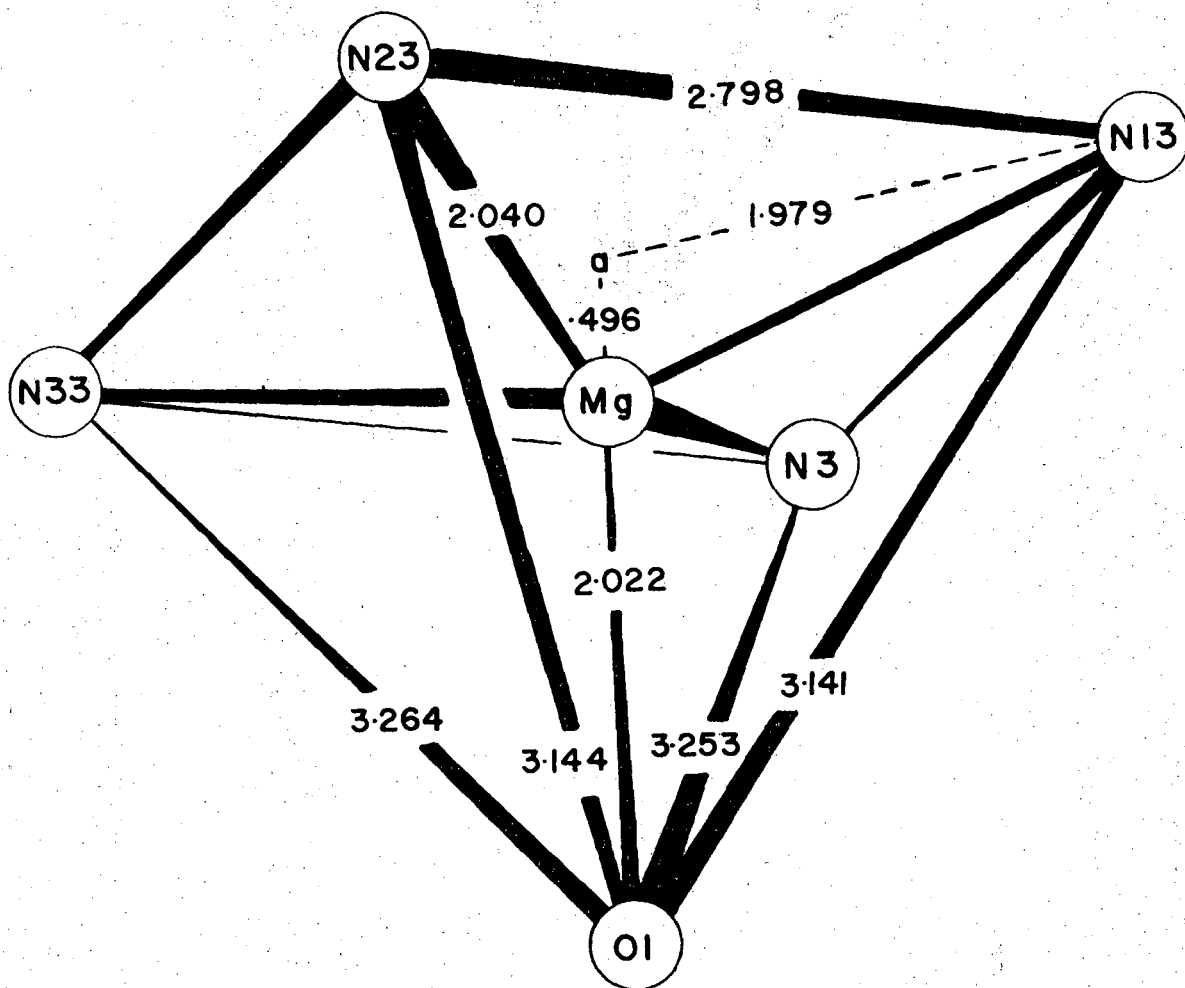


Figure 2. The central region of the MgPc molecule. The equivalent Mg-N and N...N distances have been averaged.



XBL 691-15

Table I. Final Atomic Fractional Co-ordinates and Thermal Parameters<sup>a</sup> of All Nonhydrogen Atoms in the Asymmetric Unit<sup>b</sup>.

ATOM	X	Y	Z	B11	B22	B33	B12	B13	B23
MG	.33142(16)	-.01498(5)	.53984(7)	3.98(5)	3.13(5)	3.05(5)	-.17(4)	.84(4)	-.20(4)
O1	.2195(1)	.0569(1)	.4624(2)	4.44(12)	4.81(12)	3.45(11)	.33(9)	1.05(11)	.21(9)
N1	.4600(1)	.1644(1)	.5118(2)	4.01(12)	3.54(13)	4.14(13)	-.16(10)	.84(10)	-.02(11)
C2	.4447(2)	.1069(2)	.4351(2)	3.57(15)	3.66(16)	3.94(16)	.13(13)	.74(12)	.28(14)
N3	.4029(1)	.0386(1)	.4368(2)	3.91(12)	3.57(13)	3.54(12)	-.23(10)	1.07(9)	-.07(10)
C4	.4045(2)	-.0051(2)	.3447(2)	3.22(14)	3.87(16)	3.69(15)	.19(12)	.76(12)	.12(14)
C5	.4481(2)	.0384(2)	.2785(2)	3.43(14)	4.16(17)	3.53(15)	.43(13)	.89(12)	.31(13)
C6	.4637(2)	.0228(2)	.1769(3)	4.28(17)	4.65(19)	4.20(18)	.38(15)	1.07(14)	.11(16)
C7	.5024(2)	.0800(2)	.1320(3)	4.57(18)	6.33(23)	4.16(18)	.44(16)	1.71(15)	.64(18)
C8	.5282(2)	.1505(2)	.1888(3)	4.53(18)	5.40(21)	5.15(21)	-.28(16)	1.82(15)	1.07(18)
C9	.5159(2)	.1651(2)	.2920(3)	4.20(17)	4.38(19)	4.52(19)	-.10(14)	.87(14)	.16(16)
C10	.4735(2)	.1092(2)	.3352(2)	3.34(14)	4.13(17)	4.08(15)	.18(13)	.97(12)	.55(14)
N11	.3724(1)	-.0761(1)	.3163(2)	4.08(12)	3.69(13)	3.52(12)	.00(11)	.92(10)	-.00(10)
C12	.3361(2)	-.1186(2)	.3789(2)	3.72(15)	3.62(16)	3.22(15)	.01(12)	.73(12)	-.07(13)
N13	.3237(1)	-.0975(1)	.4789(2)	4.13(12)	3.33(12)	3.26(12)	-.48(10)	.86(10)	.00(10)
C14	.2872(2)	-.1587(2)	.5185(2)	4.09(12)	3.33(15)	3.24(15)	.18(12)	.54(12)	.04(13)
C15	.2729(2)	-.2229(2)	.4362(2)	4.01(15)	3.40(16)	3.44(15)	.15(12)	.37(12)	-.19(13)
C16	.2356(2)	-.2965(2)	.4328(3)	4.72(17)	3.78(17)	4.26(18)	-.43(14)	.66(14)	-.26(15)
C17	.2292(2)	-.3426(2)	.3390(3)	5.95(19)	3.92(18)	5.12(20)	-.81(15)	1.01(15)	-1.02(17)
C18	.2600(2)	-.3163(2)	.2520(3)	6.16(20)	4.28(19)	4.34(18)	-.20(16)	.91(15)	-1.44(16)
C19	.2973(2)	-.2445(2)	.2552(3)	4.76(17)	4.16(19)	4.15(18)	.30(14)	1.26(14)	-.33(15)
C20	.3035(2)	-.1975(2)	.3493(2)	3.89(15)	3.38(15)	3.51(15)	.44(12)	.80(12)	-.16(13)
N21	.2658(1)	-.1628(1)	.6125(2)	4.34(13)	4.06(13)	3.12(12)	-.34(10)	.86(10)	-.37(11)
C22	.2798(2)	-.1049(2)	.6888(2)	3.63(14)	3.90(17)	3.41(15)	-.05(13)	.71(11)	.13(13)
N23	.3129(1)	-.0324(1)	.6814(2)	4.25(12)	3.32(12)	3.34(12)	-.18(10)	.75(9)	-.03(10)
C24	.3223(2)	-.0057(2)	.7812(2)	3.81(15)	3.77(16)	3.08(15)	.51(13)	.42(13)	-.26(13)
C25	.2929(2)	-.0447(2)	.8562(2)	3.46(14)	4.13(16)	3.19(15)	.15(12)	.82(12)	.05(13)
C26	.2908(2)	-.0350(2)	.9660(3)	4.28(17)	4.53(18)	3.69(17)	-.37(14)	.87(13)	-.22(15)
C27	.2598(2)	-.0961(2)	1.0147(3)	5.70(19)	6.57(24)	3.90(18)	-.68(17)	1.64(15)	-.22(18)
C28	.2307(2)	-.1645(2)	.9560(3)	6.33(20)	5.98(23)	4.41(20)	-1.40(17)	2.20(16)	.40(18)
C29	.2323(2)	-.1750(2)	.8466(3)	4.68(17)	4.91(19)	3.84(18)	-.58(15)	1.16(13)	-.22(15)
C30	.2653(2)	-.1138(2)	.7976(2)	3.56(15)	4.09(16)	3.40(15)	-.13(12)	.89(12)	.07(14)
N31	.3563(1)	.0763(1)	.8103(2)	4.34(13)	3.38(13)	3.55(12)	.07(11)	.80(10)	-.30(10)
C32	.3895(2)	.1197(2)	.7458(2)	3.88(15)	3.36(15)	3.64(16)	.32(12)	.44(12)	-.11(13)
N33	.3927(1)	.1035(1)	.6386(2)	4.10(12)	3.53(12)	3.59(12)	-.27(10)	.87(10)	-.10(10)
C34	.4381(2)	.1605(2)	.6071(2)	3.87(15)	3.22(15)	3.91(16)	.08(12)	.81(13)	.05(13)
C35	.4626(2)	.2191(2)	.6961(2)	4.04(15)	2.99(15)	4.36(16)	.03(13)	.54(13)	.11(13)
C36	.5073(2)	.2885(2)	.7066(3)	5.21(19)	4.02(19)	5.41(21)	-.44(15)	1.10(16)	-.08(17)
C37	.5217(2)	.3295(2)	.8050(3)	6.02(20)	3.97(19)	6.33(23)	-1.01(16)	.81(17)	-.85(18)
C38	.4916(2)	.3028(2)	.8917(3)	6.67(22)	4.51(21)	5.64(22)	-.62(17)	.44(18)	-1.04(18)
C39	.4472(2)	.2341(2)	.8830(3)	5.32(19)	4.17(19)	4.76(20)	-.25(15)	.65(15)	-.76(16)
C40	.4329(2)	.1930(2)	.7834(3)	3.98(15)	3.06(15)	4.00(16)	.40(12)	.15(13)	-.35(14)
N41	.1310(2)	.0761(2)	.6137(2)	6.61(16)	5.85(17)	5.69(16)	.23(14)	2.05(13)	-.37(15)
C42	.1031(2)	.0185(2)	.6650(4)	6.30(21)	5.47(23)	6.92(26)	-.36(17)	1.69(18)	-.86(21)
C43	.0955(2)	.0237(3)	.7703(4)	6.63(23)	8.29(31)	6.77(28)	-.14(21)	2.67(20)	.94(26)
C44	.1177(3)	.0911(4)	.8279(4)	6.87(24)	11.00(39)	5.03(25)	2.46(24)	1.91(20)	-.51(28)
C45	.1465(3)	.1524(3)	.7776(4)	6.70(23)	6.34(26)	7.67(30)	1.52(20)	.41(20)	-1.65(25)
C46	.1513(2)	.1420(3)	.6704(4)	6.93(22)	5.59(23)	7.06(26)	-.05(18)	1.91(19)	.38(21)
N47	.1301(2)	-.0224(2)	.2762(3)	5.50(15)	5.37(18)	6.38(19)	-.09(12)	.47(13)	-.99(14)
C48	.1117(2)	-.0118(3)	.1670(4)	7.65(24)	6.57(26)	7.11(27)	-.94(20)	2.80(20)	-.97(24)
C49	.0834(3)	-.0709(4)	.0897(4)	7.93(26)	10.01(36)	7.38(30)	-1.52(24)	3.13(22)	-2.71(30)
C50	.0757(3)	-.1452(3)	.1281(5)	5.90(22)	8.09(33)	9.81(36)	.09(22)	1.41(23)	-4.11(32)
C51	.0940(3)	-.1571(3)	.2386(6)	5.98(22)	5.18(26)	12.05(41)	-.07(19)	-1.40(24)	-.54(31)
C52	.1199(2)	-.0948(3)	.3098(4)	5.71(21)	6.70(27)	8.07(29)	.13(19)	-1.10(19)	.17(25)

XBL 691-74

<sup>a</sup>The form of the anisotropic thermal ellipsoid (expressed in units of Å<sup>2</sup>) is:  $\exp(-0.25 \sum_{i=1}^3 \sum_{j=1}^3 B_{ij} b_i b_j h_i h_j)$ , where  $b_i$  = ith reciprocal axis length and  $h_i$  = ith Miller index.

<sup>b</sup>The numbers in parenthesis here and in succeeding tables are the estimated standard deviations of the least significant digit(s).

Table II. Final Fractional Atomic Positional and Isotropic Thermal Parameters for All Hydrogen Atoms in the Asymmetric Unit.

ATOM	x	y	z	B( $\text{\AA}^2$ )
H01-1	.1932(19)	.0644(20)	.4984(27)	5.4(11)
H01-2	.1921(23)	.0354(22)	.3934(33)	9.5(13)
H 6	.4466(15)	-.0286(16)	.1380(21)	3.84(68)
H 7	.5107(17)	.0713(17)	.0612(25)	4.99(79)
H 8	.5569(16)	.1896(16)	.1579(22)	4.22(71)
H 9	.5336(16)	.2126(17)	.3314(23)	4.17(74)
H16	.2172(15)	-.3157(16)	.4956(22)	4.00(71)
H17	.2052(17)	-.3967(18)	.3370(23)	4.91(75)
H18	.2502(15)	-.3461(16)	.1843(22)	4.00(68)
H19	.3209(16)	-.2256(16)	.1971(22)	4.30(72)
H26	.3110(14)	.0135(15)	1.0058(19)	2.59(59)
H27	.2605(18)	-.0924(18)	1.0928(28)	6.51(89)
H28	.2104(17)	-.2066(18)	.9920(24)	5.19(80)
H29	.2112(15)	-.2228(16)	.8035(22)	3.87(68)
H36	.5302(15)	.3060(15)	.6496(21)	2.97(65)
H37	.5534(20)	.3819(22)	.8118(27)	7.8(10)
H38	.5014(18)	.3326(19)	.9602(25)	6.18(91)
H39	.4257(17)	.2154(17)	.9468(24)	5.15(79)
H42	.0905(19)	-.0261(20)	.6223(27)	7.0(10)
H43	.0763(24)	-.0185(24)	.8020(33)	10.0(14)
H44	.1176(22)	.0972(23)	.8993(33)	9.5(13)
H45	.1667(21)	.2036(23)	.8082(30)	8.9(12)
H46	.1759(20)	.1839(21)	.6336(28)	8.1(10)
H48	.1203(18)	.0418(18)	.1438(25)	5.83(86)
H49	.0762(27)	-.0581(27)	.0121(38)	12.5(17)
H50	.0680(23)	-.1907(25)	.0713(33)	11.1(13)
H51	.0827(26)	-.2016(26)	.2727(35)	10.8(16)
H52	.1311(22)	-.0981(21)	.3931(31)	8.8(12)

Table III. Observed and Calculated Structure Factor Amplitudes

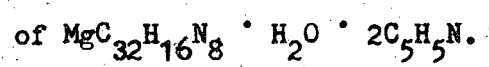


Table with multiple columns containing numerical data, likely representing structure factors and their calculated values. The table is organized in a grid-like format with various numerical entries.

Table with columns for various numerical values and alphanumeric labels. The table contains a large volume of data, including values like 123.45, 67.89, and labels such as K.L., L., and others.

Table IV. Intramolecular Bond Distances (in Å) of  $\text{MgPc} \cdot \text{H}_2\text{O} \cdot 2 \text{C}_5\text{H}_5\text{N}$ . Standard deviations are 0.002 Å for Mg-N, 0.003 Å for Mg-O, 0.003-0.004 Å for C-N in the Pc ring, 0.004-0.005 Å for C-C in the Pc ring, 0.006 Å for C-N in the pyridine rings, 0.007-0.010 Å for C-C in the pyridine rings, 0.02-0.03 Å for C-H in the Pc ring, 0.03-0.04 Å for O-H in the  $\text{H}_2\text{O}$ , and 0.03-0.05 Å for C-H in the pyridine rings.



<u>Atoms</u>	<u>Distance</u>	<u>Atoms</u>	<u>Distance</u>	<u>Atoms</u>	<u>Distance</u>
Mg-O(1)	2.022	C(22)-N(23)	1.366	C(49)-C(50)	1.366
Mg-N(3)	2.039	C(22)-C(30)	1.451	C(50)-C(51)	1.340
Mg-N(13)	2.043	N(23)-C(24)	1.370	C(51)-C(52)	1.372
Mg-N(23)	2.038	C(24)-C(25)	1.453	H(01)1-O(1)	0.73
Mg-N(33)	2.039	C(24)-N(31)	1.335	H(01)2-O(1)	0.93
N(1)-C(2)	1.339	C(25)-C(26)	1.387	H(6)-C(6)	1.00
N(1)-C(34)	1.340	C(25)-C(30)	1.392	H(7)-C(7)	0.94
C(2)-N(3)	1.364	C(26)-C(27)	1.376	H(8)-C(8)	0.97
C(2)-C(10)	1.459	C(27)-C(28)	1.388	H(9)-C(9)	0.95
N(3)-C(4)	1.371	C(28)-C(29)	1.382	H(16)-C(16)	0.98
C(4)-C(5)	1.454	C(29)-C(30)	1.398	H(17)-C(17)	1.00
C(4)-N(11)	1.330	N(31)-C(32)	1.326	H(18)-C(18)	0.96
C(5)-C(6)	1.388	C(32)-N(33)	1.379	H(19)-C(19)	0.97
C(5)-C(10)	1.400	C(32)-C(40)	1.457	H(26)-C(26)	0.97
C(6)-C(7)	1.376	N(33)-C(34)	1.362	H(27)-C(27)	0.97
C(7)-C(8)	1.397	C(34)-C(35)	1.461	H(28)-C(28)	0.96
C(8)-C(9)	1.378	C(35)-C(36)	1.389	H(29)-C(29)	0.99
C(9)-C(10)	1.388	C(35)-C(40)	1.392	H(36)-C(36)	0.95
N(11)-C(12)	1.333	C(36)-C(37)	1.371	H(37)-C(37)	1.03
C(12)-N(13)	1.368	C(37)-C(38)	1.392	H(38)-C(38)	0.97
C(12)-C(20)	1.457	C(38)-C(39)	1.379	H(39)-C(39)	1.01
N(13)-C(14)	1.358	C(39)-C(40)	1.384	H(42)-C(42)	0.92
C(14)-C(15)	1.452	N(41)-C(42)	1.324	H(43)-C(43)	0.92
C(14)-N(21)	1.343	N(41)-C(46)	1.316	H(44)-C(44)	0.90
C(15)-C(16)	1.396	C(42)-C(43)	1.355	H(45)-C(45)	0.97
C(15)-C(20)	1.392	C(43)-C(44)	1.348	H(46)-C(46)	1.00
C(16)-C(17)	1.384	C(44)-C(45)	1.372	H(48)-C(48)	0.98
C(17)-C(18)	1.400	C(45)-C(46)	1.371	H(49)-C(49)	0.97
C(18)-C(19)	1.371	N(47)-C(48)	1.321	H(50)-C(50)	1.03
C(19)-C(20)	1.396	N(47)-C(52)	1.323	H(51)-C(51)	0.91
N(21)-C(22)	1.341	C(48)-C(49)	1.383	H(52)-C(52)	1.00

Table V. Intramolecular Bond Angles (in  $^{\circ}$ ) of  $\text{MgPc} \cdot \text{H}_2\text{O} \cdot 2 \text{C}_5\text{H}_5\text{N}$ . Standard deviations are  $0.1^{\circ}$  for all angles involving Mg,  $0.2-0.3^{\circ}$  for all angles in the Pc ring, and  $0.4-0.6^{\circ}$  for all angles in the pyridine rings.

<u>Atoms</u>	<u>Angle</u>	<u>Atoms</u>	<u>Angle</u>
O(1)-Mg-N(3)	106.5	N(11)-C(12)-N(13)	127.2
O(1)-Mg-N(13)	101.2	N(11)-C(12)-C(20)	123.8
O(1)-Mg-N(23)	101.5	N(13)-C(12)-C(20)	109.0
O(1)-Mg-N(33)	107.0	Mg-N(13)-C(12)	124.9
N(3)-Mg-N(13)	86.5	Mg-N(13)-C(14)	125.1
N(3)-Mg-N(23)	152.0	C(12)-N(13)-C(14)	108.3
N(3)-Mg-N(33)	86.4	N(13)-C(14)-C(15)	110.0
N(13)-Mg-N(23)	86.8	N(13)-C(14)-N(21)	127.4
N(13)-Mg-N(33)	151.8	C(15)-C(14)-N(21)	122.6
N(23)-Mg-N(33)	86.8	C(14)-C(15)-C(16)	132.8
C(2)-N(1)-C(34)	123.3	C(14)-C(15)-C(20)	106.0
N(1)-C(2)-C(3)	127.5	C(16)-C(15)-C(20)	121.2
N(1)-C(2)-C(10)	122.9	C(15)-C(16)-C(17)	117.4
N(3)-C(2)-C(10)	109.6	C(16)-C(17)-C(18)	120.8
Mg-N(3)-C(2)	125.6	C(17)-C(18)-C(19)	122.1
Mg-N(3)-C(4)	124.9	C(18)-C(19)-C(20)	117.3
C(2)-N(3)-C(4)	108.4	C(12)-C(20)-C(15)	106.7
N(3)-C(4)-C(5)	109.3	C(12)-C(20)-C(19)	132.2
N(3)-C(4)-N(11)	127.6	C(15)-C(20)-C(19)	121.2
C(5)-C(4)-N(11)	123.1	C(14)-N(21)-C(22)	123.6
C(4)-C(5)-C(6)	132.6	N(21)-C(22)-N(23)	127.4
C(4)-C(5)-C(10)	106.6	N(21)-C(22)-C(30)	122.9
C(6)-C(5)-C(10)	120.8	N(23)-C(22)-C(30)	109.6
C(5)-C(6)-C(7)	118.0	Mg-N(23)-C(22)	125.3
C(6)-C(7)-C(8)	121.2	Mg-N(23)-C(24)	126.2
C(7)-C(8)-C(9)	121.2	C(22)-N(23)-C(24)	108.1
C(8)-C(9)-C(10)	117.8	N(23)-C(24)-C(25)	109.3
C(2)-C(10)-C(5)	106.0	N(23)-C(24)-N(31)	127.1
C(2)-C(10)-C(9)	133.1	C(25)-C(24)-N(31)	123.6
C(5)-C(10)-C(9)	120.9	C(24)-C(25)-C(26)	132.1
C(4)-N(11)-C(12)	123.9	C(24)-C(25)-C(30)	106.6

C(26)-C(25)-C(30)	121.3	C(36)-C(35)-C(40)	120.3
C(25)-C(26)-C(27)	117.6	C(35)-C(36)-C(37)	118.2
C(26)-C(27)-C(28)	121.4	C(36)-C(37)-C(38)	121.0
C(27)-C(28)-C(29)	121.7	C(37)-C(38)-C(39)	121.7
C(28)-C(29)-C(30)	117.0	C(38)-C(39)-C(40)	117.0
C(22)-C(30)-C(25)	106.4	C(32)-C(40)-C(35)	106.5
C(22)-C(30)-C(29)	132.6	C(32)-C(40)-C(39)	131.7
C(25)-C(30)-C(29)	121.0	C(35)-C(40)-C(39)	121.8
C(24)-N(31)-C(32)	124.0	C(42)-N(41)-C(46)	116.4
N(31)-C(32)-N(33)	127.8	N(41)-C(42)-C(43)	124.1
N(31)-C(32)-C(40)	123.0	C(42)-C(43)-C(44)	118.9
N(33)-C(32)-C(40)	109.2	C(43)-C(44)-C(45)	118.9
Mg-N(33)-C(32)	125.5	C(44)-C(45)-C(46)	118.1
Mg-N(33)-C(34)	126.1	N(41)-C(46)-C(45)	123.7
C(32)-N(33)-C(34)	108.3	C(48)-N(47)-C(52)	116.0
N(1)-C(34)-N(33)	127.5	N(47)-C(48)-C(49)	123.8
N(1)-C(34)-C(35)	123.1	C(48)-C(49)-C(50)	118.3
N(33)-C(34)-C(35)	109.4	C(49)-C(50)-C(51)	118.7
C(34)-C(35)-C(36)	133.1	C(50)-C(51)-C(52)	119.4
C(34)-C(35)-C(40)	106.6	N(47)-C(52)-C(51)	123.8

coordinate magnesium atom in the crystals  $\text{Ce}_2\text{Mg}_3(\text{NO}_3)_{12} \cdot 24 \text{H}_2\text{O}$  ( $2.06 \pm .01 \text{ \AA}$ )<sup>21</sup>,  $\text{Mg}(\text{NH}_4)_2(\text{SO}_4)_2 \cdot 6 \text{H}_2\text{O}$  ( $2.07 \pm .01 \text{ \AA}$ )<sup>22</sup>, and  $\text{MgSO}_4 \cdot 6 \text{H}_2\text{O}$  ( $2.06 \pm .02 \text{ \AA}$ )<sup>23</sup>.

Other five-coordinate metalloporphyrins whose crystal structures have been determined include methoxyiron-(III)-mesoporphyrin-IX-dimethyl ester ( $\text{MeOFeMeso}$ )<sup>24</sup>, chlorohemin<sup>25</sup>, and vanadyldeoxophylloerythroetioporphyrin<sup>26</sup>. The nonplanarities of the metal atoms are 0.455 Å for the first, 0.475 Å for the second, and 0.48 Å for the third case. A major difference is that the metal chloride or oxide vector in each of the other three studied is colinear with the Ct-M vector to within  $0.06^\circ$ , where Ct is the center of the square formed by the four central nitrogen atoms. For the MgPc there is a distortion of  $3.66 \pm .15^\circ$  for the Ct-O(1) vector. The distortion in MgPc, which results in the four different N··O distances in Figure 2, is most likely due to the strong interaction between the water and pyridine molecules.

In MgPc the O··N distances of  $2.739 \pm .004 \text{ \AA}$  to N(41) and  $2.753 \pm .004 \text{ \AA}$  to N(47) are somewhat shorter than the average hydrogen bonded O··N distance of 2.80 Å. The O-H-N angles to the N(41) and N(47) atoms are  $172 \pm 4^\circ$  and  $167 \pm 4^\circ$ , respectively. The closest approaches between the Pc and pyridine molecules are shown in Table VI. The relatively short O··N distances and the stability of the air-exposed crystals indicate that the hydrogen bonds are relatively strong.

Table VI. Intermolecular Spacing Less Than 3.5 Å for C<sup>···</sup>C and C<sup>···</sup>N Approaches and Less Than 3.0 Å for C<sup>···</sup>H and N<sup>···</sup>H Approaches. Standard deviations are 0.02–0.04 Å for distances involving hydrogens and 0.004–0.006 Å for those not involving hydrogen.

Position of Adjacent Molecule 2	Atom of 1	Atom of 2	Distance (Å)
$1-x, -y, 1-z^a$	C(7)	C(24)	3.239
	C(8)	C(22)	3.310
	C(19)	C(36)	3.327
	C(8)	N(23)	3.406
	N(1)	N(11)	3.417
	C(6)	C(32)	3.426
	N(11)	C(34)	3.430
	C(7)	N(23)	3.466
	N(1)	C(12)	3.466
	C(6)	N(31)	3.470
$x, y, z^b$	C(15)	C(52)	3.433
	C(25)	C(43)	3.451
	C(14)	C(52)	3.456
	C(14)	H(52)	2.88
$x, y, 1+z$	C(27)	C(49)	3.419
	C(26)	H(6)	2.93
$x, y, -1+z$	C(6)	H(26)	2.89
	N(11)	H(27)	2.93
$\frac{1}{2}x, \frac{1}{2}y, \frac{1}{2}z$	N(1)	H(50)	2.66
	C(9)	H(51)	2.80
	C(5)	H(17)	2.84
$\frac{1}{2}x, \frac{1}{2}y, \frac{3}{2}z$	C(40)	H(29)	2.80
$\frac{1}{2}x, -\frac{1}{2}y, \frac{3}{2}z$	N(21)	H(45)	2.61
	C(29)	H(46)	2.84

<sup>a</sup>Position of the other molecule in the "dimer."

<sup>b</sup>Only the closest pyridine-MgPc distances are listed.

Chemically equivalent bond lengths and angles for the Pc were averaged in accordance with  $C_{4v}$  ( ~~$C_{4h}$~~ ) symmetry and are shown in Figure 3. The only departures from the mean bond lengths of Figure 3 larger than 0.006 Å are (in Å): +0.012 for C(32)-N(33), -0.011 for N(13)-C(14), -0.009 for N(31)-C(32), and +0.007 for C(14)-N(21). All of these are less than three times the standard deviation  $\sigma$  of the individual bond lengths. The largest differences from the mean angles of Figure 3 are  $3.5\sigma$  for Mg-C(23)-C(24),  $3.0\sigma$  for Mg-C(33)-C(34), and  $3.0\sigma$  for Mg-C(13)-C(12). These correspond to deviations of 0.6-0.7°.

Because of the deviations from planarity, which are shown in Figure 4, not only do the atomic positions in MgPc not conform to the  $C_{4v}$  symmetry, but they also differ from even mirror symmetry by more than thirty times the standard deviations of the atomic positions for some of the atoms. However, the pyrrole and benzene rings are all planar to within 0.02 Å. The largest deviations from the respective planes are 0.014 Å for pyrrole N(33) and 0.022 Å for benzene C(5)-C(10). Most of the deviations from planarity for the MgPc molecule can be described by three sets of operations shown in Figure 5: a) the tilt of the pyrrole groups around the line through atoms C(2) and C(4), b) the rotation of both pyrrole and benzene groups around the line between N(3) and the midpoint between atoms C(7) and C(8), and c) the tilt of the benzene rings around bond C(5)-C(10). The first of these can be as large as 30° or more for the porphyrin diacids<sup>28</sup>. The third of these, which is the



Figure 3. Averaged bond distances (in Å) and bond angles (in °) of MgPc. Standard deviations of the bond distances and angles are 0.006 Å and 0.4°.

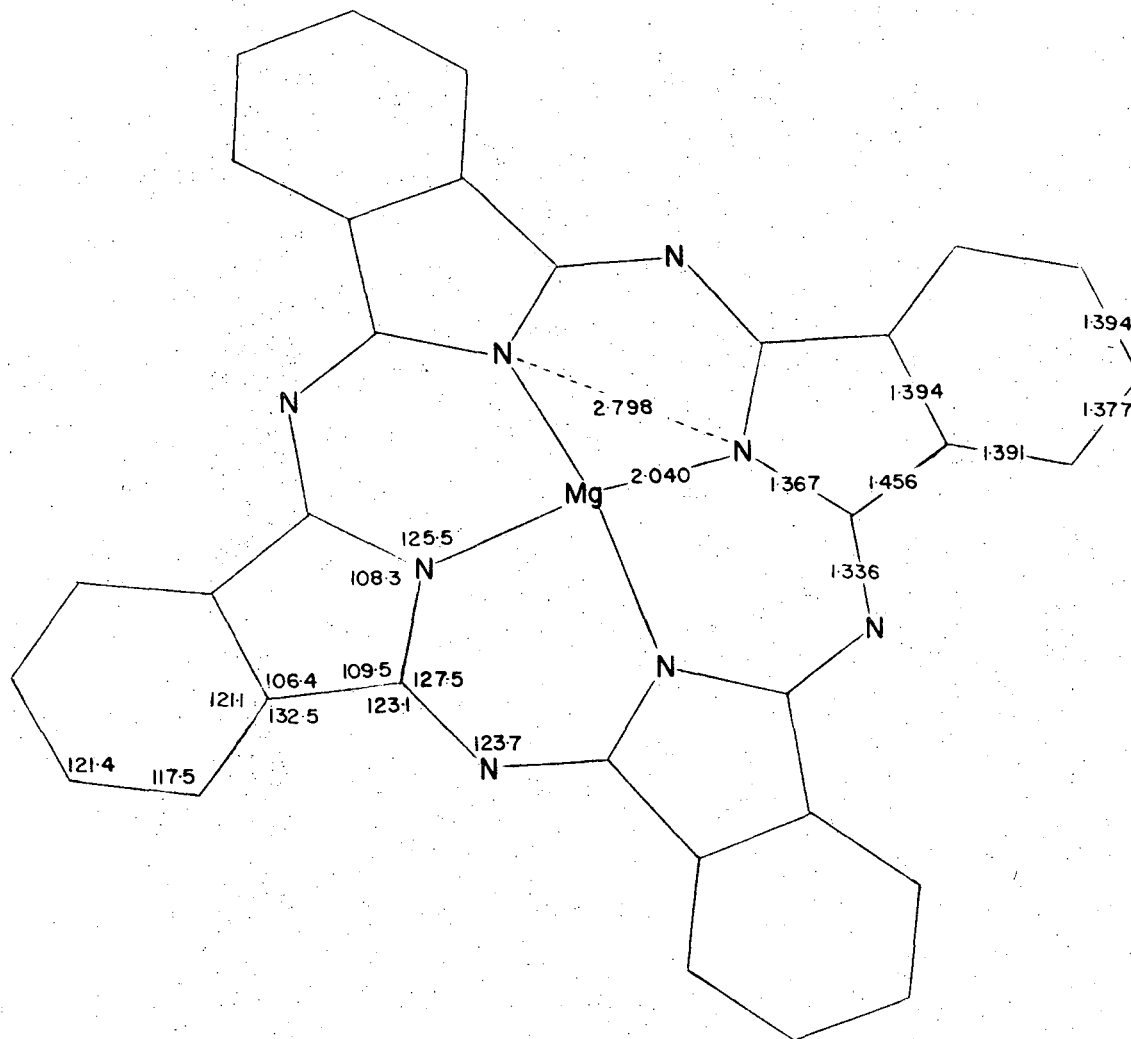


Figure 4. Deviations ( $\times 100$  in  $\text{\AA}$ ) from the least squares plane of the four central nitrogen atoms.

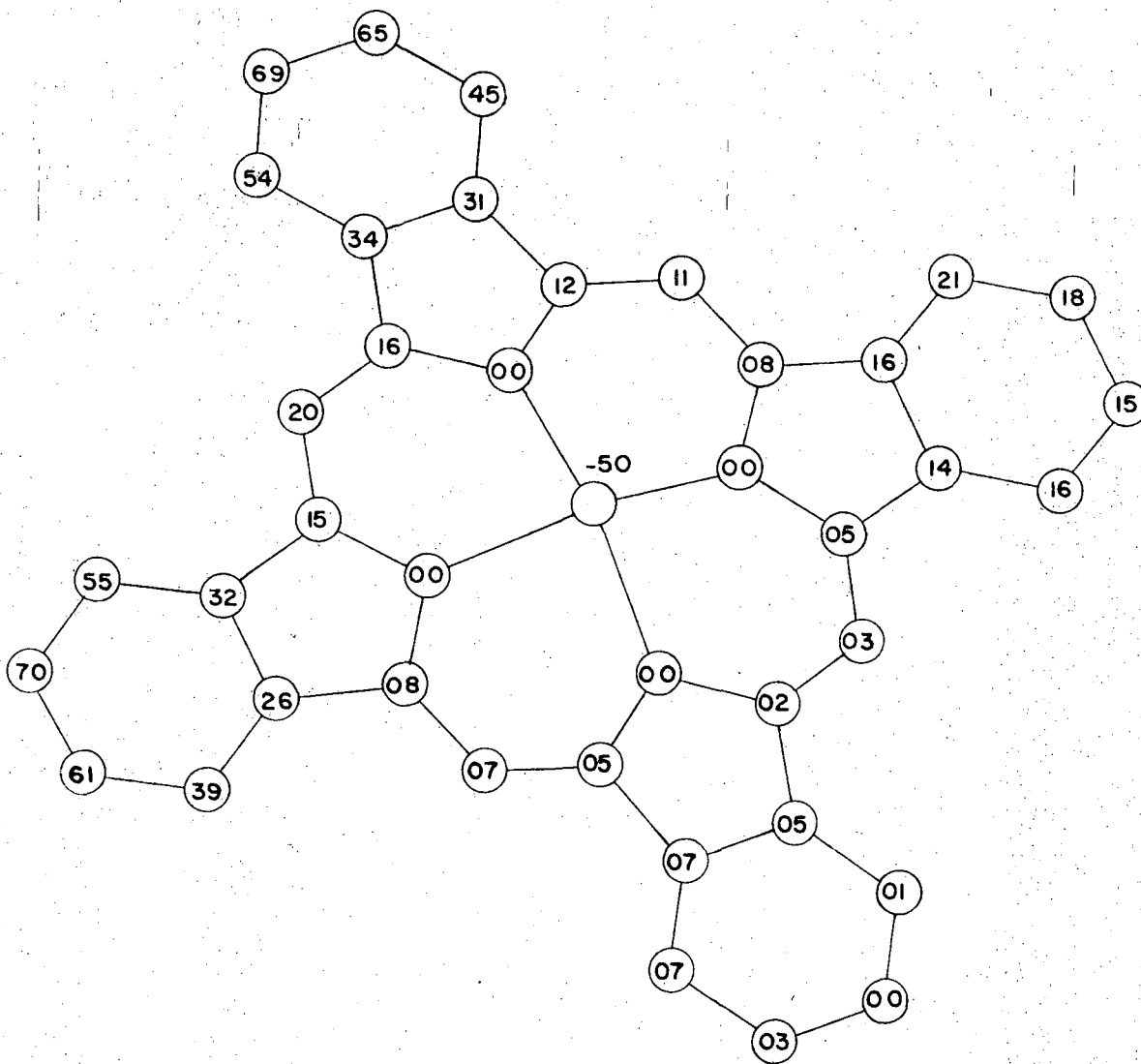
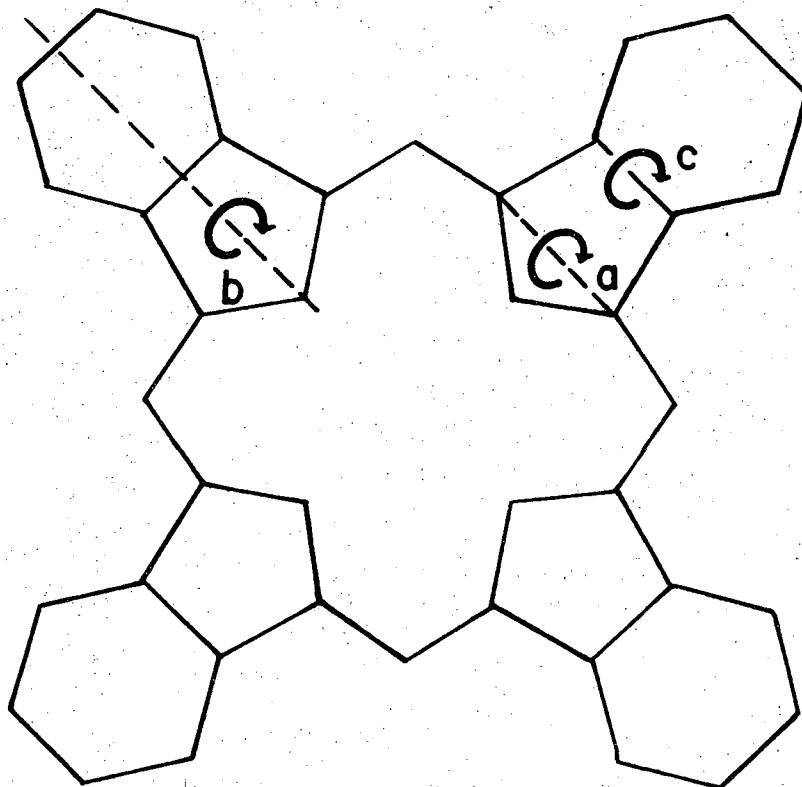


Figure 5. Rotation angles which describe the nonplanarity  
in phthalocyanin.



XBL 695-461

angle between the planes through a pyrrole and its fused benzene ring, is an indicator of the amount of conjugation between the pyrrole and benzene rings. The amounts of the rotations for each of the three operations and for each of the four corners of the MgPc molecule are listed in Table VII.

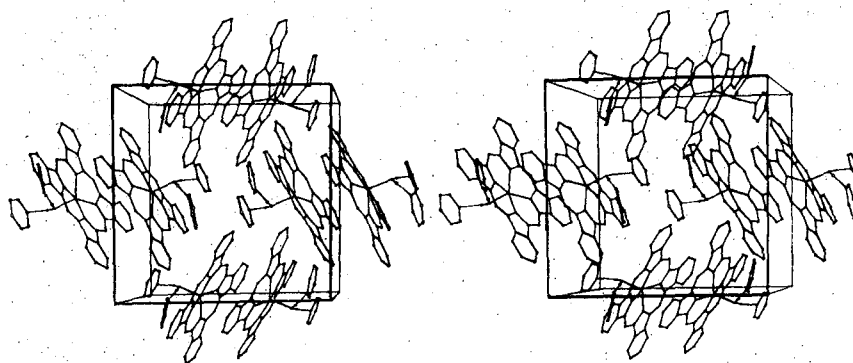
The packing arrangement of the unit cell is shown in Figure 6. The MgPc molecules are close together in pairs about the centers of symmetry at  $(\frac{1}{2}0\frac{1}{2})$  and  $(0\frac{1}{2}0)$ . A view of the "dimer" as seen perpendicular to the plane of the central nitrogens is shown in Figure 7. The planes through the pyrrole nitrogens are separated by only 3.506 Å, a distance only slightly greater than the 3.354 Å interplanar spacing of graphite<sup>29</sup> and the 3.34 Å spacing of  $\beta$ -CuPc<sup>7</sup> not involving hydrogen atoms. The closest atomic approach between molecules is 3.239 Å which is the distance between atoms C(7) of one molecule and C(24) of the other. All C...C and C...N intermolecular distances less than 3.5 Å and all C...H and N...H intermolecular distances less than 3.0 Å are listed in Table VI. In comparison, the shortest non H-atom intermolecular contacts in some other porphyrin structures are 3.43 Å in porphine<sup>30</sup>, 3.38 Å in H<sub>2</sub>Pc<sup>3</sup> and NiPc<sup>5</sup>, and 3.39 Å in MeOFeMeso<sup>24</sup>, which are all longer than the shortest distance in MgPc.

Packing forces can explain qualitatively some of the deviations from planarity of the Pc ring. The ruffling is in the proper direction to maximize the distance between overlapping groups in the "dimer". The closest intermolecular approach, between C(24) and

Table VII. Rotation Angles (in  $^{\circ}$ ) for Nonplanarity of MgPc.

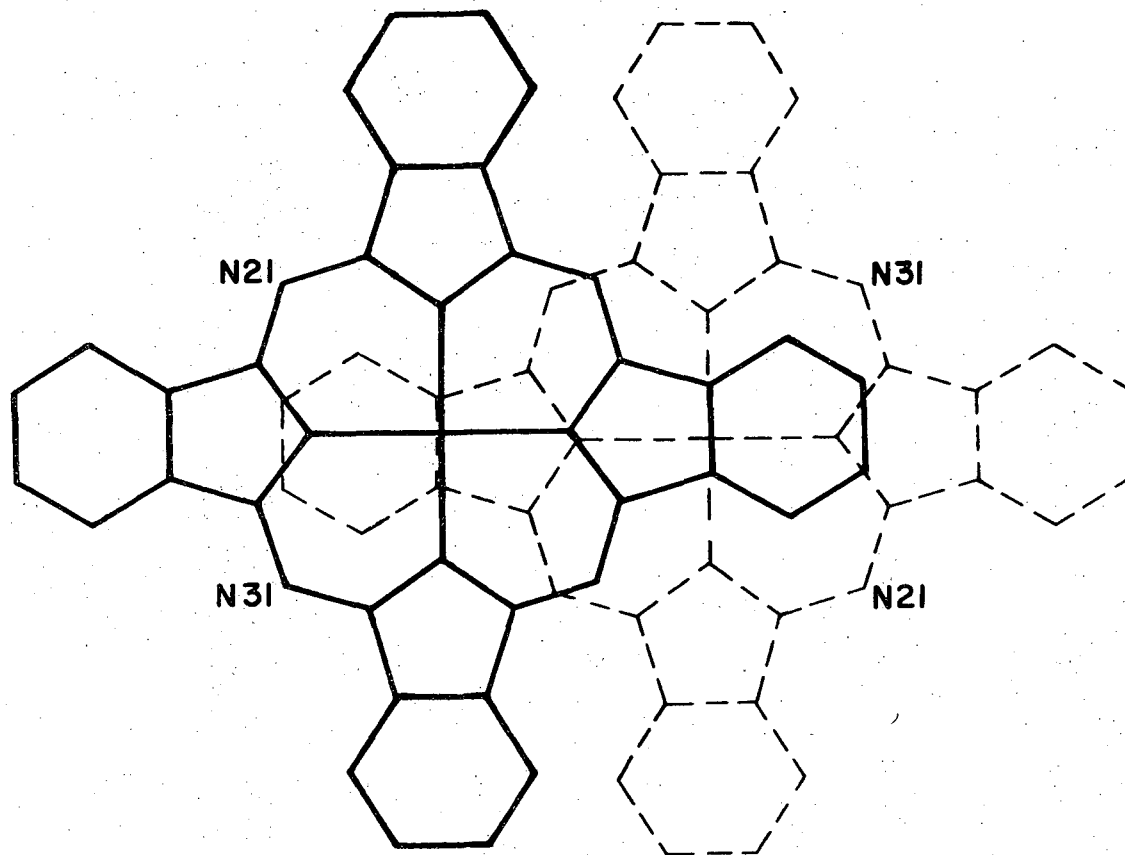
<u>Atoms</u>	<u><math>n_a</math></u>	<u><math>n_b</math></u>	<u><math>n_c</math></u>
C(2) - C(10)	3.5	0.8	3.5
C(12) - C(20)	1.2	-0.8	-2.3
C(22) - C(30)	6.8	-2.7	-1.6
C(32) - C(40)	7.4	1.3	-0.7

Figure 6. Stereoscopic view of the contents of the unit cell looking down the  $c$  axis. All C,N,O, and Mg atoms as well as the two hydrogens of the water molecule are shown. The hydrogen bonds connecting the water molecule to the two pyridine molecules are drawn in.



XBL 691-162

Figure 7. Normal projection of parallel phthalocyanins in the dimer. One molecule is drawn with solid lines, the other with dashed lines.



XBL 694-368

C(7), governs the ruffling of groups C(2) through C(10) and C(22) through C(30), and the approach between atoms C(19) and C(36) twists those groups out of the plane. Benzene ring C(5)-C(10), the least planar of any of the benzene rings, is involved in the closest intermolecular approach.

The "radius of the central hole"<sup>31</sup> of a porphyrin may be defined as the distance from the pyrrole nitrogen to the center (Ct) of the molecule. Through a compilation of the results of many porphyrin and metalloporphyrin structures, Hoard<sup>31</sup> has shown that the metal atom lies in the plane of the four nitrogen atoms of porphyrin molecules only when the M-N distance is less than 2.01 Å. The M-N distance in porphyrins is usually 0.05-0.10 Å larger than in Pc's. Since the Mg-N distance in MgPc is  $2.040 \pm .003$  Å, we expect that the Mg-N distance in Mg-porphyrins, when the magnesium atom is in a similar environment, will be at least  $2.070 \pm .02$  Å. This distance is analogous to the largest metalloporphyrin M-N distance thus far reported, *i.e.* in MeOFeMeso<sup>24</sup>, in which the iron atom is 0.46 Å out of the plane of the central nitrogens. From molecular orbital calculations Zerner, Gouterman, and Kobayashi<sup>32</sup> have predicted that the magnesium atom in porphyrins will have ~0.5 positive charge on it. For the chlorophyll molecule Katz *et al* have shown<sup>33,34</sup> that intermolecular aggregation most likely involves the coordination of ketone and aldehyde oxygen atoms of one molecule with the central magnesium atom of the other.



The central magnesium atom then would be in an environment similar to that in MgPc. This suggests the possibility that there is a similar non-planar orientation of Mg in porphyrins in general and very likely chlorophyll in particular, when they are in a hydrated biological environment or when the chlorophyll is aggregated.

The existence of hydrated penta coordinate magnesium atoms may help to explain the role of water in both the pyridine-Mg porphyrin complexing reported by Seely<sup>10</sup> and the biosynthesis of Mg porphyrins. Seely has reported at least a twofold enhancement of poly(vinyl pyridine) complex formation when 0.016% H<sub>2</sub>O was added to the nitromethane solutions of the Mg porphyrins or MgPc. The water molecules might act as a pivot between the polymer and porphyrin molecules. This would allow more movement of the porphyrin molecules so that other pyridine molecules would be available for complexing.

Plane et al<sup>12</sup> have studied the effect of pyridine as a catalyst<sup>in the insertion</sup> and removal of magnesium atoms in water solutions of deuteroporphyrins. When pyridine or some other catalyst is present, a complex similar to the MgPc·H<sub>2</sub>O·2C<sub>5</sub>H<sub>5</sub>N might be formed. The hydrogen-bonding of the bridging water molecule with its donation of positive charge to the pyridines would leave the oxygen more electronegative. The more electronegative oxygen, in turn, would attract the magnesium atom to form a stable complex with the magnesium atom half-way out of the plane. This would be in contrast to a more nearly planar molecule when pyridine is not present. From steric considerations alone, it would be more difficult to insert and remove the magnesium atom from the more planar configuration.

In the biosynthesis of chlorophyll, a similar Mg coordination compound might be involved with the imidazole of a histidine, for example, replacing the pyridine molecules. In fact, Baum and Plane<sup>35</sup> found that the imidazole as well as several other nitrogen bases can act as catalysts similar to pyridine.

References

- 2 J.M. Robertson, J.Chem.Soc., 615 (1935)
- 3 J.M. Robertson, ibid., 1195 (1936)
- 4 R.P. Linstead and J.M. Robertson, ibid., 1736 (1936)
- 5 J.M. Robertson and I. Woodward, ibid., 219 (1937)
- 6 J.M. Robertson and I. Woodward, ibid., 36 (1940)
- 7 C.J. Brown, ibid., A, 2488 (1968)
- 8 C.J. Brown, ibid., A, 2494 (1968)
- 9 L.H. Vogt, A. Zalkin and D.H. Templeton, Inorg.Chem., 6, 1725 (1967)
- 10 G.R. Seeley, J.Phys.Chem., 71, 2091 (1967)
- 11 N.A. Matwiyoff and H. Taube, J.Amer.Chem.Soc., 90, 2796 (1968)
- 12 R. Snellgrove and R.A. Plane, ibid., 90, 3185 (1968)
- 13 K. Sauer, E.A. Dratz and L. Coyne, Proc.Nat.Acad.Sci.U.S., 61, 17 (1968); K. Ballschmiter and J.J. Katz, J.Amer.Chem.Soc., 91, 2661 (1969)
- 14 D.T. Cromer and J.B. Mann, Acta Cryst., A24, 321 (1968)
- 15 R.F. Stewart, E.R. Davidson, and W.T. Simpson, J.Chem.Phys., 42, 3175 (1965).
- 16 D.T. Cromer, Acta Cryst., 18, 17 (1965)

- 17 R.E. Long, Ph.D. Thesis, University of California, Los Angeles, Calif., 1965.
- 18 C.K. Johnson, Oak Ridge National Report-3794, Revised, Oak Ridge, Tennessee, June, 1965.
- 19 A.J.C. Wilson, Nature, 150, 152 (1942).
- 20 C.A. Taylor and H. Lipson, "Optical Transforms," G. Bell and Sons, Ltd., London, 1964.
- 21 D.H. Templeton, A. Zalkin and J.D. Forrester, Bull. Amer. Phys. Soc., 7, 608 (1962).
- 22 T.N. Margulis and D.H. Templeton, Z. Kristallogr., 117, 344 (1962).
- 23 A. Zalkin, H. Ruben and D.H. Templeton, Acta Cryst., 17, 235 (1964).
- 24 J.L. Hoard, M.J. Hamor, T.A. Hamor, and W.S. Caughey, J. Amer. Chem. Soc., 87, 2312 (1965).
- 25 D.F. Koenig, Acta Cryst., 18, 663 (1965).
- 26 R.C. Petterson and L.E. Alexander, J. Amer. Chem. Soc., 90, 387 (1968).
- 27 G.C. Pimentel and A.L. McClellan, "The Hydrogen Bond," W.H. Freeman and Co., San Francisco, Calif., 1960, p 289.
- 28 A. Stone and E.B. Fleischer, J. Amer. Chem. Soc., 90, 2735 (1968).
- 29 J.B. Nelson and D.P. Riley, Proc. Roy. Soc., 57, 477, 486 (1945).
- 30 L.E. Webb and E.B. Fleischer, J. Chem. Phys., 43, 3100 (1965).
- 31 J.L. Hoard in "Structural Chemistry and Molecular Biology," A. Rich and N. Davidson, Eds., W.H. Freeman and Co., San Francisco, Calif., 1968, pp 573-594.

- 32 M. Zerner, M. Gouterman, and H. Kobayashi, Theor.Chim.Acta,  
6, 363 (1966).
- 33 J.J. Katz, G.L. Closs, F.C. Pennington, M.R. Thomas, and  
H.H. Strain, J.Amer.Chem.Soc., 85, 3801 (1963).
- 34 G.L. Closs, J.J. Katz, F.C. Pennington, M.R. Thomas, and  
H.H. Strain, ibid., 85, 3809 (1963).
- 35 S.J. Baum and R.A. Plane, J.Amer.Chem.Soc., 88, 910 (1966).

## The Crystal and Molecular Structure of Methyl Pheophorbide a

### Experimental Procedure

Weissenberg photographs of a wedge-shaped fragment of Methyl pheophorbide a (MePPb) with dimensions  $0.2 \times 0.1 \times .05$  mm indicated Laue symmetry  $2/m$ . The intrinsic molecular non-centricity and the systematic absences on Weissenberg photographs ( $0k0$ ,  $k \neq 2n$ ) imply that the probable space group is  $P2_1$ . Both the cell dimensions and intensity data were collected on a General Electric XRD-5 x-ray diffractometer equipped with a copper x-ray tube, a manual quarter-circle Eulerian-cradle goniostat and a .0003 inch thick nickel filter at the receiving slit. The distances from the crystal to the x-ray source and to the receiving slit are 14.5 and 17.8 cm, respectively. The crystal was aligned so that its reciprocal  $101$  line was parallel to the instrument  $\varphi$  axis. The  $\chi$ ,  $\varphi$ , and  $2\theta$  values of 25 independent general reflections, each of which had

its alpha doublet resolved ( $\lambda = 1.5405 \text{ \AA}$  for  $\text{CuK}\alpha_1$ ), were used in a least squares refinement of the unit cell parameters and crystal orientation. The unit cell dimensions are  $a = 8.035 \pm 0.004 \text{ \AA}$ ,  $b = 28.531 \pm 0.006 \text{ \AA}$ ,  $c = 7.321 \pm 0.002 \text{ \AA}$ , and  $\beta = 110.96 \pm 0.02^\circ$ . An average density of  $1.252 \pm 0.005 \text{ g cm}^{-3}$  was obtained from flotation of the crystals in three independent solutions of aqueous  $\text{ZnBr}_2$ , aqueous  $\text{KBr}$ , and aqueous  $\text{NaI}$ . The calculated density is 1.285 for a formula weight of 606.7, for  $Z = 2$ , and for a unit cell volume of  $1567 \text{ \AA}^3$ .

All the independent reflections lying within half of a sphere in reciprocal space corresponding to spacing  $\geq 1.006 \text{ \AA}$  ( $2\theta \leq 100^\circ$ ) were counted for ten seconds with both crystal and counter stationary and at a takeoff angle of  $4^\circ$ . Individual backgrounds were measured for those reflections seriously affected by streaking from lower orders; for the rest, backgrounds were taken from a plot of the background counts as a function of the Bragg scattering angle. Of the 3214 reflections measured, the intensities of 3103 were above background. The rms difference between  $I(hkl)$  and  $I(\bar{h}\bar{k}\bar{l})$  was 6.2% of  $I(hkl)$ . The intensities of the Bijvoet pairs of reflections were averaged to produce 1662 independent reflections of which 1616 had net intensities greater than zero counts. The intensities of the three standard reflections, measured periodically to check the alignment and decay, varied by less than  $\pm 2\%$ . No correction was made for absorption ( $\mu = 6.9 \text{ cm}^{-1}$ ).

The atomic scattering factors used in this analysis were those of Cromer and Mann<sup>12</sup> for the non-hydrogen atoms and those of Stewart, Davidson, and Simpson<sup>13</sup> for the hydrogen atoms. The function minimized during the least-squares refinements was  $(R_2)^2 = \frac{\sum w (|kF_o| - |F_c|)^2}{\sum w |kF_o|^2}$ , where  $|F_o|$  and  $|F_c|$  are the observed and calculated structure amplitudes, respectively, and  $k$  is the scale factor. The weight  $w$  assigned to a reflection was  $w = 0$  if  $I = 0$ . Otherwise it was calculated from the larger of the counting statistics and the difference between duplicate measurements<sup>14</sup>.

Computer programs run on the CDC 6600 computer include: WILSON, an unpublished Wilson-plot program by Maddox and Maddox; R. E. Long's phase determination program<sup>15</sup>; LS200, our unpublished modified version of the Ganzel-Sparks-Trueblood least squares program; ORTEP, Johnson's molecular crystallographic plotting program<sup>16</sup>; and RIGBOD, a rigid-body rotation program written specifically for this problem.

Powder pattern data for methyl pheophorbide were obtained from a Philips cylindrical camera of radius 57.29 mm using ~~vanadium~~ filtered FeK $\alpha$  radiation ( $\lambda = 1.9373 \text{ \AA}$ ). We corrected for the film shrinkage of 0.34%.



### Solution of the Structure

The structure was solved by trial and error methods. An idealized model based on porphin geometry<sup>2</sup> was systematically changed in its orientation and used to generate structure factor values. The 147 reflections with  $(\sin\theta/\lambda) \leq 0.22 \text{ \AA}^{-1}$  were compared with the calculated values.

Three positional and three angular coordinates are sufficient to specify a molecule's location and orientation in the unit cell. Our calculations were greatly simplified by the elimination of three of these parameters. The  $y$  coordinate of the center was fixed at 0.5 since the space group is polar in that direction. Two of the angles were determined from an examination of a three dimensional Patterson calculation which indicated the molecular plane. The program called RIGBOD calculated an  $R_1$ -value for each combination of coordinates, where  $R_1 = \frac{\sum |k|F_o| - |F_c|}{\sum k|F_o|}$ . The  $x$ ,  $z$ , and  $\phi$  (the angle in the plane) coordinates were varied from 0.00 to 0.25, 0.00 to 0.475, and 0 to 80°, respectively, in increments of 0.025 for  $x$  and  $z$  and 10° for  $\phi$ . Typical  $R$ -values were 66-73%, and there were two minima with  $R = 64\%$ . The two orientations which corresponded to the two minima had identical  $x$  and  $z$  values but differed by approximately 45° in  $\phi$ .

The atomic positions for one of these two orientations refined to an R value of 0.49. We discontinued using this proposed orientation as a trial structure because of the difficulty in locating additional atoms at chemically reasonable locations.

The other trial structure was refined eventually to the structure presented below. Fourier and least-squares techniques were used to adjust tentative atomic positions and to locate additional atoms. A total of 45 atoms were located in this way. The nitrogen and oxygen atoms were recognized from their molecular positions.

The molecular structure, with isotropic temperature factors, refined to 0.128. The 45 atoms were given anisotropic thermal parameters. The positions of 31 of the 38 hydrogen atoms were located from difference Fourier maps, assigned  $B = 6$ , and included (but not refined) in the least squares calculations.  $R_1$  dropped to 0.069. The inner pyrrole hydrogen atoms were not among the hydrogen atoms included in these calculations.

We calculated a difference Fourier map which showed four peaks in the middle of the molecule. The technique of LaPlaca and Ibers<sup>17</sup> was used to decide whether the peaks correspond to physical reality or were artifacts of the high noise level produced by random and systematic errors in the data. If the peaks are due to noise, then they should shift markedly or even disappear as the number of terms in the difference Fourier synthesis is varied. The noise level was estimated from the esd of the electron density:  $\sigma(\rho) = (\sum(F_o - F_c)^2)^{1/2}/V$  where  $V$  is the unit cell volume<sup>18</sup>. Table I lists the average peak heights for the four peaks and the esd of the electron density. All four peaks are present at nearly the same locations on each of the five difference Fourier maps calculated with different amounts of data. Because there are only two hydrogen atoms in the center of the molecule, we assigned an occupancy of  $\frac{1}{2}$  to each of the four hydrogen "half-atoms" and refined their positions in further calculations. The positions of two of the five remaining hydrogen atoms were calculated and included in all subsequent computations, but attempts to locate the hydrogen atoms on the methyl ester of the carboxyl group off Ring IV were unsuccessful. Group temperature factors were assigned to the hydrogen atoms of each of six methyl groups, to the four pyrrole half-hydrogen atoms, to the six hydrogen atoms attached directly to the chlorin ring, and to the eight remaining hydrogen atoms. Attempts to refine the

Table I. Peak Heights and Their Esd's of the Four Inner Hydrogen Atoms of Methyl Pheophorbide as a Function of the Number of Reflections Used to Calculate the Five Difference Fourier Maps.

<u>Maximum</u> $\sin \theta/\lambda$ ( $\text{\AA}^{-1}$ )	<u>Number of</u> <u>Reflections</u>	<u>Average Peak</u> <u>Height <math>\rho</math> (<math>e^-</math>)</u>	$\sigma(\rho)$ ( $e^-$ )	$\rho/\sigma(\rho)$
0.29	335	0.074	0.022	3.3
0.36	635	0.108	0.025	4.3
0.42	999	0.131	0.026	5.0
0.46	1302	0.162	0.027	6.0
0.497	1609	0.162	0.028	5.8

positions of all of the hydrogen atoms were unsuccessful. The positions of fifteen of the hydrogen atoms were fixed at 1.0 Å from their respective carbon atoms while the positions of the remaining 22 (including the four pyrrole half hydrogen atoms) were refined.

In the refinements, the  $y$  coordinate of one of the nitrogen atoms was fixed at  $y = \frac{1}{2}$ . In the final refinements half the atoms were refined in each cycle. On the final two cycles, the maximum shift of any parameter was less than 0.1 of its standard deviation. The final  $R_1$ -value based upon the atomic parameters of Tables II and III is 0.051 for the 1616 observed data and 0.053 for all 1662 data. The weighted residual value  $R_2 = 0.063$  and the standard deviation of an observation of unit weight is 2.14. The observed and calculated structure factor values are presented in Table IV, and the intramolecular bond distances and bond angles calculated from these atomic coordinates are presented in Tables V and VI. The final values of  $w(\Delta F)^2$  are independent of both the intensities and Bragg scattering angle of the reflections. The highest peak on the final difference Fourier map is  $0.15 \text{ e } \text{Å}^{-3}$ . At the positions on which the fifteen hydrogen atoms were fixed, the lowest and mean electron densities are  $-0.07$  and  $-0.03 \text{ e } \text{Å}^{-3}$ , respectively. The numbering scheme is shown in Figure 2.

Table II. Final Atomic Fractional Coordinates and Thermal Parameters<sup>a</sup> of All Nonhydrogen Atoms in the Asymmetric Unit<sup>b</sup>.

ATOM	X	Y	Z	B <sup>11</sup>	B <sup>22</sup>	B <sup>33</sup>	B <sup>12</sup>	B <sup>13</sup>	B <sup>23</sup>
N(1)	.2659(6)	.5090	.7105(7)	3.13(21)	5.00(24)	6.20(24)	.60(23)	1.68(21)	.55(20)
N(2)	-.0450(8)	.4385(2)	.4893(8)	5.53(28)	3.53(25)	7.16(32)	.04(27)	2.18(24)	-.32(21)
N(3)	-.2717(7)	.5119(2)	.4655(6)	3.06(22)	5.59(27)	5.59(23)	-.22(22)	.81(18)	-.36(18)
N(4)	.0265(8)	.5785(2)	.6912(9)	3.54(24)	4.59(30)	5.84(26)	.13(29)	1.39(20)	-.33(24)
C(1)	.3873(7)	.5327(2)	.8123(8)	3.36(26)	5.17(26)	5.51(26)	.46(23)	1.40(21)	.81(22)
C(2)	.5617(7)	.5109(2)	.8787(8)	3.68(28)	5.56(28)	5.42(25)	.81(23)	1.66(21)	1.23(21)
C(3)	.5381(7)	.4661(2)	.8143(8)	4.05(26)	5.34(26)	6.48(29)	1.19(22)	2.06(22)	1.39(22)
C(4)	.3486(7)	.4580(2)	.7087(7)	3.87(27)	5.68(29)	5.59(27)	.46(23)	1.64(22)	1.10(21)
C(5)	.2703(7)	.4168(2)	.6244(9)	4.60(28)	4.71(26)	7.13(32)	.22(21)	2.75(25)	.30(22)
C(6)	.0675(8)	.4068(2)	.5278(9)	5.94(32)	4.64(27)	6.57(31)	-.12(28)	2.76(26)	.12(24)
C(7)	.0205(10)	.3615(2)	.4543(10)	6.58(40)	4.98(32)	7.96(37)	-.38(27)	2.78(31)	-.18(26)
C(8)	-.1594(10)	.3661(2)	.3689(11)	7.07(41)	4.87(32)	8.11(37)	-.80(26)	2.35(32)	-1.01(25)
C(9)	-.2003(8)	.4148(2)	.3928(9)	5.14(31)	4.82(30)	6.45(31)	-.86(25)	1.56(25)	-.46(22)
C(10)	-.3683(8)	.4340(2)	.3340(9)	4.82(30)	5.50(27)	6.27(30)	-.92(24)	1.75(24)	-.34(24)
C(11)	-.4968(7)	.4807(2)	.3640(8)	3.97(28)	5.47(27)	5.77(28)	-.41(26)	1.05(23)	.01(23)
C(12)	-.5675(7)	.5051(2)	.3050(8)	4.13(30)	6.19(34)	5.68(27)	-.29(26)	1.76(23)	.72(24)
C(13)	-.5284(6)	.5511(2)	.3719(7)	3.21(28)	6.01(30)	4.67(24)	-.05(21)	.60(20)	.18(22)
C(14)	-.3430(7)	.5537(2)	.4688(7)	3.46(27)	5.22(29)	4.96(26)	-.06(21)	1.08(21)	.61(20)
C(15)	-.2812(6)	.5974(2)	.5470(7)	3.51(23)	5.46(27)	5.09(25)	.96(21)	.97(20)	.13(20)
C(16)	-.1075(7)	.6094(2)	.6618(8)	3.92(25)	4.26(23)	5.43(26)	.33(21)	1.42(20)	.00(20)
C(17)	-.0474(7)	.6541(2)	.7714(8)	3.20(25)	5.38(27)	5.97(28)	.60(21)	1.35(20)	.02(23)
C(18)	-.1576(7)	.6508(2)	.8282(9)	3.33(25)	5.93(29)	5.54(26)	-.24(22)	1.08(21)	-.40(24)
C(19)	-.1802(7)	.6034(2)	.7889(8)	4.52(26)	3.79(24)	5.86(26)	.90(21)	1.35(22)	.05(19)
C(20)	.3476(7)	.5782(2)	.8467(8)	3.25(23)	5.34(27)	5.92(27)	-.19(21)	1.60(20)	.03(22)
C(21)	.7292(8)	.5345(3)	.9996(11)	3.53(30)	6.88(36)	7.49(37)	-.49(28)	1.45(26)	.77(32)
C(22)	.6729(9)	.4292(3)	.8426(11)	3.65(32)	8.35(45)	9.18(41)	1.32(29)	1.58(28)	1.43(33)
C(23)	.8346(14)	.4349(4)	.8980(17)	8.88(64)	10.72(61)	15.77(86)	2.14(52)	1.52(56)	-2.44(60)
C(24)	.1260(11)	.3174(4)	.4722(14)	8.52(47)	9.64(35)	11.82(55)	-.27(33)	4.06(43)	-.49(33)
C(25)	-.2969(10)	.3287(3)	.2756(13)	7.93(43)	5.17(31)	11.35(51)	-1.61(29)	2.90(39)	-1.26(32)
C(26)	-.3578(13)	.3056(3)	.4197(18)	10.42(61)	7.87(48)	15.28(78)	-3.31(46)	5.74(57)	-2.34(50)
C(27)	-.7511(7)	.4849(3)	.1883(10)	3.85(30)	8.83(41)	7.45(34)	-1.82(29)	.27(26)	.59(30)
C(28)	-.6044(8)	.5963(3)	.3759(8)	4.20(30)	6.63(31)	5.33(27)	.69(25)	1.30(23)	.83(23)
C(29)	-.4432(6)	.6298(2)	.4868(8)	3.71(26)	5.82(27)	5.50(26)	-.52(22)	1.08(21)	.20(22)
C(30)	-.1023(8)	.6560(2)	.9537(9)	4.24(28)	5.60(30)	6.31(30)	-.00(24)	1.78(23)	-.34(25)
C(31)	-.0409(10)	.6985(3)	1.0813(10)	5.32(35)	7.10(39)	6.95(37)	.29(28)	2.32(27)	-1.03(32)
C(32)	.2272(11)	.6834(3)	.7085(13)	5.59(38)	5.60(33)	10.08(50)	-.40(30)	4.24(40)	-.04(31)
C(33)	-.4347(7)	.6664(2)	.3453(10)	3.33(27)	6.14(34)	7.98(37)	1.55(24)	1.12(26)	.92(27)
C(34)	-.5272(12)	.7416(3)	.2155(15)	9.11(54)	4.86(31)	12.96(58)	-.08(32)	3.17(45)	1.69(40)
C(35)	-.1337(11)	.7419(3)	.9924(12)	6.79(42)	7.13(41)	8.22(40)	-1.22(33)	2.54(34)	-2.29(38)
C(36)	-.1471(21)	.8255(3)	1.0239(19)	25.52(141)	5.76(44)	14.42(78)	.41(59)	8.55(87)	.05(46)
H(1)	-.7581(5)	.6092(2)	.3103(7)	3.46(19)	8.63(25)	7.95(23)	1.46(18)	.97(16)	1.02(20)
H(2)	-.3617(7)	.6620(2)	.2286(9)	4.15(31)	9.27(29)	12.00(36)	2.93(25)	6.75(30)	6.55(28)
H(3)	-.5272(6)	.7040(2)	.3527(7)	7.55(27)	5.81(21)	9.19(26)	1.78(21)	3.00(21)	.40(20)
H(4)	-.2666(10)	.7448(2)	.8529(11)	10.62(41)	8.76(32)	11.12(38)	2.48(30)	.86(33)	.60(31)
H(5)	-.0574(9)	.7796(2)	1.0903(10)	13.77(49)	8.06(34)	12.80(43)	-2.34(32)	3.83(36)	-4.62(32)

<sup>a</sup> The form of the anisotropic thermal ellipsoid

(expressed in units of Å<sup>2</sup>) is:  $\exp\left(-\frac{1}{2} \sum_{i,j=1}^3 \sum_{k=1}^3 B_{ij} b_i b_j h_i h_j\right)$ , where  $b_i$  =  $i$ th reciprocal axis

length and  $h_i$  =  $i$ th Miller index.

<sup>b</sup> The numbers in parentheses here and in succeeding

tables are the estimated standard deviations of

the least significant digit(s).

Table III. Final Fractional Positional and Isotropic Thermal Parameters<sup>A</sup> for All Hydrogen Atoms in the Asymmetric Unit.

<u>Atom</u>	<u>x</u>	<u>y</u>	<u>z</u>	<u>B</u> (Å <sup>2</sup> )
H(1)N(1)	.163(12)	.499(3)	.680(12)	2.4(11)
H(1)N(2)	-.038(15)	.458(3)	.528(15)	2.4
H(1)N(3)	-.159(12)	.502(3)	.499(11)	2.4
H(1)N(4)	.016(19)	.562(4)	.667(18)	2.4
H(1)C(5)	.350	.389	.639	4.8(4)
H(1)C(10)	-.471(7)	.414(2)	.252(7)	4.8
H(1)C(17)	-.101(7)	.677(2)	.697(8)	4.8
H(1)C(18)	.229(7)	.655(2)	.961(8)	4.8
H(1)C(20)	.432(7)	.601(2)	.903(7)	4.8
H(1)C(21)	.702(8)	.565(3)	1.052(9)	7.2(8)
H(2)C(21)	.799(9)	.545(2)	.946(9)	7.2
H(3)C(21)	.811(9)	.517(2)	1.122(9)	7.2
H(1)C(22)	.659(6)	.386(2)	.835(7)	4.8
H(1)C(23)	.913	.407	.914	10.4(8)
H(2)C(23)	.884	.467	.930	10.4
H(1)C(24)	.224	.326	.425	13.5(17)
H(2)C(24)	.193	.314	.615	13.5
H(3)C(24)	.038(12)	.291(4)	.398(14)	13.5
H(1)C(25)	-.247	.306	.206	10.4
H(2)C(25)	-.403	.342	.168	10.4

H(1)C(26)	-.438	.331(3)	.471	12.7(15)
H(2)C(26)	-.257	.295	.538	12.7
H(3)C(26)	-.431	.277	.366	12.7
H(1)C(27)	-.746	.454	.126	15.8(20)
H(2)C(27)	-.802	.508	.078	15.8
H(3)C(27)	-.838	.485	.258	15.8
H(1)C(29)	-.450	.646	.605	4.8
H(1)C(30)	-.244(12)	.652(3)	.901(12)	10.4
H(2)C(30)	-.033(11)	.633(3)	1.034(12)	10.4
H(1)C(31)	-.074(12)	.694(3)	1.155(14)	10.4
H(2)C(31)	.113(12)	.712(3)	1.137(11)	10.4
H(1)C(32)	.196(7)	.718(2)	.738(7)	5.6(7)
H(2)C(32)	.329(8)	.681(2)	.735(9)	5.6
H(3)C(32)	.162(7)	.673(2)	.563(9)	5.6
H(1)C(34)	-.610(15)	.738(4)	.083(19)	16.7(22)
H(2)C(34)	-.408	.749	.209	16.7
H(3)C(34)	-.565	.770	.271	16.7

<sup>a</sup>Those parameters listed without standard deviations  
are not independent.



Table IV. Observed and Calculated Structure Factor Amplitudes of Methyl Pheophorbide. 70

h	k	l	F <sub>o</sub>	F <sub>c</sub>	h	k	l	F <sub>o</sub>	F <sub>c</sub>	h	k	l	F <sub>o</sub>	F <sub>c</sub>
1	0	0	14.58	6.2	2	0	0	2.257	2.08	3	0	0	4.76	7.7
2	0	0	14.58	6.2	4	0	0	11.14	12.6	5	0	0	15.87	16.1
3	0	0	14.58	6.2	6	0	0	22.28	25.2	8	0	0	35.74	35.2
4	0	0	14.58	6.2	8	0	0	33.42	37.8	10	0	0	51.06	50.6
5	0	0	14.58	6.2	10	0	0	44.56	50.4	12	0	0	65.40	65.0
6	0	0	14.58	6.2	12	0	0	55.70	63.0	14	0	0	79.74	79.3
7	0	0	14.58	6.2	14	0	0	66.84	75.6	16	0	0	94.08	93.6
8	0	0	14.58	6.2	16	0	0	77.98	88.2	18	0	0	108.42	108.0
9	0	0	14.58	6.2	18	0	0	89.12	100.8	20	0	0	122.76	122.3
10	0	0	14.58	6.2	20	0	0	100.26	113.4	22	0	0	137.10	136.7
11	0	0	14.58	6.2	22	0	0	111.40	126.0	24	0	0	151.44	151.0
12	0	0	14.58	6.2	24	0	0	122.54	138.6	26	0	0	165.78	165.3
13	0	0	14.58	6.2	26	0	0	133.68	151.2	28	0	0	180.12	179.7
14	0	0	14.58	6.2	28	0	0	144.82	163.8	30	0	0	194.46	194.0
15	0	0	14.58	6.2	30	0	0	155.96	176.4	32	0	0	208.80	208.3
16	0	0	14.58	6.2	32	0	0	167.10	189.0	34	0	0	223.14	222.7
17	0	0	14.58	6.2	34	0	0	178.24	201.6	36	0	0	237.48	237.0
18	0	0	14.58	6.2	36	0	0	189.38	214.2	38	0	0	251.82	251.3
19	0	0	14.58	6.2	38	0	0	200.52	226.8	40	0	0	266.16	265.7
20	0	0	14.58	6.2	40	0	0	211.66	239.4	42	0	0	280.50	280.0
21	0	0	14.58	6.2	42	0	0	222.80	252.0	44	0	0	294.84	294.3
22	0	0	14.58	6.2	44	0	0	233.94	264.6	46	0	0	309.18	308.7
23	0	0	14.58	6.2	46	0	0	245.08	277.2	48	0	0	323.52	323.0
24	0	0	14.58	6.2	48	0	0	256.22	289.8	50	0	0	337.86	337.3
25	0	0	14.58	6.2	50	0	0	267.36	302.4	52	0	0	352.20	351.7
26	0	0	14.58	6.2	52	0	0	278.50	315.0	54	0	0	366.54	366.0
27	0	0	14.58	6.2	54	0	0	289.64	327.6	56	0	0	380.88	380.3
28	0	0	14.58	6.2	56	0	0	300.78	340.2	58	0	0	395.22	394.7
29	0	0	14.58	6.2	58	0	0	311.92	352.8	60	0	0	409.56	409.0
30	0	0	14.58	6.2	60	0	0	323.06	365.4	62	0	0	423.90	423.3
31	0	0	14.58	6.2	62	0	0	334.20	378.0	64	0	0	438.24	437.7
32	0	0	14.58	6.2	64	0	0	345.34	390.6	66	0	0	452.58	452.0
33	0	0	14.58	6.2	66	0	0	356.48	403.2	68	0	0	466.92	466.3
34	0	0	14.58	6.2	68	0	0	367.62	415.8	70	0	0	481.26	480.7
35	0	0	14.58	6.2	70	0	0	378.76	428.4	72	0	0	495.60	495.0
36	0	0	14.58	6.2	72	0	0	389.90	441.0	74	0	0	509.94	509.3
37	0	0	14.58	6.2	74	0	0	401.04	453.6	76	0	0	524.28	523.7
38	0	0	14.58	6.2	76	0	0	412.18	466.2	78	0	0	538.62	538.0
39	0	0	14.58	6.2	78	0	0	423.32	478.8	80	0	0	552.96	552.3
40	0	0	14.58	6.2	80	0	0	434.46	491.4	82	0	0	567.30	566.7
41	0	0	14.58	6.2	82	0	0	445.60	504.0	84	0	0	581.64	581.0
42	0	0	14.58	6.2	84	0	0	456.74	516.6	86	0	0	595.98	595.3
43	0	0	14.58	6.2	86	0	0	467.88	529.2	88	0	0	610.32	609.7
44	0	0	14.58	6.2	88	0	0	479.02	541.8	90	0	0	624.66	624.0
45	0	0	14.58	6.2	90	0	0	490.16	554.4	92	0	0	639.00	638.3
46	0	0	14.58	6.2	92	0	0	501.30	567.0	94	0	0	653.34	652.7
47	0	0	14.58	6.2	94	0	0	512.44	579.6	96	0	0	667.68	667.0
48	0	0	14.58	6.2	96	0	0	523.58	592.2	98	0	0	682.02	681.3
49	0	0	14.58	6.2	98	0	0	534.72	604.8	100	0	0	696.36	695.7
50	0	0	14.58	6.2	100	0	0	545.86	617.4	102	0	0	710.70	709.9
51	0	0	14.58	6.2	102	0	0	557.00	630.0	104	0	0	725.04	724.3
52	0	0	14.58	6.2	104	0	0	568.14	642.6	106	0	0	739.38	738.7
53	0	0	14.58	6.2	106	0	0	579.28	655.2	108	0	0	753.72	753.0
54	0	0	14.58	6.2	108	0	0	590.42	667.8	110	0	0	768.06	767.3
55	0	0	14.58	6.2	110	0	0	601.56	680.4	112	0	0	782.40	781.7
56	0	0	14.58	6.2	112	0	0	612.70	693.0	114	0	0	796.74	796.0
57	0	0	14.58	6.2	114	0	0	623.84	705.6	116	0	0	811.08	810.3
58	0	0	14.58	6.2	116	0	0	634.98	718.2	118	0	0	825.42	824.7
59	0	0	14.58	6.2	118	0	0	646.12	730.8	120	0	0	839.76	839.0
60	0	0	14.58	6.2	120	0	0	657.26	743.4	122	0	0	854.10	853.3
61	0	0	14.58	6.2	122	0	0	668.40	756.0	124	0	0	868.44	867.7
62	0	0	14.58	6.2	124	0	0	679.54	768.6	126	0	0	882.78	882.0
63	0	0	14.58	6.2	126	0	0	690.68	781.2	128	0	0	897.12	896.3
64	0	0	14.58	6.2	128	0	0	701.82	793.8	130	0	0	911.46	910.7
65	0	0	14.58	6.2	130	0	0	712.96	806.4	132	0	0	925.80	925.0
66	0	0	14.58	6.2	132	0	0	724.10	819.0	134	0	0	940.14	939.3
67	0	0	14.58	6.2	134	0	0	735.24	831.6	136	0	0	954.48	953.7
68	0	0	14.58	6.2	136	0	0	746.38	844.2	138	0	0	968.82	968.0
69	0	0	14.58	6.2	138	0	0	757.52	856.8	140	0	0	983.16	982.3
70	0	0	14.58	6.2	140	0	0	768.66	869.4	142	0	0	997.50	996.7
71	0	0	14.58	6.2	142	0	0	779.80	882.0	144	0	0	1011.84	1011.0
72	0	0	14.58	6.2	144	0	0	790.94	894.6	146	0	0	1026.18	1025.3
73	0	0	14.58	6.2	146	0	0	802.08	907.2	148	0	0	1040.52	1039.7
74	0	0	14.58	6.2	148	0	0	813.22	919.8	150	0	0	1054.86	1054.0
75	0	0	14.58	6.2	150	0	0	824.36	932.4	152	0	0	1069.20	1068.3
76	0	0	14.58	6.2	152	0	0	835.50	945.0	154	0	0	1083.54	1082.7
77	0	0	14.58	6.2	154	0	0	846.64	957.6	156	0	0	1097.88	1097.0
78	0	0	14.58	6.2	156	0	0	857.78	970.2	158	0	0	1112.22	1111.3
79	0	0	14.58	6.2	158	0	0	868.92	982.8	160	0	0	1126.56	1125.7
80	0	0	14.58	6.2	160	0	0	880.06	995.4	162	0	0	1140.90	1140.0
81	0	0	14.58	6.2	162	0	0	891.20	1008.0	164	0	0	1155.24	1154.3
82	0	0	14.58	6.2	164	0	0	902.34	1020.6	166	0	0	1169.58	1168.7
83	0	0	14.58	6.2	166	0	0	913.48	1033.2	168	0	0	1183.92	1183.0
84	0	0	14.58	6.2	168	0	0	924.62	1045.8	170	0	0	1198.26	1197.3
85	0	0	14.58	6.2	170	0	0	935.76	1058.4	172	0	0	1212.60	1211.7
86	0	0	14.58	6.2	172	0	0	946.90	1071.0	174	0	0	1226.94	1226.0
87	0	0	14.58	6.2	174	0	0	958.04	1083.6	176	0	0	1241.28	1240.3
88	0	0	14.58	6.2	176	0	0	969.18	1096.2	178	0	0	1255.62	1254.7
89	0	0	14.58	6.2	178	0	0	980.32	1108.8	180	0	0	1270.00	1269.0
90	0	0	14.58	6.2	180	0	0	991.46	1121.4	182	0	0	1284.34	1283.3
91	0	0	14.58	6.2	182	0	0	1002.60	1134.0	184	0	0	1298.68	1297.7
92	0	0	14.58	6.2	184	0	0	1013.74	1146.6	186	0	0	1313.02	1312.0
93	0	0	14.58	6.2	186	0	0	1024.88	1159.2	188	0	0	1327.36	1326.3
94	0	0	14.58	6.2	188	0	0	1036.02	1171.8	190	0	0	1341.70	1340.7
95	0	0	14.58	6.2	190	0	0	1047.16	1184.4	192	0	0	1356.04	1355.0
96	0	0	14.58	6.2	192	0	0	1058.30	1197.0	194	0	0	1370.38	1369.3
97	0	0	14.58	6.2	194	0	0	1069.44	1209.6	196	0	0	1384.72	1383.7
98	0	0	14.58	6.2	196	0	0	1080.58	1222.2	198	0	0	1399.06	1398.0
99	0	0	14.58	6.2	198	0								

Table V. Intramolecular Bond Distances<sup>a</sup> (in Å) of  
Methyl Pheophorbide.

<u>Atoms</u>	<u>Distance</u>	<u>Atoms</u>	<u>Distance</u>
N(1)-C(1)	1.364(8)	C(11)-C(12)	1.392(8)
N(1)-C(4)	1.372(8)	C(12)-C(13)	1.398(8)
N(2)-C(6)	1.348(8)	C(12)-C(27)	1.528(8)
N(2)-C(9)	1.373(8)	C(13)-C(14)	1.404(7)
N(3)-C(11)	1.394(8)	C(13)-C(28)	1.431(8)
N(3)-C(14)	1.328(7)	C(14)-C(15)	1.388(8)
N(4)-C(16)	1.347(8)	C(15)-C(16)	1.390(7)
N(4)-C(19)	1.340(8)	C(15)-C(29)	1.526(7)
C(1)-C(2)	1.448(7)	C(16)-C(17)	1.492(8)
C(1)-C(20)	1.381(8)	C(17)-C(18)	1.551(7)
C(2)-C(3)	1.353(8)	C(17)-C(30)	1.550(8)
C(2)-C(21)	1.482(9)	C(18)-C(19)	1.490(8)
C(3)-C(4)	1.459(7)	C(18)-C(32)	1.515(10)
C(3)-C(22)	1.472(9)	C(19)-C(20)	1.408(7)
C(4)-C(5)	1.371(8)	C(22)-C(23)	1.225(13)
C(5)-C(6)	1.412(8)	C(25)-C(26)	1.469(14)
C(6)-C(7)	1.429(9)	C(28)-C(29)	1.580(8)
C(7)-C(8)	1.361(10)	C(28)-O(1)	1.211(7)
C(7)-C(24)	1.496(10)	C(29)-C(33)	1.490(9)
C(8)-C(9)	1.453(9)	C(30)-C(31)	1.503(10)
C(8)-C(25)	1.511(10)	C(31)-C(35)	1.471(11)
C(9)-C(10)	1.376(8)	C(33)-O(2)	1.203(9)
C(10)-C(11)	1.404(9)	C(33)-O(3)	1.318(8)

C(34)-O(3)	1.469(10)	C(24)-H(3)C(24)	1.05(10)
C(35)-O(4)	1.187(11)	C(25)-H(1)C(25)	1.00
C(35)-O(5)	1.315(10)	C(25)-H(2)C(25)	1.00
C(36)-O(5)	1.491(12)	C(26)-H(1)C(26)	1.12(9)
N(1)-H(1)N(1)	0.78(9)	C(26)-H(2)C(26)	1.00
N(2)-H(1)N(2)	0.62(10)	C(26)-H(3)C(26)	1.00
N(3)-H(1)N(3)	0.90(9)	C(27)-H(1)C(27)	1.00
N(4)-H(1)N(4)	0.51(11)	C(27)-H(2)C(27)	1.00
C(5)-H(1)C(5)	1.00	C(27)-H(3)C(27)	1.00
C(10)-H(1)C(10)	1.01(5)	C(29)-H(1)C(29)	1.00
C(17)-H(1)C(17)	0.87(5)	C(30)-H(1)C(30)	1.07(9)
C(18)-H(1)C(18)	0.94(5)	C(30)-H(2)C(30)	0.93(8)
C(20)-H(1)C(20)	0.93(5)	C(31)-H(1)C(31)	0.69(9)
C(21)-H(1)C(21)	1.01(7)	C(31)-H(2)C(31)	1.21(9)
C(21)-H(2)C(21)	0.85(7)	C(32)-H(1)C(32)	1.05(6)
C(21)-H(3)C(21)	1.04(6)	C(32)-H(2)C(32)	0.77(6)
C(22)-H(1)C(22)	1.24(5)	C(32)-H(3)C(32)	1.05(6)
C(23)-H(1)C(23)	1.00	C(34)-H(1)C(34)	0.97(13)
C(23)-H(2)C(23)	1.00	C(34)-H(2)C(34)	1.00
C(24)-H(1)C(24)	1.00	C(34)-H(3)C(34)	1.00
C(24)-H(2)C(24)	1.00		

<sup>a</sup>For those distances which are listed without esd's,  
the distance was held fixed.

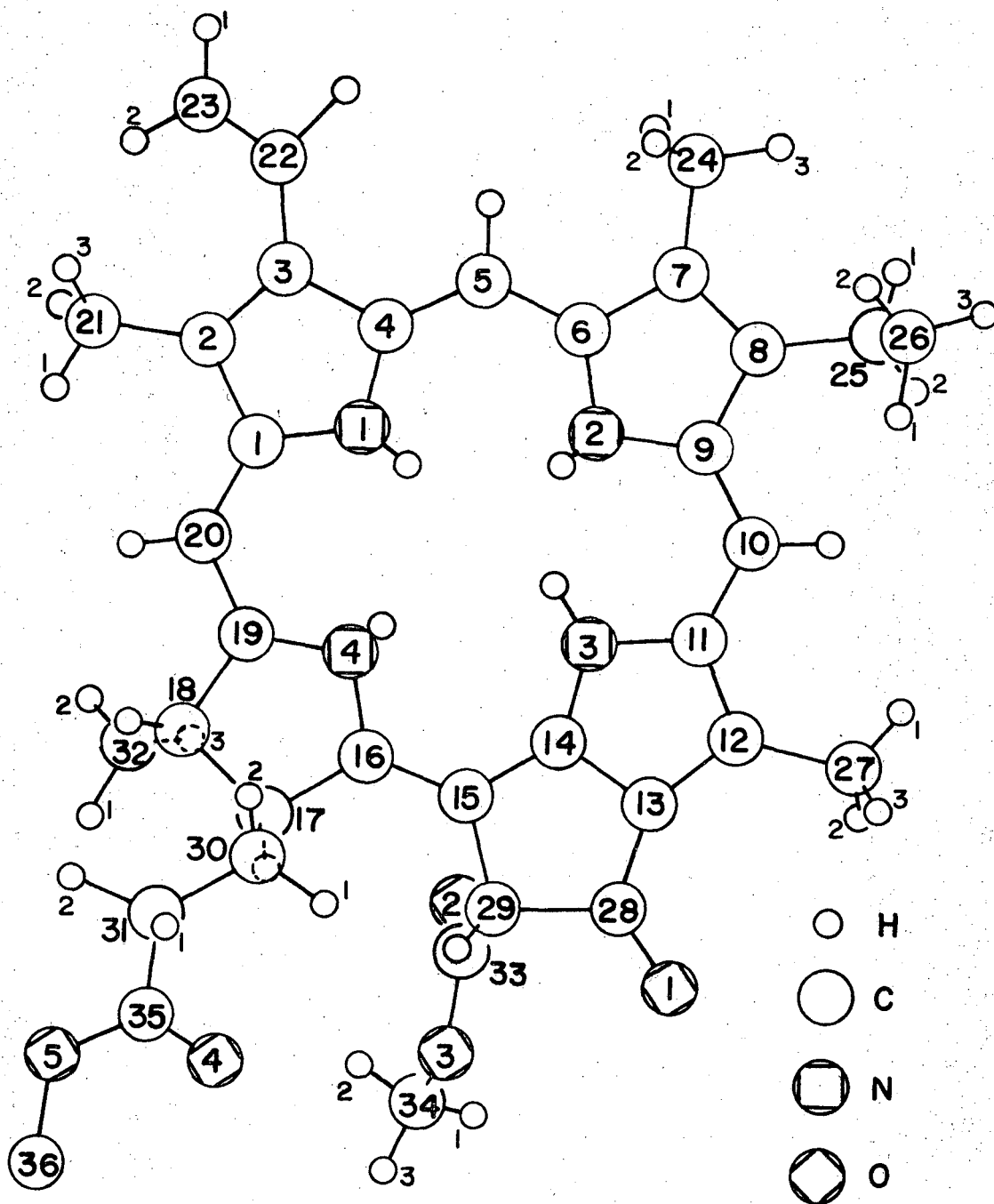
Table VI. Intramolecular Bond Angles (in Degrees) of  
Methyl Pheophorbide<sup>a</sup>.

<u>Atoms</u>	<u>Angle</u>	<u>Atoms</u>	<u>Angle</u>
C(1)-N(1)-C(4)	110.5	C(7)-C(8)-C(9)	106.6
C(6)-N(2)-C(9)	106.3	C(7)-C(8)-C(25)	128.7
C(11)-N(3)-C(14)	108.9	C(9)-C(8)-C(25)	124.7
C(16)-N(4)-C(19)	108.2	N(2)-C(9)-C(8)	109.3
N(1)-C(1)-C(2)	107.8	N(2)-C(9)-C(10)	125.0
N(1)-C(1)-C(20)	125.2	C(8)-C(9)-C(10)	125.7
C(2)-C(1)-C(20)	127.0	C(9)-C(10)-C(11)	125.2
C(1)-C(2)-C(3)	106.9	N(3)-C(11)-C(10)	121.1
C(1)-C(2)-C(21)	124.7	N(3)-C(11)-C(12)	107.8
C(3)-C(2)-C(21)	128.4	C(10)-C(11)-C(12)	131.1
C(2)-C(3)-C(4)	108.9	C(11)-C(12)-C(13)	107.0
C(2)-C(3)-C(22)	128.6	C(11)-C(12)-C(27)	126.1
C(4)-C(3)-C(22)	122.5	C(13)-C(12)-C(27)	126.9
N(1)-C(4)-C(3)	105.9	C(12)-C(13)-C(14)	107.0
N(1)-C(4)-C(5)	127.4	C(12)-C(13)-C(28)	144.0
C(3)-C(4)-C(5)	126.7	C(14)-C(13)-C(28)	109.0
C(4)-C(5)-C(6)	128.8	N(3)-C(14)-C(13)	109.3
N(2)-C(6)-C(5)	124.8	N(3)-C(14)-C(15)	136.2
N(2)-C(6)-C(7)	111.4	C(13)-C(14)-C(15)	114.5
C(5)-C(6)-C(7)	123.7	C(14)-C(15)-C(16)	127.2
C(6)-C(7)-C(8)	106.4	C(14)-C(15)-C(29)	106.4
C(6)-C(7)-C(24)	127.0	C(16)-C(15)-C(29)	126.5
C(8)-C(7)-C(24)	126.6	N(4)-C(16)-C(15)	120.5

N(4)-C(16)-C(17)	112.7	C(13)-C(28)-O(1)	130.4
C(15)-C(16)-C(17)	126.7	C(29)-C(28)-O(1)	123.5
C(16)-C(17)-C(18)	101.6	C(15)-C(29)-C(28)	103.9
C(16)-C(17)-C(30)	110.8	C(15)-C(29)-C(33)	112.2
C(18)-C(17)-C(30)	111.9	C(28)-C(29)-C(33)	107.4
C(17)-C(18)-C(19)	101.4	C(17)-C(30)-C(31)	115.6
C(17)-C(18)-C(32)	112.6	C(30)-C(31)-C(35)	113.8
C(19)-C(18)-C(32)	112.6	C(29)-C(33)-O(2)	125.2
N(4)-C(19)-C(18)	113.6	C(29)-C(33)-O(3)	112.1
N(4)-C(19)-C(20)	123.3	O(2)-C(33)-O(3)	122.6
C(18)-C(19)-C(20)	123.1	C(31)-C(35)-O(4)	126.6
C(1)-C(20)-C(19)	128.8	C(31)-C(35)-O(5)	112.5
C(3)-C(22)-C(23)	126.2	O(4)-C(35)-O(5)	120.9
C(8)-C(25)-C(26)	111.7	C(33)-O(3)-C(34)	115.3
C(13)-C(28)-C(29)	106.1	C(35)-O(5)-C(36)	117.6

<sup>a</sup> Standard deviations are 0.7-0.9° for those angles involving atoms C(23), C(26), O(4) or O(5); for the other angles the esd's are 0.4-0.6°.

Figure 2. Numbering scheme for methyl pheophorbide a. Hydrogen atoms are numbered by the atoms to which they are attached.

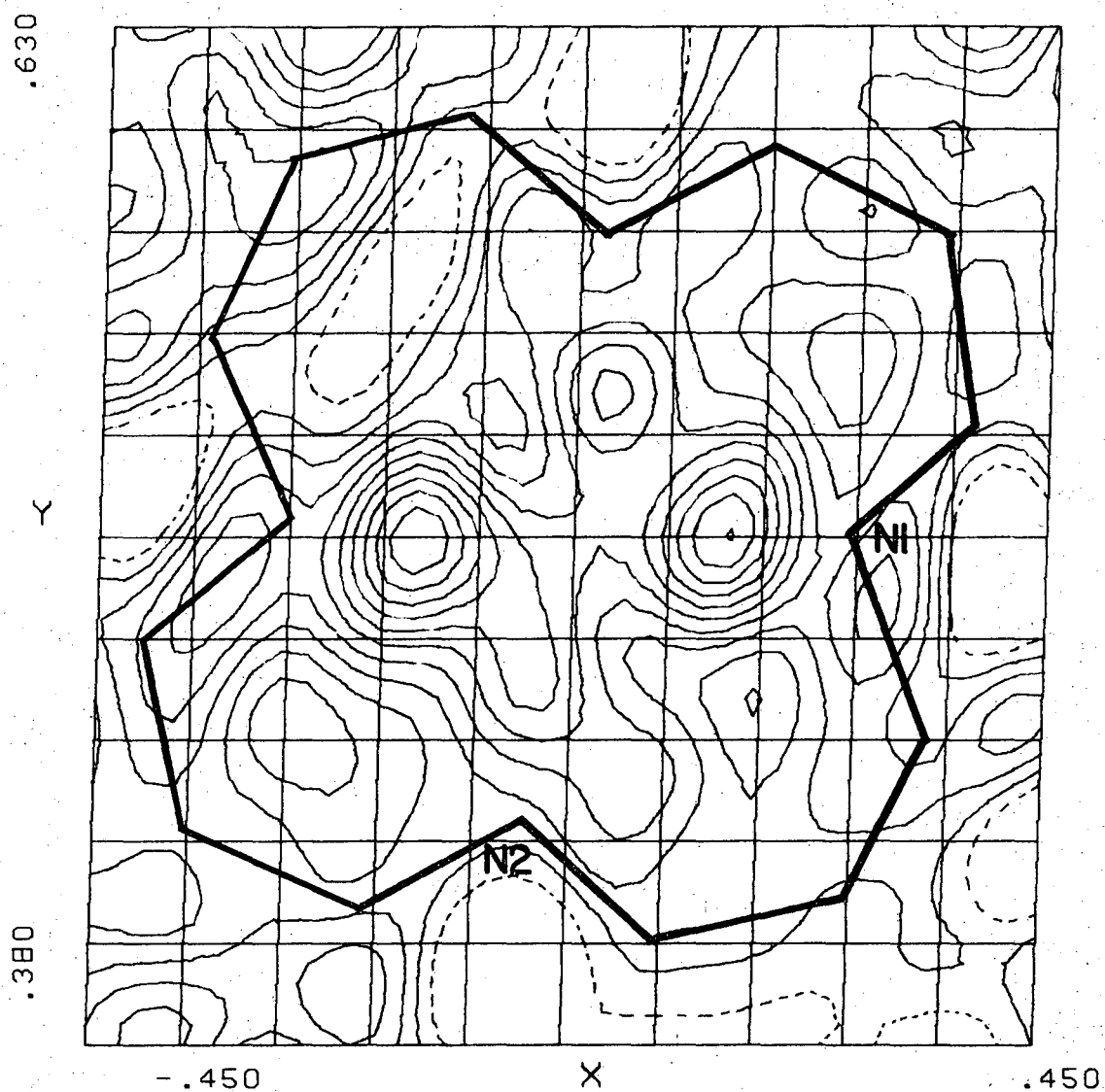


As a final check on the positions of the four inner pyrrole half-hydrogen atoms, we eliminated them from the calculation and refined only the four pyrrole nitrogen atoms. The difference Fourier map in the center of the molecule, calculated with only those data whose  $\sin\theta/\lambda \leq 0.47$  and shown in Figure 3, agreed closely with the results obtained at an earlier stage of the refinement. Four peaks were present, and peak heights adjacent to the nitrogen atoms of Rings I and III were approximately twice as high as those adjacent to Rings II and IV.

The atomic positions of the last cycle were employed in a check of anomalous dispersion<sup>19</sup>. The intensities of the 3214 unaveraged  $hkl$  and  $\bar{h}\bar{k}\bar{l}$  were used in this calculation. The calculated effects were too small compared to the errors in the data to permit an unambiguous assignment of absolute configuration, but there was slightly better agreement with the handedness proposed by Fleming<sup>23</sup> than with the reverse one. Fleming's configuration is used in all Tables and Figures.

In retrospect, we examined the 24 proposed atomic positions of the initial trial structure which led to the correct structure. The distance between the center of the proposed and actual molecules was 0.21 Å and the angle between the two molecules was  $\sim 10^\circ$ . The shortest interatomic distances between atoms of the proposed and actual structures were 0.17 and 0.21 Å while the longest and rms distances were 0.74 and 0.48 Å.

Figure 3. Difference Fourier in the chlorin plane of methyl pheophorbide. Positive contours are indicated by solid thin lines and zero contours by dotted lines. The contour interval is  $0.0243 \text{ e } \text{\AA}^{-3}$ . The solid heavy lines designate intramolecular bonds involving the pyrrole nitrogen and methine carbon atoms.



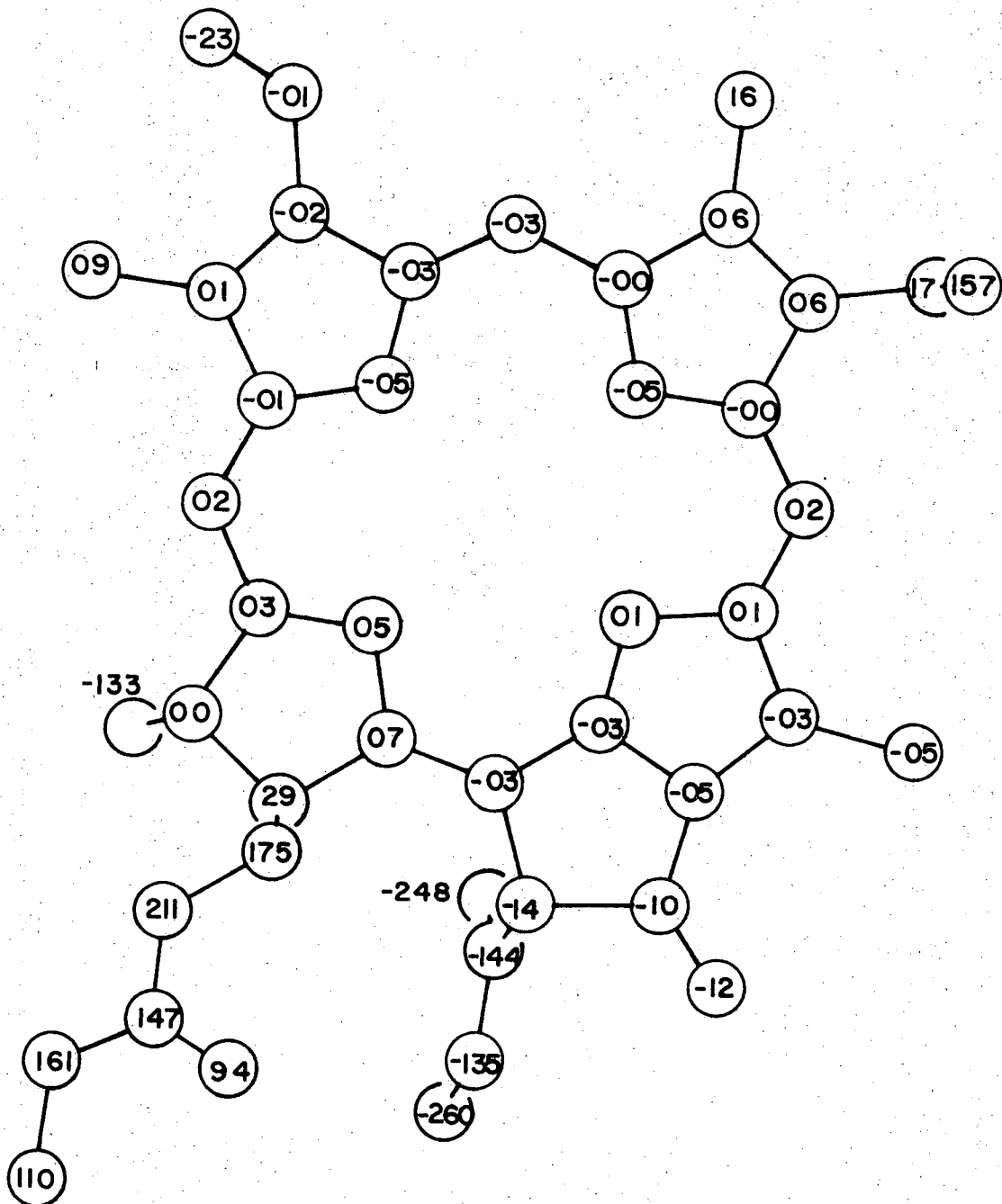


### Molecular Structure

The chlorin ring is nearly flat although the departures from planarity are statistically significant. The deviations from the least squares plane through atoms N(1) - N(4), C(1) - C(16), and C(19) and C(20) are presented in Figure 4. (This plane is called the chlorin plane in later discussions.) Rings I, II, and III are each planar to within 0.01 Å and Ring V is planar to within 0.02 Å. Ring IV is not planar. In Ring IV, atoms C(17) and C(18) are, respectively, 0.22 Å above and 0.04 Å below the least squares plane through atoms N(4), C(16), and C(19). This chlorin conformation is similar to that found in the phyllochlorin ester<sup>8</sup>. Relative to the plane through the nitrogen atoms (itself planar to within 0.01 Å), Rings I and II are tipped up, while Rings III, IV, and V are tipped down.

The inner hydrogen atoms of the triclinic modification of tetraphenylporphine<sup>3</sup> (tri-TPP) are on diagonally opposite pyrrole rings and repel each other. The repulsion is manifested in a diagonal N...N distance of 4.20 Å for the nitrogen atoms which contain hydrogen atoms. This distance is 0.14 Å larger than the diagonal N...N distance for those nitrogen atoms which do not contain hydrogen atoms. In the MePPb, although the electron density at sites H(1)N(1) and H(1)N(3) is greater than at sites H(1)N(2) and H(1)N(4) (see Figure 3), the N(1)...N(3) distance of 4.06 Å is considerably shorter than the N(2)...N(4) distance of 4.23 Å.

Figure 4. Deviations ( $\times 100$  in  $\text{\AA}$ ) from the least squares plane through atoms N(1) - N(4), C(1) - C(16), C(19) and C(20).



We conclude that the distortion is due to some other factor, most likely the presence of the fifth isocyclic ring. In the VO-DPEP structure<sup>9</sup>, the analogous distances are 3.96 Å and 4.08 Å.

The C(17)-C(18) bond length of  $1.551 \pm 0.007$  in MePPb, compared with  $1.34 \pm 0.02$  Å in the porphyrin VO-DPEP<sup>9</sup>, exhibits the single-bond character which distinguishes a chlorin from a porphyrin. Correspondingly the C(16)-C(17)-C(18) and C(17)-C(18)-C(19) angles are decreased from an average of  $107 \pm 3^\circ$  in VO-DPEP to an average of  $101.5 \pm 0.5^\circ$  in MePPb. The C(16)-C(17) and C(18)-C(19) bond distances are increased from 1.43 and 1.46 Å, each  $\pm 0.02$ , to respectively 1.492 and 1.490, each  $\pm 0.008$ . Since Ring V contains a  $\beta$ -keto ester, we examined the Ring V bond distances to determine the amount of keto-enol tautomerism. The short C-O distance ( $1.211 \pm .007$  Å) and the long C-C distance ( $1.580 \pm .008$  Å) preclude the possibility of much tautomerism. Thus our results are in agreement with the results obtained from infrared absorption<sup>24</sup>.

The C(13)-C(28) bond distance of  $1.431 \pm 0.008$  Å is smaller than the  $1.526 \pm 0.007$  Å distance for bond C(15)-C(29). We have concluded that the ketone carbonyl is in conjugation with the chlorin ring system.

The vinyl group on Ring I is also in conjugation with the main chlorin ring. The C(3)-C(22) bond length of  $1.472 \pm 0.009$  Å in MePPb is considerably shorter than the  $1.56 \pm 0.02$  Å distance for a similar bond in VO-DPEP<sup>9</sup>, which links an ethyl group to Ring I.

There is considerable steric hinderance between that vinyl group in MePPb and the methyl group also attached to Ring I. Not only is the vinyl group shifted out of the chlorin plane by  $14^\circ$ , but the three angles C(3)-C(2)-C(21), C(2)-C(3)-C(22), and C(3)-C(22)-C(23) are also increased in such a way as to increase the distance between methyl carbon C(21) and C(23) of the vinyl group. Thus angle C(3)-C(2)-C(21) =  $128.4^\circ$  is greater than angle C(1)-C(2)-C(21) =  $124.7^\circ$ ; angle C(2)-C(3)-C(22) =  $128.6^\circ$  is greater than angle C(4)-C(3)-C(22) =  $122.5^\circ$ ; and the  $126.2^\circ$  angle for C(3)-C(22)-C(23) is approximately four degrees larger than the comparable angle in buta-1,3-diene<sup>25</sup>. The non-planarity and angular distortions increase the C(21)···H(2)C(23) distance from  $\sim 2.1 \text{ \AA}$  to the  $2.43 \text{ \AA}$  value which is observed.

The Ring II ethyl and Ring V carboxyl groups are oriented in such a way as to minimize intramolecular repulsion. The plane through atom C(8) and the ethyl group is perpendicular to the plane through Ring II to within the experimental error. The orientation coplanar with Ring II would be energetically unfavorable because of the strong repulsion between atom C(26) and either H(1)C(10) or C(24). The least-squares plane through the carboxyl group off Ring V intersects the Ring V plane at an angle of  $80^\circ$ . A much smaller intersection angle is not allowed because of the potential interatomic repulsion between atoms H(1)C(17) and either atoms O(2) or O(3).

### Molecular Dimensions

To compare the dimensions of this molecule with those of porphyrin derivatives, we averaged the bond parameters of MePPb and of tri-TPP<sup>3</sup> in accordance with  $C_{4v}$  ( $4mm$ ) symmetry. Their averaged bond parameters are listed in Table VII. The  $\alpha$ ,  $\beta$  and  $m$  notations designate the  $\alpha$ - and  $\beta$ - pyrrole carbon atoms and the methine carbon atom. With the exclusion of the saturated bond C(17)-C(18) of Ring IV, the two average geometries are the same within the experimental precisions. However, the spread of values in MePPb is three times that of tri-TPP even though the uncertainties are only  $1\frac{1}{2}$  times as great.

On closer inspection, the variability of the bond distances is not random but is systematic. We postulate that the variability is the result of the unequal contribution of three main resonance structures which is in turn caused by the presence of both the saturated C(17)-C(18) bond and the side groups conjugated to the chlorin ring.

Three unionized Kekule structures of the chlorin ring of methyl pheophorbide a with diagonally opposite hydrogen atoms may be described according to the valence-bond technique of Pauling<sup>25</sup> (Figure 1). Two contain inner hydrogen atoms on Rings I and III whereas one contains the hydrogen atoms on Rings II and IV. If we consider, first, the  $C_{\alpha}-C_{\beta}$  and  $C_{\beta}-C_{\beta}$  type bonds of the pyrrole rings, we see that the pyrrole groups in structures Ia, Ib and II of Figure 1 differ, i.e. structure Ia has similar rings II and III, structure Ib

Table VII. Average Bond Distances of Methyl Pheophorbide and the Triclinic Modification of Tetraphenylporphin<sup>a</sup>.

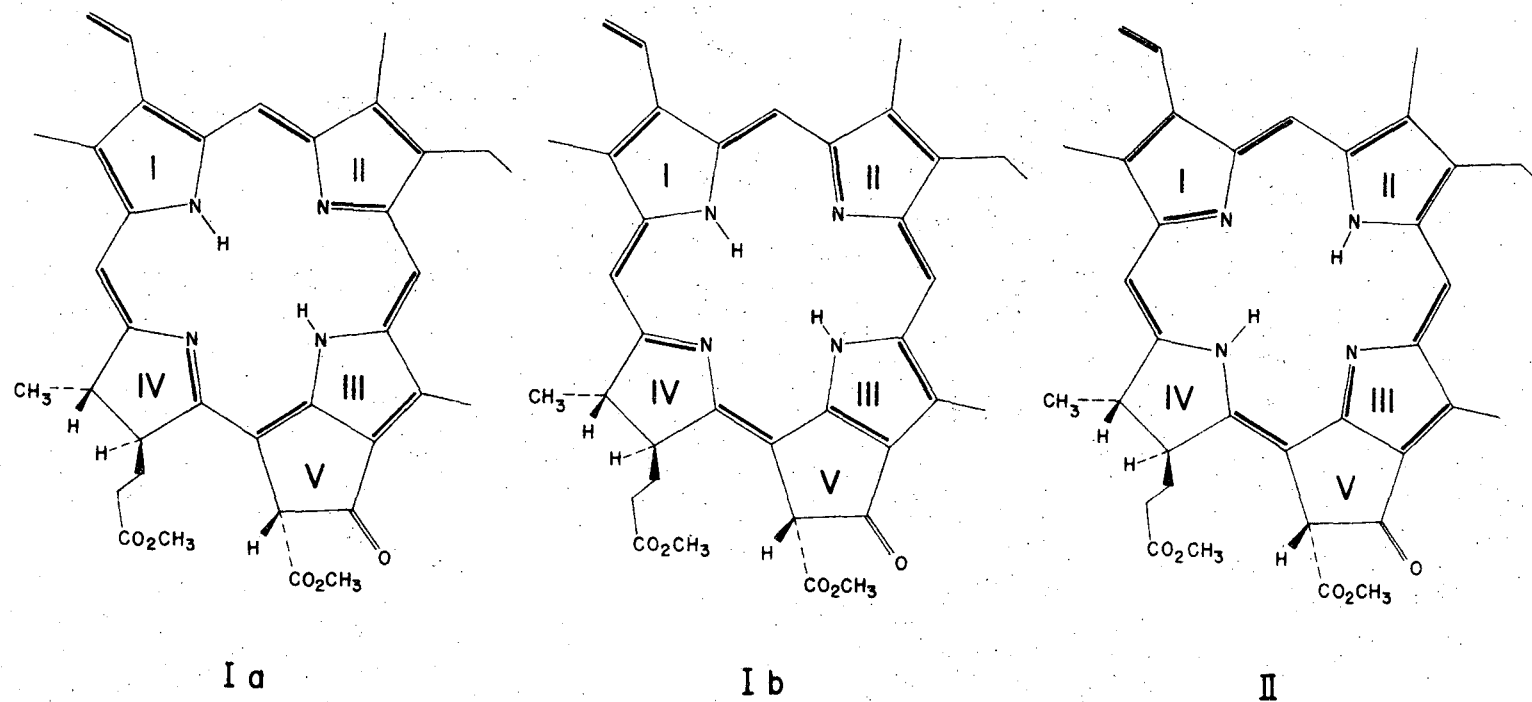
<u>Bond or Angle</u> <sup>b</sup>	<u>Methyl Pheophorbide</u>	<u>Tetraphenylporphin</u>
N-C <sub>α</sub>	1.358 ± 0.021 Å	1.369 ± 0.007 Å
C <sub>α</sub> -C <sub>β</sub>	1.446 ± 0.033	1.441 ± 0.015
C <sub>β</sub> -C <sub>β</sub>	1.371 ± 0.024 <sup>c</sup>	1.353 ± 0.006
C <sub>α</sub> -C <sub>m</sub>	1.391 ± 0.015	1.399 ± 0.006
C <sub>α</sub> -N-C <sub>α</sub>	108.5 ± 1.7 °	107.7 ± 1.5 °
N-C <sub>α</sub> -C <sub>β</sub>	109.7 ± 2.7	108.8 ± 1.4
N-C <sub>α</sub> -C <sub>m</sub>	125.4 ± 4.9	126.1 ± 0.6
C <sub>β</sub> -C <sub>α</sub> -C <sub>m</sub>	124.8 ± 4.8	125.0 ± 1.8
C <sub>α</sub> -C <sub>β</sub> -C <sub>β</sub>	107.1 ± 0.9 <sup>c</sup>	107.4 ± 0.5
C <sub>α</sub> -C <sub>m</sub> -C <sub>α</sub>	127.5 ± 1.7	125.6 ± 0.4

<sup>a</sup> Derived from Reference 3.

<sup>b</sup> The α, β and m designate the α- and β- pyrrole carbon atoms and the methine carbon atom.

<sup>c</sup> Does not include bond C(17)-C(18).

Figure 1. Three resonance structures of methyl pheophorbide a.



XBL 696-727

has similar rings I and II, and structure II has similar rings I and III. If we examine the bond lengths of Table V in detail, the  $C_{\alpha}-C_{\beta}$  and  $C_{\beta}-C_{\beta}$  bonds unequivocally correspond to valence bond structure Ib. Considering the  $C_{\alpha}-C_m$  bonds, the bond distances conform more to structure Ib than to any other single structure of Figure 1, although there is some evidence of a contribution of Ia in the shortening of bond C(14)-C(15). The shortest N-C bond length is N(3)-C(14) which can be contributed only from VB structure II, and bond N(1)-C(1) is shorter than bond N(1)-C(4), which can occur only from structure II. Otherwise, the C-N bond lengths conform more to Ib than to any other.

The distribution of inner hydrogen atoms most consistent with the unequal contribution of resonance structures of Figure 3 is their predominant localization on Rings I and III. Examples already exist for both ordered and disordered pyrrole atoms. Among porphyrin and phthalocyanin structures tri-TPP<sup>3</sup> has inner hydrogen atoms localized on just two diagonally opposite nitrogen atoms while phthalocyanin<sup>27</sup>, tetragonal-TPP<sup>4</sup> and porphin<sup>2</sup> all have four disordered half-hydrogen atoms. Our electron density results correspond to hydrogen atoms on all four rings, but with an excess on Rings I and III.

Nuclear magnetic resonance studies of several symmetrical porphyrins<sup>28</sup> have shown that the ring currents and presumably the shapes of all four pyrrole groups are identical. This implies



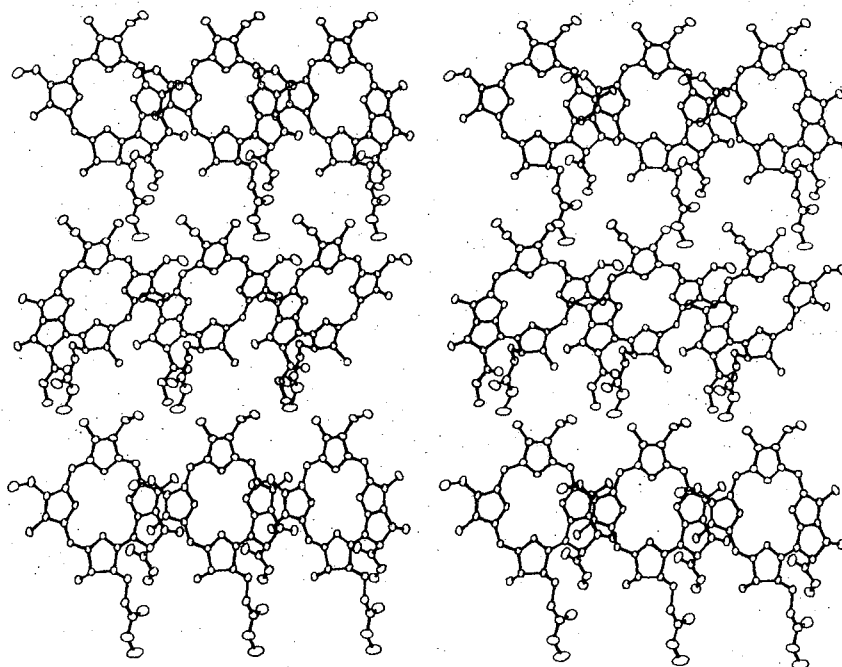
that the hydrogen atoms are not localized when the porphyrins are in solution. Katz and coworkers, in their n.m.r. study<sup>29</sup> of chlorophyll and its derivatives, found two distinct peaks for the two inner hydrogen atoms of methyl pheophorbide. Since no two pyrrole groups<sup>are</sup> chemically equivalent, we conclude that the hydrogen atoms of chlorophyll in solution are localized on two nitrogen atoms. We would expect from steric considerations that the hydrogens would lie on diagonally opposite nitrogen atoms. The molecular orbital calculations of Weiss, Gouterman and Kobayashi<sup>30</sup> have predicted that they will lie on pyrrole Rings I and III.

### Packing

The molecules pack in sheets nearly perpendicular to the ac plane with all of the molecules related by translations within the sheet. The angle between the normal to the plane through the chlorin ring and the normal to the ac plane is  $74^\circ$ . The intermolecular spacings to the adjacent parallel molecules at positions  $1+x$ ,  $y$ ,  $z$  and  $1+x$ ,  $y$ ,  $1+z$  are  $3.492 \text{ \AA}$  and  $3.525 \text{ \AA}$ . These distances are somewhat larger than the intermolecular spacings of  $3.43 \text{ \AA}$  and  $3.39 \text{ \AA}$  for porphin<sup>2</sup> and methoxyiron(III)mesoporphyrin-IX-dimethyl ester<sup>31</sup> and are a consequence of the lack of chlorin-chlorin attractive interaction. There are no chlorin-chlorin intermolecular distances less than  $3.5 \text{ \AA}$ , and the side groups, many of which are not coplanar with the chlorin ring, determine the interplanar spacings. There is one contact between atom H(2)C(23) of the molecule at position  $x$ ,  $y$ ,  $z$  and C(27) of the molecule at  $2+x$ ,  $y$ ,  $1+z$ .

The intermolecular angle between the molecules in one sheet and those in the adjacent sheets, which are related by the screw axis symmetry element, is  $32^\circ$ . The ethyl, the C(32) methyl and both ester groups are all in the region between the sheets, whereas the other side groups are between molecules within a sheet. A view of the packing as seen down the reciprocal c axis is shown in Figure 5. The intermolecular bond distances are presented in Table VIII.

Figure 5. Stereoscopic view of two screw-axis-related methyl pheophorbide molecules and neighboring molecules related to them by translations in  $x$  and  $y$ .



XBL 698-1331

Table VIII. Intermolecular Spacings Less than 3.5 Å for C...C  
and C...N Approaches and Less than 3.0 Å for C...H Approaches.

<sup>a</sup> The equivalent position numbers are 1 for  $x$ ,  $y$ ,  $z$   
and 2 for  $-x$ ,  $-y$ ,  $-z$ .

Atom 1	Atom 2	Distance	Position Number	Atom 2: Translations in		
			of Atom 2 <sup>a</sup>	x	y	z
N(1)	H(2)C(27)	2.94	1	1	0	1
N(2)	C(23)	3.460	1	$\bar{1}$	0	0
N(3)	H(3)C(21)	2.82	1	$\bar{1}$	0	$\bar{1}$
	C(21)	3.473	1	$\bar{1}$	0	$\bar{1}$
C(1)	H(2)C(27)	2.95	1	1	0	1
C(26)	H(3)C(34)	2.75	2	$\bar{1}$	$\bar{1}$	1
	O(4)	3.434	2	$\bar{1}$	$\bar{1}$	1
C(27)	H(2)C(23)	2.91	1	$\bar{2}$	0	$\bar{1}$
C(30)	O(1)	3.329	1	1	0	1
C(31)	O(1)	3.427	1	1	0	1
C(34)	H(2)C(31)	2.87	1	$\bar{1}$	0	$\bar{1}$
C(36)	H(2)C(24)	2.81	2	0	0	$\bar{2}$
	H(1)C(23)	2.92	2	1	0	$\bar{2}$
O(1)	H(3)C(32)	2.83	1	$\bar{1}$	0	0
	H(1)C(18)	2.85	1	$\bar{1}$	0	$\bar{1}$
O(2)	H(1)C(20)	2.93	1	$\bar{1}$	0	$\bar{1}$
O(3)	H(2)C(31)	2.76	1	$\bar{1}$	0	$\bar{1}$
O(5)	H(2)C(24)	2.91	2	0	0	2

### Powder Pattern

The powder pattern of methyl pheophorbide was obtained to compare with those of chlorophyll a<sup>32</sup>, chlorophyll b<sup>33</sup>, bactero-chlorophyll<sup>33</sup> and pheophytin and its metal derivatives<sup>34</sup>. The five most intense lines in the powder pattern of MePPb are at d-spacings of 14.28, 3.62, 3.41, 6.67 and 6.17 Å which correspond to the following reflections: 020;  $11\bar{2}$ ,  $10\bar{2}$  and  $23\bar{1}$ ;  $13\bar{2}$  and 012; 120 and 011; and 021 and  $11\bar{1}$ . The powder pattern of MePPb is quite different from those of either the chlorophylls or the pheophytinates. Thus it is likely that the crystalline packing of methyl pheophorbide a is different from any of those mentioned above.

Packing of Chlorophyll in Photosynthetic Lamellae

Steinman<sup>35</sup>, Frey-Wyssling<sup>36</sup>, and Park<sup>37</sup> have demonstrated that the chloroplast membranes are composed of 200 Å units which exist in highly ordered arrays. These particles, called quantasomes, may be the morphological photosynthetic unit<sup>38</sup>. Each quantasome contains approximately 230 chlorophyll molecules<sup>37</sup>. It is generally accepted that the number of energy traps is much less than the number of chlorophyll molecules. Therefore a mechanism for the transfer of energy from one chlorophyll molecule to another is required.

Chlorophyll is very hygroscopic<sup>24</sup>. In fact, the presence of small quantities of water are necessary to form microcrystalline chlorophyll<sup>33</sup>. What is biologically interesting is that chlorophyll·water complexes have a similar electron paramagnetic resonance spectrum to photosynthesizing chloroplasts, whereas anhydrous chlorophyll does not<sup>39</sup>. Previous structural determinations of the molecules of  $\text{MgTPP}\cdot\text{H}_2\text{O}$ <sup>5</sup> and  $\text{MgPc}\cdot\text{H}_2\text{O}\cdot 2\text{C}_5\text{H}_5\text{N}$ <sup>6</sup> lead us to believe that the water molecules are coordinated as a fifth ligand to the central magnesium atom which is 0.3-.05 Å out of the molecular plane. An infrared absorption study of chlorophyll·water aggregates<sup>24</sup> indicates that the water molecule is hydrogen-bonded both to the Ring V ketone carbonyl and to the the O(2) ester carbonyl oxygen atoms of the adjacent molecule. The OH stretch absorption frequencies for the hydrogen atoms of the water molecule

are at  $3240\text{ cm}^{-1}$  for the hydrogen bond involving O(1) and  $3460\text{ cm}^{-1}$  for O(2). We have used a correlation<sup>40</sup> between O-H stretch absorption frequencies and the corresponding O...O distances to estimate that the O(water)...O(1) and O(water)...O(2) distances are 2.78 and 2.89 Å, respectively.

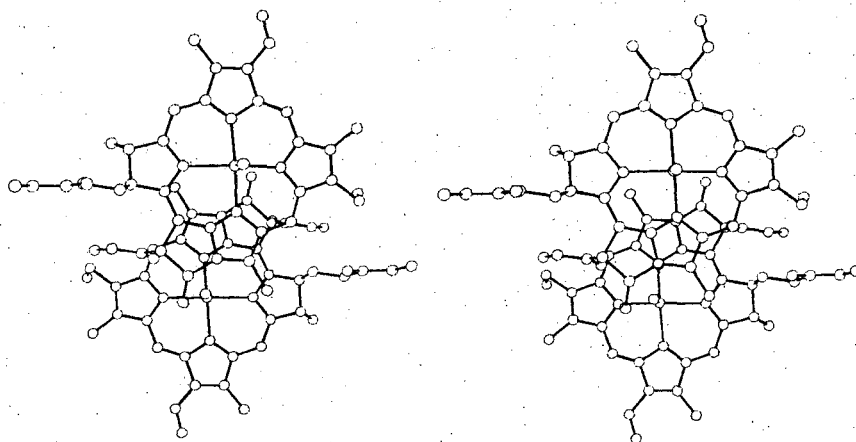
Our molecular model of chlorophyll has dimensions similar to MePPb but with a magnesium atom substituted for the inner hydrogen atoms. We placed the magnesium atom at a distance of 0.50 Å out of the plane and a water molecule 2.02 Å above the magnesium atom. The environment of the magnesium atom was derived from the results of the structural determinations of  $\text{MgPc}\cdot\text{H}_2\text{O}\cdot 2\text{C}_5\text{H}_5\text{N}^6$  and  $\text{MgTPP}\cdot\text{H}_2\text{O}^5$ .

The simplest model for the periodic arrangement of chlorophyll subject to these boundary conditions is one in which adjacent molecules are related by a simple translation. Adjacent molecules are then parallel, and Rings I and III overlap. However, even when the molecules are at their maximum possible interplanar spacing of 5.19 Å, there is considerable crowding between the Ring V carboxyl group of one molecule and Ring I of the other. If the Ring V carboxyl group is rotated around bond C(29)-C(33), considerable intramolecular crowding between atoms O(3) and H(1)C(17) results when the carboxyl group is rotated by more than  $\sim 42^\circ$ . Even in this orientation the intermolecular distance between atom C(34) and atom H(1)C(18) (which is above the ring) is too short. Thus we were induced to eliminate the model involving only translations.

In the second model which we considered, we combined a twofold rotation symmetry element with the translation to form a  $2_1$  screw axis. The  $2_1$  screw axis relates neighboring molecules, which are not necessarily parallel in this model. Now the Rings III and V of one molecule overlap with Rings V and III of an adjacent molecule. One such arrangement of chlorophyll molecules for which the intermolecular contacts are chemically reasonable is shown in Figure 6, a stereoscopic view of a pair of molecules. We have several conclusions about such a dimer: 1) The magnesium atom must be substantially out of the chlorin plane to maximize intermolecular spacings between the Ring V carboxyl group and the chlorin ring. It is 0.50 Å out of the plane in this model, a distance identical to that found in aquo-magnesium phthalocyanin.<sup>7</sup> 2) The molecules must be non-parallel to increase the distance between the Ring V carboxyl group and the atoms of Ring II. In our model the interplanar angle is  $14^\circ$ , but orientations with larger interplanar angles cannot be excluded a priori. 3) If the molecules are separated by their maximum possible distance, atom C(27) of one molecule collides with atom C(30) of the adjacent one. This particular intermolecular distance is increased as the intermolecular distance is decreased, subject to the hydrogen-bonding constraints. The decrease in intermolecular distance is limited, however by possible contacts between the Ring V carboxyl group of one molecule



Figure 6. Stereoscopic view of proposed model of a chlorophyll·  
water dimer. Only the first carbon atom of the phytyl group  
is shown.



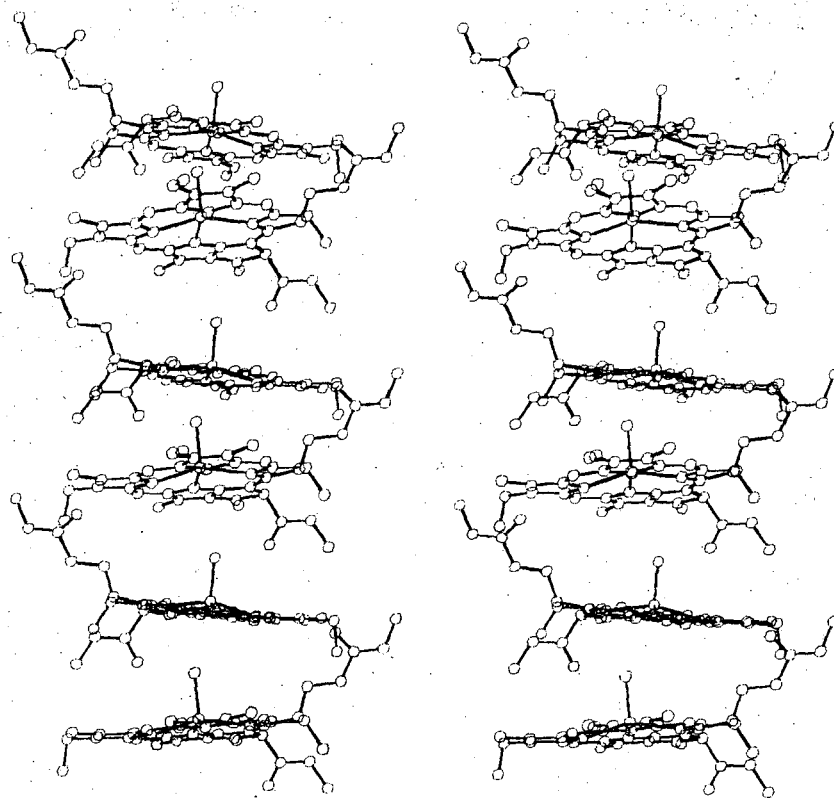
XBL 6910-5917

and Ring II of the other. We have used an interplanar spacing of 5.49 Å, which is half the distance between the  $n$ th and  $(n+2)$ th molecule. This distance is 0.22 Å less than the maximum possible interplanar spacing subject to these constraints. 4) The Ring IV alkyl chain and the ethyl group of Ring II must be rotated from the positions in the crystal structure of methyl pheophorbide to avoid intermolecular collisions.

Nuclear magnetic resonance studies of chlorophyll aggregates<sup>29</sup> have indicated that the major area of overlap involves Rings III and V, although the chemical shift caused by aggregation is very small. Thus our postulated model agrees with the n.m.r. data.

Plant lamellae, when stained with  $\text{KMnO}_4$  and viewed under the electron microscope, exhibit a banded structure<sup>41</sup>. The bands appear to be layers of protein and lipid, and at least the phytyl chain of the chlorophyll molecules may be in the lipid fraction. In their study of the permeability of thin films, Danielli and Davson<sup>42</sup> suggested that membranes are composed of protein molecules which are adsorbed onto a lipid layer. We propose a model (Figure 7) for the aggregation of hydrated chlorophyll molecules within the lipid layer. In this Figure, the phytyl group of chlorophyll has been replaced by a methyl group. The phytyl groups, which radiate out opposite sides of the chlorophyll-water polymer, extend toward the protein bands on each side and are necessary to firmly orient the chlorophyll heads which are in the center.

Figure 7. Stereoscopic view of proposed model of a chlorophyll·  
water polymer which might exist in photosynthetic lamellae. Only  
the first carbon atom of the phytyl group is shown. The region  
on both sides of the depicted polymer contains phytyl chains,  
lipids and , farther out, proteins.



As a variation of the model, the chlorophyll-water polymer could be bent enough to form a circular cover for the quantasome. The phytyl chains would be in one of two possible configurations. In the first, half the phytyl chains would project out from the quantasome and half would project in. In the other possibility, all phytyl chains and some of the lipids would be on the surface of the quantasome. In any of these linear and nonlinear models, the chlorin groups are oriented in such a way that any molecule can absorb a photon and transmit the energy to an adjacent molecule via the water molecule. Energy can be transmitted to the  $O(1)$  carbonyl, which is in resonance with the rest of the chlorin group. In this way, energy can be shuttled until it is trapped in some unique chlorophyll-protein complex.

Anhydrous Chlorophyll Dimers

Houssier and Sauer<sup>43</sup> have studied the circular dichroism (CD) and magnetic circular dichroism (MCD) of anhydrous solutions of chlorophyll a and two of its analogues. One analogue, protochlorophyll a, is unsaturated in bond C(17)-C(18) while the other, pyrochlorophyll a, has no carboxymethyl group attached to Ring V. Houssier and Sauer found that the CD and MCD spectra of dimers of chlorophyll a and of pyrochlorophyll a are similar but that dimer spectra of chlorophyll a and protochlorophyll a are different. Since the CD and MCD spectra are sensitive to the overall geometry of the dimer, they concluded that the carboxymethyl group off Ring V is not involved in stabilizing the dimer but that the carboxyphytyl group is involved. In addition, they accepted the proposal of Katz et al.<sup>29</sup> that there is always a Mg...O(1) interaction in the dimer.

We have used the computer program called ORTEP<sup>16</sup> to investigate possible dimer configurations of chlorophyll and protochlorophyll. The chlorophyll model which we used was derived from the VO-DPEP structure<sup>9</sup>, and the magnesium atom was arbitrarily placed in the plane. Stereoscopic pictures of plausible arrangements of the anhydrous chlorophyll and protochlorophyll dimers, subject to these constraints, are presented in Figures 8 and 9. The interplanar angles are 45° for chlorophyll a and 14° for protochlorophyll a.

Figure 8. Anhydrous chlorophyll dimer<sup>a</sup>.

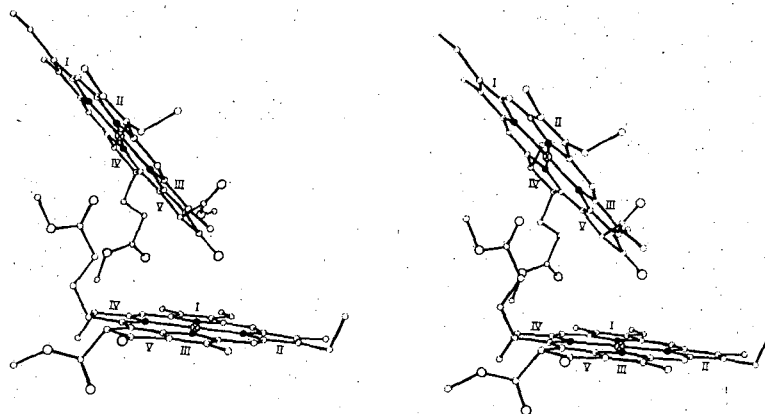
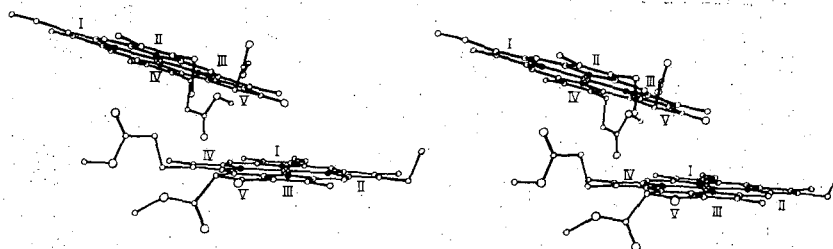


Figure 9. Anhydrous protochlorophyll dimer<sup>a</sup>.



ABL 695-4276

<sup>a</sup> Solid circles, larger circles, and  $\odot$  designate nitrogen atoms, oxygen atoms and magnesium atoms, respectively. The other atoms are carbon.

References

- 2 L. E. Webb and E. B. Fleischer, J. Chem. Phys., 43, 3100 (1965).
- 3 S. J. Silvers and A. Tulinsky, J. Amer. Chem. Soc., 89,  
3331 (1967).
- 4 M. J. Hamor, T. A. Hamor and J. L. Hoard, ibid., 86, 1938 (1964).
- 5 R. Timkovitch and A. Tulinsky, ibid., 91, 4430 (1969).
- 6 J. M. Robertson, J. Chem. Soc., 1195 (1936).
- 7 M. S. Fischer, D. H. Templeton, A. Zalkin and M. Calvin,  
submitted for publication in J. Amer. Chem. Soc.
- 8 W. Hoppe, G. Will, J. Gassmann and H. Weichselgartner, Z.  
Kristallogr., 128, 18 (1969).
- 9 R. C. Pettersen, Acta Cryst., in press.
- 10 H. Fischer and H. Wenderoth, Ann. Chem., 545, 140 (1940).
- 11 R. B. Woodward, Pure Appl. Chem., 2, 383 (1961).
- 12 D. T. Cromer and J. B. Mann, Acta Cryst., A24, 321 (1968).
- 13 R. F. Stewart, E. R. Davidson and W. T. Simpson, J. Chem. Phys.,  
42, 3175 (1965).

- 14 B. G. DeBoer, A. Zalkin and D. H. Templeton, Inorg. Chem., 11, 2288 (1968). In our weight scheme, five percent of the intensity was included in its uncertainty.
- 15 R. E. Long, Ph. D. Thesis, University of California, Los Angeles, Calif., 1965.
- 16 C. K. Johnson, Oak Ridge National Report -- 3794, Revised, Oak Ridge, Tennessee, June, 1965.
- 17 S. La Placa and J. A. Ibers, Acta Cryst., 18, 511 (1965).
- 18 D. W. J. Cruickshank, ibid, 7, 519 (1954).
- 19 The imaginary components  $\Delta f''$  of the anomalous scattering factors for the O, C and N atoms were estimated from the expression of James<sup>20</sup>:  $\Delta f'' = K\mu_a$ , where  $\mu_a$  is the absorption coefficient for that atom and K is constant for the wavelength. The constant  $K = 813 \pm 13$  was calculated from tabulated values of  $\Delta f''$ <sup>21</sup> and  $\mu_a$ <sup>22</sup> for atomic numbers eleven through sixteen and for CuK $\alpha$  radiation. The value of K and the  $\mu_a$  of C, N, and O were used to calculate their  $\Delta f''$  values, which are 0.011, 0.022 and 0.037 e, respectively.
- 20 R. W. James, "The Optical Principles of the Diffraction of X-Rays," Cornell University Press, Ithaca, 1965, p 138.
- 21 D. T. Cromer, Acta Cryst., 18, 17 (1965).
- 22 "International Tables for X-Ray Crystallography," Vol. III. Kynoch Press, Birmingham, England, 1962, p 177.
- 23 I. Fleming, Nature, 216, 151 (1967).



- 24 K. Ballschmiter and J. J. Katz, J. Amer. Chem. Soc., 91, 2661 (1969).
- 25 A. Almendinger, O. Bastiansen and M. Traetteberg, Acta Chem. Scand., 12, 1221 (1958).
- 26 L. Pauling, "The Nature of the Chemical Bond," Third edition, Cornell University Press, Ithaca, 1960, pp 183-220.
- 27 B. F. Hoskins, S. A. Mason and J. C. B. White, Chem. Commun., 554 (1969).
- 28 E. D. Becker, R. B. Bradley and C. J. Watson, J. Amer. Chem. Soc., 83, 3743 (1961).
- 29 G. L. Gloss, J. J. Katz, F. C. Pennington, M. R. Thomas and H. H. Strain, ibid., 85, 3809 (1963).
- 30 C. Weiss, H. Kobayashi and M. Gouterman, J. Mol. Spectrosc., 16, 415 (1965).
- 31 J. L. Hoard, M. J. Hamor, and W. S. Caughey, J. Amer. Chem. Soc., 87, 2312 (1965).
- 32 G. Donnay, Arch. Biochem. Biophys., 80, 80 (1959).
- 33 E. E. Jacobs, A. E. Vatter and A. S. Holt, ibid, 53, 228 (1954).
- 34 I. L. Kukhetevich and A. I. Bilyak, Biophys., (USSR), 10, 469 (1965).
- 35 E. Steinman, Exptl. Cell Res., 3, 367 (1952).
- 36 A. Frey-Wyssling, "Macromolecules in Cell Structure," Harvard University Press, Cambridge, Mass., 1957.

- 37 R. B. Park and J. Biggins, Science, 144, 1009 (1964).
- 38 R. B. Park, J. Chem. Educ., 39, 424 (1962).
- 39 J. J. Katz, K. Ballschmiter, M Garcia-Morin, H. H. Strain and R. A. Uphaus, Proc. Nat. Acad. Sci. U. S., 60, 100 (1968).
- 40 K Nakamoto, M. Margoshes and R. E. Rundle, J. Amer. Chem. Soc., 77, 6480 (1955).
- 41 R. B. Park in "Plant Biochemistry," J. Bonner and J. Varner, Eds., Academic Press, New York, N. Y., 1965, p 133.
- 42 J. F. Danielli and H. Davson, J. Cellular Comp. Physiol., 5, 495 (1935).
- 43 C. Houssier and K. Sauer, to be published, 1970.

The electronic absorption spectra of metalloporphyrins vary depending on the central metal ion. Gouterman<sup>3</sup> showed that the oscillator strength of the O-O absorption band of the relatively weak visible (Q) transition could be correlated with the energies of both the Q band itself and the extremely intense Soret (B) transition in the blue or near-violet. He used the limited data then available to try to establish a correlation between these three quantities and the electronegativity of the central metal. Becker<sup>4</sup> measured the spectra of the mesoporphyrin derivatives of nineteen different metals and found that they "cannot be related in a simple way with electronegativity."

In this paper, we present a <sup>statistical</sup> A correlation between spectroscopic energy levels and the structures of metal porphyrins as determined by x-ray crystallography. To do this, we first need a way of expressing differences in porphyrin structure in terms of a single controlling parameter. Through analysis of the results of ten published crystal structures of porphyrin derivatives (as listed in Table I), we found that the molecular bond distances and angles vary in a systematic way with hole size. The hole size of a porphyrin can be defined<sup>14</sup> as half the average distance between diagonally opposite nitrogen atoms.

There are four independent bond distances and six independent bond angles in a square planar ( $D_{4h}$ ) porphyrin ring. We determined each of these for each of the ten porphyrins by averaging the

Table I. Porphyrin structures used in the analysis of hole size.

<u>Porphyrin</u>	<u>Reference</u>
Nickel(II) 2,4-diacetyldeuteroporphyrin dimethyl ester	5
Copper(II) tetraphenylporphin	6
Chlorohemin (Chloroiron(III) protoporphyrin-IX)	7
Palladium(II) tetraphenylporphin	6
Chloroiron(III) tetraphenylporphin	8
Methoxyiron(III) mesoporphyrin-IX dimethyl ester	9
Aquozinc(II) tetraphenylporphin	10
Porphin	11
Tetraphenylporphin in tetragonal crystals	12
Tetraphenylporphin in triclinic crystals	13

experimentally determined values according to  $D_{4h}$  symmetry. We then used the method of least squares to obtain the best linear relationship between hole size and bond angle or bond distance. Each experimental value was weighted by  $1/\sigma^2$ , where  $\sigma^2$  is the larger of two numbers: the r.m.s. difference from the average value and the average standard deviation of the individual measurements.

These linear correlations between hole size and molecular parameters (bond angles and bond distances) now made it possible to establish a standard geometry corresponding to a metalloporphyrin with a "large" and a "small" hole. For this purpose, we used hole sizes of 2.062 Å and 1.960 Å, respectively the largest and smallest measured holes for square porphyrins. We also calculated a "medium" geometry for a hole size of 2.011 Å. The molecular parameters corresponding to the largest and smallest hole sizes are listed in Table II, along with the linear correlation coefficient<sup>15</sup>,  $r$ , which is a measure of the correlation between parameters, as well as the r.m.s. difference  $\Delta$  between the observed and the calculated bond parameters.

The numbering scheme and the general changes produced by enlarging the hole size are shown in Figure 1, which is a threefold exaggeration of the change from small to large hole size. As the hole size increases and the nitrogens are forced farther from the geometric center of the ring, the  $\alpha$ -N- $\alpha$  angle increases and the  $\alpha$ -N distance decreases. The  $\alpha$  carbons are forced outward, lengthening the  $\alpha$ -m distance and increasing the angle  $\alpha$ -m- $\alpha$ .

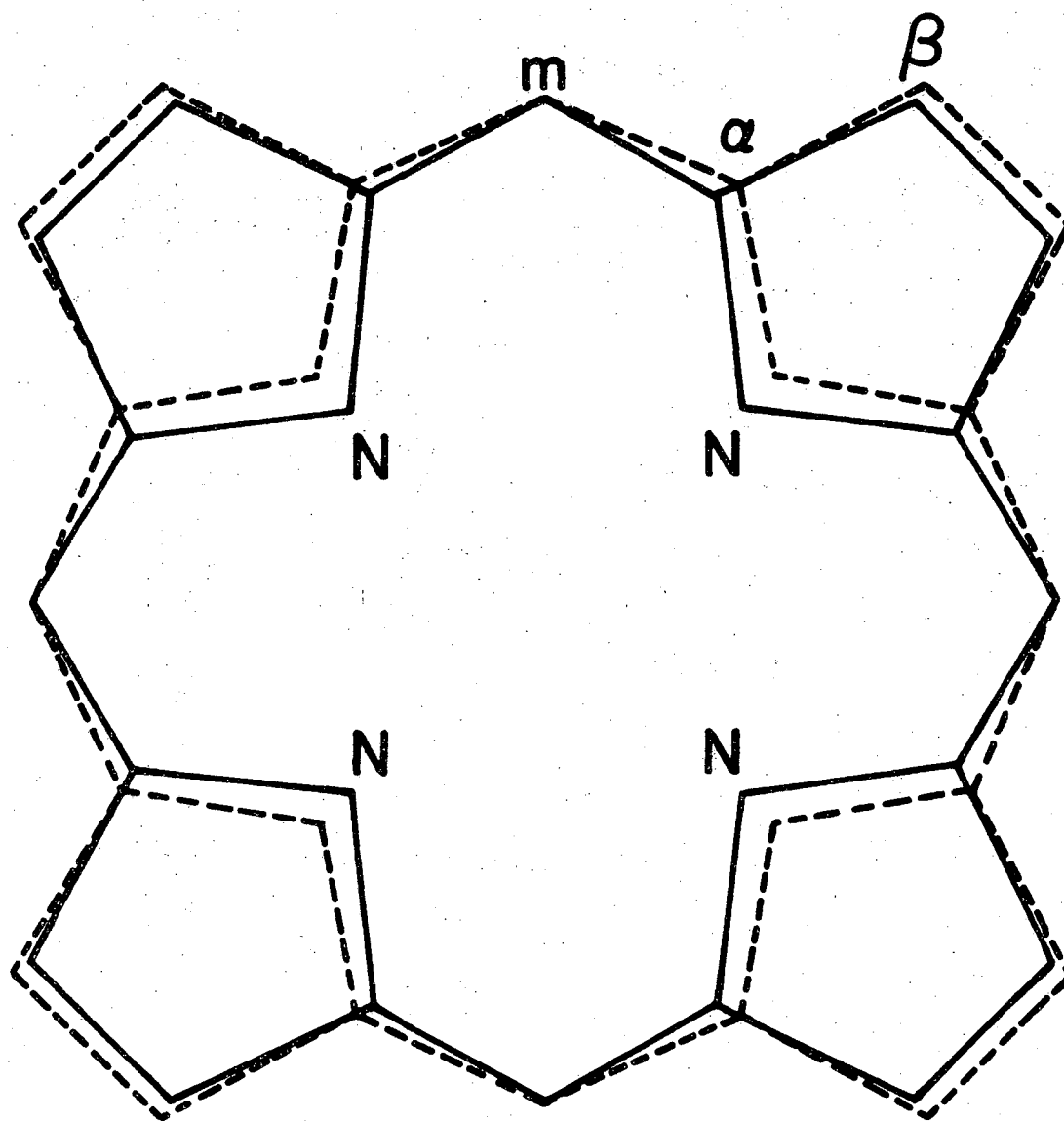
Table II. Porphyrin geometry as a function of the hole size.

<u>Bond Parameter</u>	<u>Small Hole</u>	<u>Large Hole</u>	<u>r<sup>a</sup></u>	<u><math>\Delta</math><sup>b</sup></u>
Hole size	1.960 Å	2.062 Å		
N- $\alpha$	1.394	1.363	-0.62	0.010 Å
$\alpha$ - $\beta$	1.447	1.439	-0.33	0.010
$\beta$ - $\beta$	1.351	1.350	-0.02	0.015
$\alpha$ -m	1.374	1.394	0.38	0.011
$\alpha$ -N- $\alpha$	104.71 <sup>o</sup>	108.31 <sup>o</sup>	0.75	1.15 <sup>o</sup>
N- $\alpha$ - $\beta$	110.24	108.96	-0.40	0.91
N- $\alpha$ -m	125.36	125.69	0.18	0.53
$\beta$ - $\alpha$ -m	124.53	125.48	0.41	0.57
$\alpha$ - $\beta$ - $\beta$	107.20	107.21	0.01	0.44
$\alpha$ -m- $\alpha$	123.74	126.19	0.58	0.66

<sup>a</sup>Linear correlation coefficient.

<sup>b</sup>R.m.s. difference between observed and calculated parameter.

Figure 1. Effect of expansion of the hole size on the porphyrin geometry, three times exaggerated, as derived from x-ray data. The solid lines correspond to a porphyrin with hole size of 1.858 Å, the dashed lines to a porphyrin with hole size of 2.164 Å. (These are not the values used in the calculations.)



XBL 699-5605

The molecular orbitals for the general metalloporphyrin were calculated using the self-consistent molecular orbital method of Pariser, Parr and Pople (SCMO-PPP)<sup>16</sup> and the four-orbital model and "traditional" parameters of Weiss, Kobayashi, and Gouterman<sup>17</sup>. The calculations use the input geometry to calculate repulsion and resonance integrals. Since <sup>these</sup> parameters were originally chosen<sup>17</sup> to minimize the effects of the geometry, any dependence of a calculated quantity on the input geometry should be significant. The calculations predict that the bond orders and lowest excited singlet energies should be invariant to changes in the input geometry, but that the lowest excited triplets should show a measurable dependence on the hole size. Analogous calculations using the interpolation formula for interatomic electron repulsion formulated by Pariser and Parr<sup>16</sup> gave much the same qualitative prediction. This formula is the one used by Sundbom<sup>18</sup> in her recent molecular orbital calculation on porphyrins.

The lowest triplet energies of a variety of metalloporphyrins have been measured by Becker<sup>4</sup>. Many of these data relate to compounds whose hole sizes have not been accurately determined. We have therefore developed a method of estimating the hole sizes of metalloporphyrins from ionic radii determined from x-ray measurements of inorganic crystals.

This undertaking is complicated by the demonstration by Shannon and Prewitt<sup>19</sup> that the effective ionic radius in metal fluorides and



oxides depends not only on the ionic charge but also on its coordination number and electronic spin state,<sup>19</sup> Using their data we estimated the effective ionic radius of tetracoordinated Ni(II),  $r(\text{IV Ni(II)})$ , from ionic radii of  $\text{VI Ni(II)}$ ,  $\text{Cu(II)}$  and  $\text{Zn(II)}$  by using the relationship:  $r(\text{IV Ni(II)}) = r(\text{VI Ni(II)}) + \frac{1}{2}[r(\text{IV Cu(II)}) - r(\text{VI Cu(II)}) + r(\text{IV Zn(II)}) - r(\text{VI Zn(II)})]$ . (Cu and Zn are adjacent to Ni on the periodic table.) The ionic radius of the vanadium atom was estimated from the vanadium oxygen distances of vanadyl bisacetylacetonate.<sup>20</sup> The "effective radius" of the oxygen atoms of the acetylacetonate group was found by subtracting the effective ionic radii of  $\text{VI Mn(III)}$ ,  $\text{V Zn(II)}$ ,  $\text{VI Ni(II)}$ ,  $\text{VI Cr(III)}$ , and  $\text{VI Fe(III)}$  from the metal oxygen distances of their respective acetylacetonates<sup>21-25</sup>. The other three values of ionic radius were obtained directly from Shannon and Prewitt.<sup>19</sup> Figure 2 shows a good correlation between the ionic radius as determined by these methods and the experimental hole size in the five metalloporphyrins for which both data are available.

The existence of correlations between the ionic radius and hole size and between hole size and porphyrin geometry implies that there should be a correlation between the ionic radius and porphyrin geometry. Our molecular orbital calculations therefore predict that the ionic radius should be correlated with the phosphorescence energy and the singlet-triplet separation. Figures 3 and 4 show

Figure 2. Metalloporphyrin hole size derived from x-ray data as a function of the ionic radius of the central metal in fluorides and oxides.<sup>19</sup>

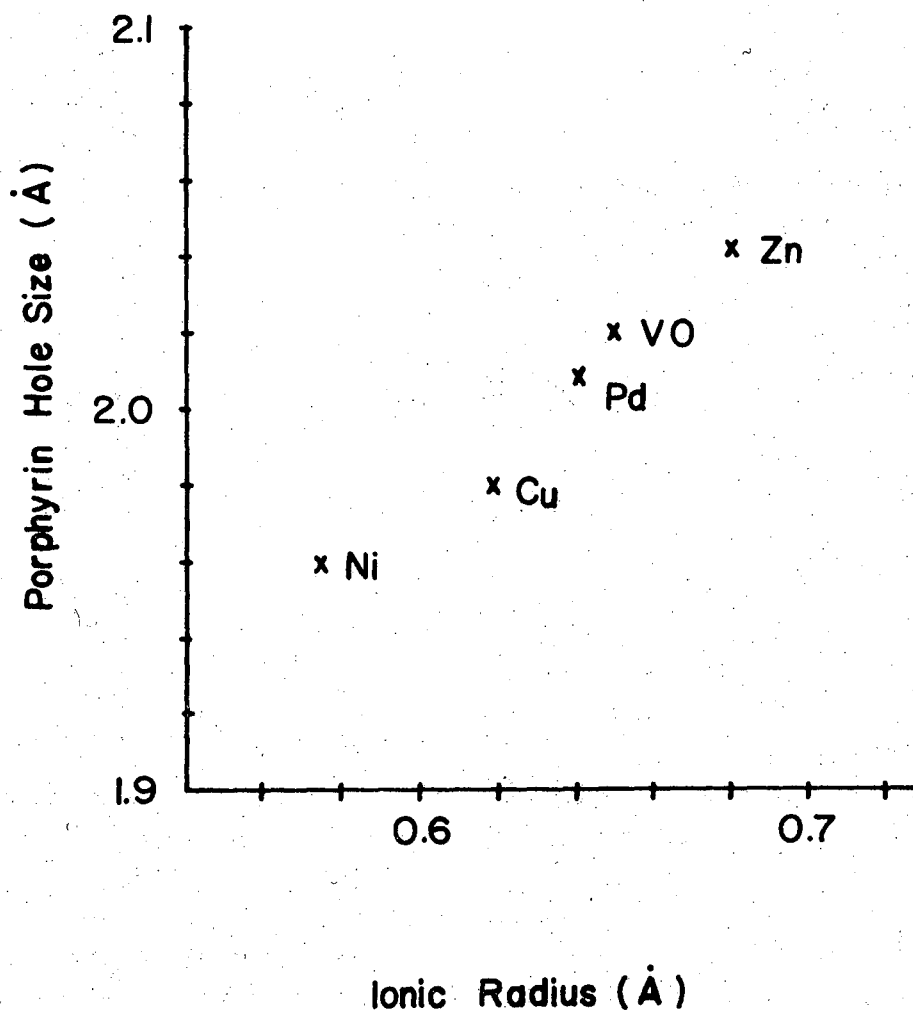


Figure 3. Points indicated by x are experimental phosphorescence energies of metalloporphyrins plotted as a function of the ionic radius of the metal. All metal ions are divalent. Line indicated by o—o is predicted lowest triplet energy of a porphyrin with hole size corresponding to a particular ionic radius.

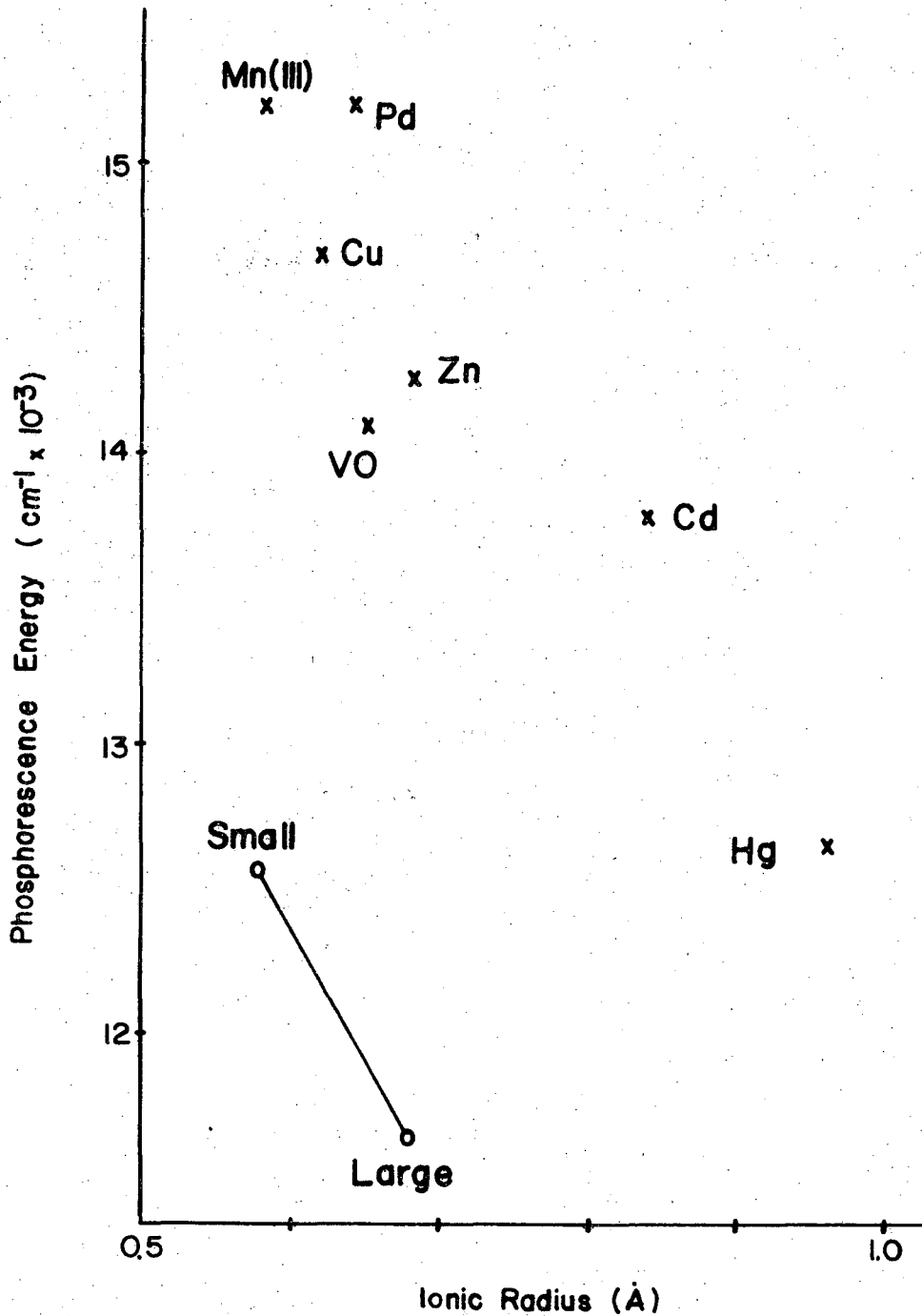
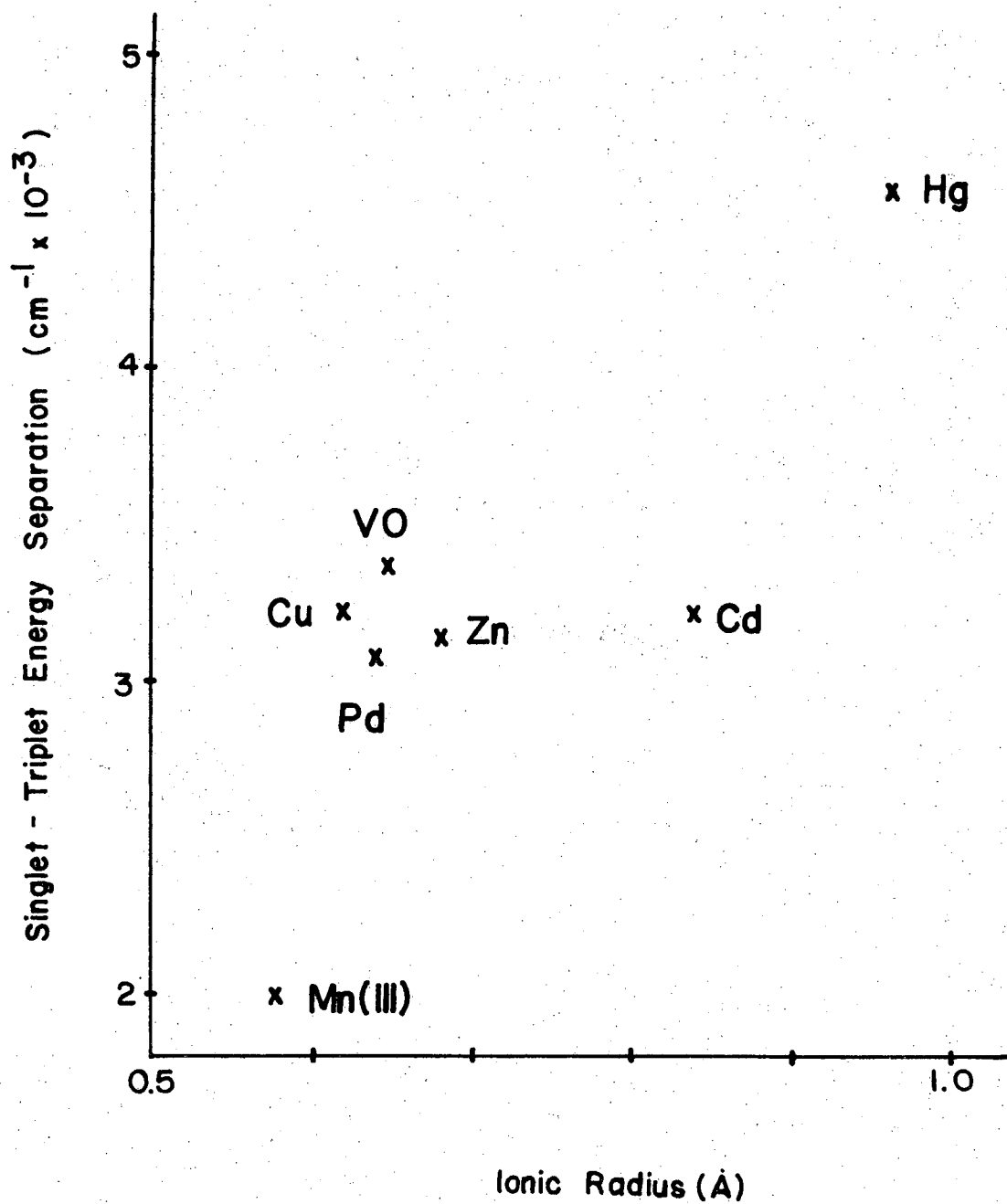


Figure 4. Experimental singlet-triplet energy separation of metalloporphyrins as a function of the ionic radius of the metal. All metal ions are divalent unless otherwise indicated.



the dependence of the experimental phosphorescence energy and singlet-triplet separation, respectively, as a function of the ionic size derived from the data of Shannon and Prewitt for the seven metalloporphyrins for which the necessary data is available. Our theoretical predictions are included in Figure 3. Figure 5 indicates the much weaker dependence of the phosphorescence energy on the electronegativity of the central metal atom. The analogous plot for the energy of the lowest singlet is found in Figure 2 of reference 4c.

The molecular orbital calculations of Figure 3 predict a stronger dependence of the phosphorescence energy on the molecular geometry than is experimentally observed.

Hoard has shown<sup>14</sup> that the central atom in metalloporphyrins is coplanar with the four inner nitrogen atoms only if the metal-nitrogen distance, M-N, is less than 2.01 Å, which corresponds to an effective ionic distance of 0.63 Å. This means that the Cd and Hg atoms in their respective porphyrins would very likely be substantially out of the plane of the central nitrogens. This would result in a much smaller hole size than the linear correlation of Figure 2 would predict. The phosphorescence energy of the Cd and Hg porphyrins would therefore be higher than we would have predicted.

Table III lists several possible correlations, the linear correlation coefficient for each and its associated probability.<sup>27</sup> The most significant experimental correlation is between the triplet energy and ionic radius of the central metal atom (Figure 3). For

Figure 5. Phosphorescence energy of metalloporphyrins as a function of the electronegativity of the metal atom. All metals are divalent unless otherwise indicated.

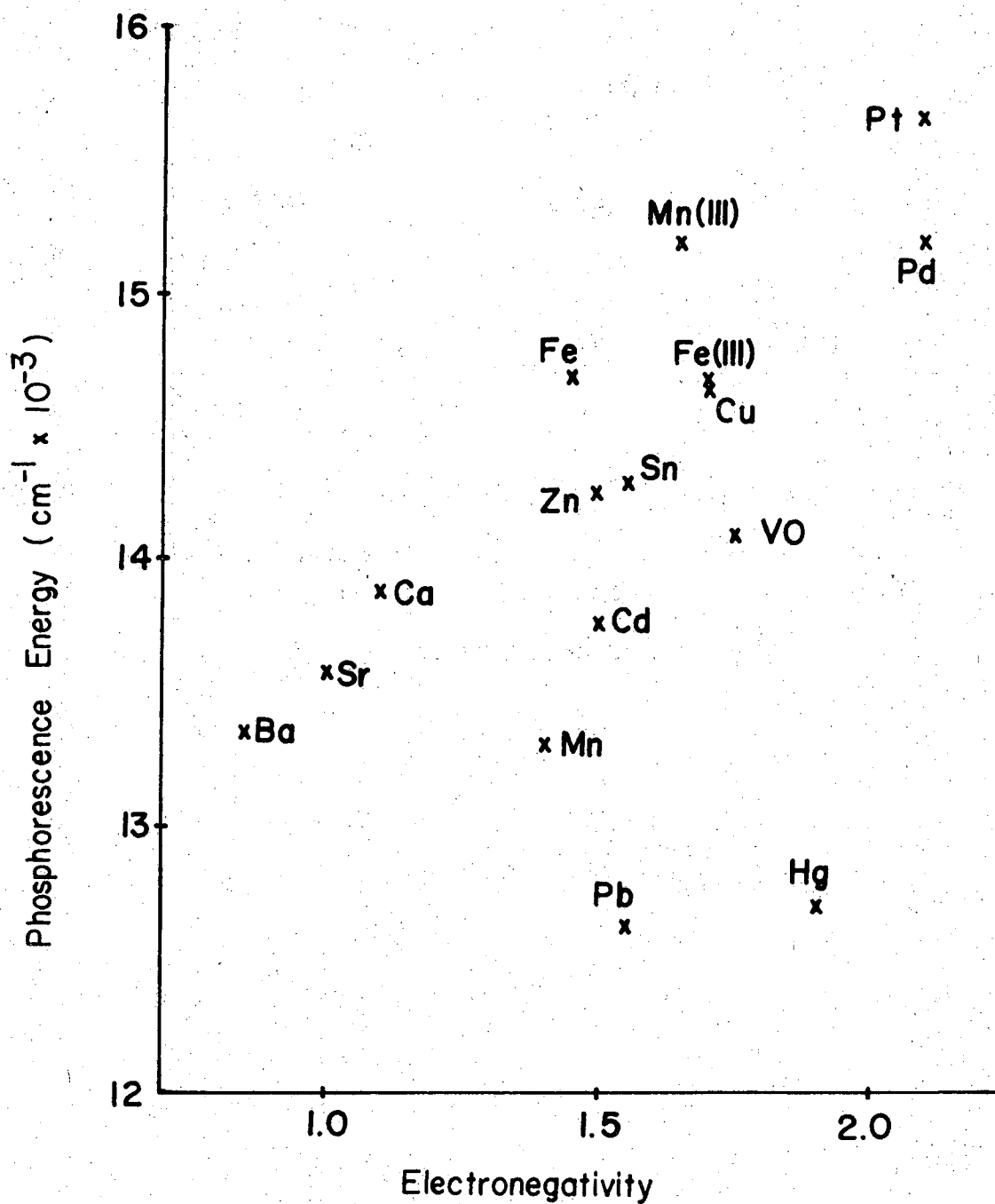


Table III. Correlations and significance levels.

		<u>Number</u>	<u>r<sup>a</sup></u>	<u>significance level<sup>b</sup></u>	
triplet energy	ionic radius <sup>19</sup>	7	-0.919	<<0.01	vs
	electronegativity <sup>28</sup>	16	0.488	0.07	s
	metallic charge <sup>29</sup>	9	-0.141	0.7	ns
singlet energy	ionic radius <sup>19</sup>	7	-0.772	0.04	s
	electronegativity <sup>28</sup>	19	0.707	< 0.01	vs
	metallic charge <sup>29</sup>	8	-0.412	0.3	ns
singlet-triplet energy separation	ionic radius <sup>19</sup>	7	0.805	0.04	s

<sup>a</sup> Linear correlation coefficient.

<sup>b</sup> vs = very significant; s = significant; ns = not significant.

triplets the direct geometric effect of the sigma strain due to increased ionic size is enough to explain the triplet dependence on ionic radius.

For singlets, statistical analysis of the data shows that  $E_Q$  varies in a significant way with the metal's electronegativity<sup>28</sup>. The correlation is masked, however, by a strong dependence on some other variable. In statistical terminology<sup>27</sup>, the linear correlation is significant but accounts for only  $r^2 = 50\%$  of the variation. The singlet dependence on ionic radius is not due to the direct geometric effect, at least according to our calculations, but must be due to some other unknown factor. In an attempt to pin down this unknown variable, we looked for a correlation between <sup>experimental</sup> singlet and triplet energy and the metallic charge as calculated by Zerner and Gouterman.<sup>29</sup> No correlation was found in either case.

We conclude that changes in the ring geometry of metalloporphyrins produce small but significant changes in the electronic properties of the molecules, as far as can be judged from the small sample of data available. The correlations between hole size and phosphorescence energy should be confirmed and extended by additional spectroscopic and crystallographic measurements on metalloporphyrins.

This means that differences in ground state geometry should be taken into account in detailed theoretical explanations of porphyrin



spectra, and the coordination number of the central metal atom should be specified. No satisfactory theory for the effect of ligands on porphyrin spectra exists. From the present study we conclude that the coordination number may have a small but significant effect on metalloporphyrin absorption energy levels simply by virtue of the change in ionic radius of the central metal. For example, the ionic radius of  $\text{Pd}^{+2}$  in the square planar arrangement is  $0.64 \text{ \AA}$ <sup>19</sup>, but the ionic radius increases to  $0.86 \text{ \AA}$  when the  $\text{Pd}^{+2}$  increases its coordination to sixfold. From Figure 3 we estimate that the increased hole size should be enough to shift the phosphorescence energy by as much as  $-1800 \text{ cm}^{-1}$  when the number of ligands of the  $\text{Pd}^{+2}$  is increased from four to six. A similar change in the coordination number of  $\text{Mg}^{+2}$  from four to six should also shift the phosphorescence energy by as much as  $-1800 \text{ cm}^{-1}$ . If these predictions are confirmed, it may be possible to use experimental measurements of the phosphorescence energies for other metalloporphyrins together with published values of the ionic radius of the cations themselves to determine the coordination number of the metals in the metalloporphyrins in varied chemical environments. If the overall correlation of phosphorescence energy with hole size is confirmed, it may be possible to use phosphorescence energy as a "spectroscopic ruler" of hole size without the necessity of gathering x-ray data.

References

- 3 M. Gouterman, J. Chem. Phys., 30, 1139 (1959).
- 4 a) R. S. Becker and J. S. Allison, J. Phys. Chem., 67, 2663 (1963);  
b) J. B. Allison and R. S. Becker, ibid., 67, 2667 (1963);  
c) R. S. Becker and J. B. Allison, ibid., 67, 2675 (1963).
- 5 T.A. Hamor, W.S. Caughey and J.L. Hoard, J. Amer. Chem. Soc.,  
87, 2305 (1965).
- 6 E.B. Fleischer, C.K. Miller and L.E. Webb, ibid., 86, 2342 (1964)
- 7 D.F. Koenig, Acta Cryst., 18, 663 (1965).
- 8 J.L. Hoard, G.H. Cohen, and M.D. Glick, J. Amer. Chem. Soc.,  
89, 1992 (1967).
- 9 J.L. Hoard, M.J. Hamor, T.A. Hamor and W.S. Caughey, ibid.,  
87, 2312 (1965).
- 10 M.D. Glick, G.H. Cohen and J.L. Hoard, ibid., 89, 1996 (1967).
- 11 L.E. Webb and E.B. Fleischer, ibid., 87, 667 (1965).
- 12 M.J. Hamor, T.A. Hamor and J.L. Hoard, ibid., 86, 1938 (1964).
- 13 S.J. Silvers and A. Tulinsky, ibid., 89, 331 (1967).

- 14 J. L. Hoard in "Structural Chemistry and Molecular Biology," 120  
A. Rich and N. Davidson, Eds., W. H. Freeman and Co., San  
Francisco, Calif., 1968, pp 573-594.
- 15 W. C. Hamilton, "Statistics in Physical Sciences," Ronald Press  
co., New York, N.Y., 1964, p 31.
- 16 R. Pariser and R. G. Parr, J. Chem. Phys., 21, 466, 767 (1953);  
J. A. Pople, Trans. Faraday Soc., 49, 1365 (1953); R. G. Parr,  
"Quantum Theory of Molecular Electronic Structure," W. A.  
Benjamin, New York, N.Y., 1964.
- 17 C. Weiss, H. Kobayashi and M. Gouterman, J. Mol. Spectr., 16,  
415 (1965).
- 18 M. Sundbom, Acta Chem. Scand., 22, 1317 (1968).
- 19 R. D. Shannon and C. T. Prewitt, Acta Cryst., 25, 925 (1969).
- 20 R. P. Dodge, D. H. Templeton and A. Zalkin, J. Chem. Phys.,  
35, 55 (1961).
- 21 B. Morosin and J. R. Brathovde, Acta Cryst., 17, 705 (1964).
- 22 H. Montgomery and E. C. Lingafelter, ibid., 16, 748 (1964).
- 23 H. Montgomery and E. C. Lingafelter, ibid., 17, 1481 (1964).
- 24 B. Morosin, ibid., 19, 131 (1965).
- 25 R. B. Roof, ibid., 9, 781 (1956).
- 26 R. C. Pettersen, ibid., In Press.
- 27 K. W. Smillie, "An Introduction to Regression and Correlation,"  
Academic Press, New York, 1966.
- 28 A. F. Clifford, J. Phys. Chem., 63, 1227 (1959).
- 29 M. Zerner and M. Gouterman, Theoret. Chim. Acta, 4, 44 (1966);  
M. Zerner and M. Gouterman, Inorg. Chem., 5, 1699 (1966).

THE CHOLINES

Choline chloride,  $[(\text{CH}_3)_3\text{NCH}_2\text{CH}_2\text{OH}]^+ \text{Cl}^-$ , is one of the most radiation sensitive molecules in the solid state (Tolbert et al., 1953). As a measure of radiation sensitivity we define a G-value as the number of molecules decomposed per 100 electron volts of absorbed radiation. The G-values of choline chloride and a number of other organic compounds (Tolbert and Lemmon, 1955; Lemmon et al., 1955; Lemmon et al., 1958) are listed in Table I. Choline chloride is radiation sensitive to far ultra-violet light, x-rays,  $\beta$ -rays and  $\gamma$ -rays. The overall decomposition reaction is  $[(\text{CH}_3)_3\text{NCH}_2\text{CH}_2\text{OH}]^+ \text{Cl}^-$  radiation  $\rightarrow$   $[(\text{CH}_3)_3\text{NH}]^+ \text{Cl}^- + \text{CH}_3\text{CHO}$ .

The decomposition is the result of a cooperative process. After a single molecule is decomposed, a chain reaction is initiated in which 300-20000 additional molecules are decomposed (Lemmon et al., 1955). At about 75° C there is a phase transformation of the crystalline choline chloride (Serlin, 1957). Choline chloride in this new phase and in solution (Lemmon et al., 1958) is stable to radiation. Thus the crystalline packing plays a crucial role in the decomposition.

The crystal structure of choline chloride at room temperature was determined by Senko and Templeton (1960) and at high temperature by Collin (1957). The structures of five analogues of choline chloride have been determined: muscarine iodide (Jellinek, 1957), acetyl choline bromide (Canepa et al., 1966), choline-O-sulfate (Okaya, 1964), L- $\alpha$ -glycerophosphorylcholine (GPC) (Abrahamson and Pascher, 1966), and GPC·CdCl<sub>2</sub>·3H<sub>2</sub>O (Sundaralingam and Jensen, 1965).

Table 1. G-values for Choline Chloride and its Analogues.

<u>Molecule</u>		<u>Name</u>	<u>G</u>
$[(\text{CH}_3)_3\text{NCH}_2\text{CH}_2\text{OH}]^+$	$\text{Cl}^-$	choline chloride	354 - 55000
	$\text{Br}^-$	bromide	92
	$\text{I}^-$	iodide	3
	$\text{NO}_3^-$	nitrate	5
	$\text{CN}^-$	cyanide	16
$[(\text{CH}_3)_3\text{NCH}_2\text{CH}_2\text{OH}]^+$	$\text{SO}_4^{=}$	sulfate	29
$[(\text{CH}_3)_3\text{NCH}_2\text{CH}_2\text{CH}_2\text{OH}]^+$	$\text{Cl}^-$		5
$[(\text{CH}_3)_3\text{NCH}_2\text{CO}_2\text{H}]^+$	$\text{Cl}^-$	betaine hydrochloride	15
$[(\text{C}_2\text{H}_5)(\text{CH}_3)_2\text{NCH}_2\text{CH}_2\text{OH}]^+$	$\text{Cl}^-$		26
$[(\text{C}_2\text{H}_5)_2(\text{CH}_3)\text{NCH}_2\text{CH}_2\text{OH}]^+$	$\text{Cl}^-$		8
$[(\text{C}_2\text{H}_5)_3\text{NCH}_2\text{CH}_2\text{OH}]^+$	$\text{Cl}^-$		14
$[(\text{C}_6\text{H}_5)(\text{CH}_3)_2\text{NCH}_2\text{CH}_2\text{OH}]^+$	$\text{Cl}^-$		2
$[(\text{CH}_3)_2\text{N}(\text{CH}_2\text{CH}_2\text{OH})_2]^+$	$\text{Cl}^-$		14
$[(\text{CH}_3)_3\text{PCH}_2\text{CH}_2\text{OH}]^+$	$\text{Cl}^-$		5
		organic alcohols	1 - 12
		alkyl halides	1 - 15
		carboxylic acids	1 - 2

None of these structures has been determined to the high accuracy obtainable by present scintillation-counting techniques. We were interested in determining high precision structures of choline chloride analogues to compare both intra- and inter- molecular distance.

Choline iodide was prepared from a 1:1 mixture of dimethyl-aminoethanol and methyl iodide in methanol. The mixture was refluxed for two hours and evaporated to dryness. When recrystallized from ethanol, the choline iodide formed thin plates; when recrystallized from dimethyl formamide it formed thicker crystals.

Choline bromide was prepared from choline iodide by dissolving the iodide in water, adding an excess of  $\text{Ag}_2\text{O}$  slowly, filtering off the  $\text{AgI}$  and titrating with  $\text{HBr}$ . The water was evaporated under high vacuum and the bromide recrystallized from slowly evaporating ethanol. Other choline salts were prepared from choline iodide by the addition of the appropriate acid to choline hydroxide.

### Betaine Hydrochloride

Clastre (1964) has published a preliminary structure report for betaine hydrochloride, in which he refined the R value for two of the two-dimensional projections down to 0.18. Bond distances which we calculated from his published atomic coordinates implied that the C-N bond lengths ranged from 1.49 to 1.63 Å in length. We undertook this structure investigation to provide an accurate structure, to locate the positions of the hydrogen atoms, and to investigate the packing.



### Experimental

Small colorless crystals of betaine hydrochloride were kindly supplied to us by Dr. R. M. Lemmon. These were then recrystallized in the form of colorless needles by the evaporation of a water-methanol solution to dryness at room temperature. The unit-cell dimensions were obtained from careful measurements of the Bragg scattering angles for the  $h00$ ,  $0k0$ , and  $00l$  reflections, as measured on a manually operated General Electric XRD-5 diffractometer. The alpha doublet ( $\lambda = 1.5405 \text{ \AA}$  for  $\text{CuK}\alpha_1$ ) was resolved for those reflections of highest order. The crystal used for both the determination of cell dimensions and the collection of data was mounted on the crystallographic  $b$  axis, and the  $\beta$  angle was obtained directly from the angle on the  $\varphi$  circle between the  $h00$  and the  $00l$  reflections. The unit cell parameters (at  $23^\circ$ ) are shown in Table 1. The absence of reflections  $h0l$  with  $l$  odd and  $0k0$  with  $k$  odd indicate the space group  $P2_1/c$ . The crystal, which was mounted on the needle axis, measured  $0.09 \times 0.09 \times 0.43$  mm. The four most prominent faces were the  $(100)$ ,  $(001)$ ,  $(\bar{1}00)$  and  $(00\bar{1})$ . The observed density of  $1.314 \pm .005 \text{ g cm}^{-3}$ , which was determined by flotation in a chloroform-ethylene dichloride mixture, agrees well with the value  $1.313 \text{ g cm}^{-3}$  calculated for a molecular weight of 153.5, for  $Z = 4$ , and for a unit cell volume of  $776 \text{ \AA}^3$ .

Integrated intensities were measured with a card controlled, automated General Electric XRD-5 diffractometer. The copper radiation was filtered by a 0.001 inch thick nickel foil placed

Table 1. Unit Cell Parameters

	This Work	Glastre
a	$7.428 \pm .002 \text{ \AA}$	$7.45 \pm .02 \text{ \AA}$
b	$9.108 \pm .005$	$9.15 \pm .02$
c	$11.550 \pm .003$	$11.65 \pm .02$
$\beta$	$96.71 \pm .03$	97.0

between the crystal and the receiving slit, and a  $\theta$ - $2\theta$  scan was employed. The intensities were measured for all reflections lying within half a sphere in reciprocal space corresponding to d-spacings  $\geq 1.006 \text{ \AA}$  ( $2\theta \geq 100^\circ$ ). The intensities of equivalent reflections were averaged to give 794 independent reflections of which 782 were above background. The 32 largest intensities were remeasured at lower x-ray flux to avoid flooding of the counter. Crystal decay, monitored by 24 periodic measurements of six standard reflections, was less than 5%. The calculated linear absorption coefficient  $\mu$  is  $39 \text{ cm}^{-1}$  (for CuK $\alpha$ ). The data are uncorrected for absorption effects, which may vary by a factor of the order of 1.15 for the extreme cases.

Net intensities  $I$  and their standard deviations  $\sigma(I)$  were calculated from the expressions  

$$I = I_{\text{gross}} - (t_I/2t_B) (B_1 + B_2)$$
and 
$$\sigma^2(I) = I_{\text{gross}} + (t_I/2t_B)^2 (B_1 + B_2)$$
,
where  $B_1$  and  $B_2$  are the number of counts for each background reading and  $t_I$  and  $t_B$  are the times spent counting the peak and the background. For  $n$  measurements of the intensity of a particular reflection ( $n$  was always  $\geq 2$ ), the intensities were averaged and  $\sigma(\bar{I})$ , the standard deviation of the mean, was calculated from  $\sigma_L(I)$  equal to the larger of  $[\sum(I_i - \bar{I})^2]^{1/2}/(n-1)$  and  $[\sum \sigma^2(I_i)]^{1/2}/n$  by using the relationship  $\sigma^2(\bar{I}) = \sigma_L^2(I) + (pI)^2$ , where  $p$ , a constant, was set equal to 0.04 to reduce the weights of the most intense reflections.

The full matrix least squares program used was our local unpublished version for the CDC 6600 computer. The atomic scattering

factors used during this analysis were those given by Cromer and Mann (1968) for the  $\text{Cl}^-$ , Cl, O, N and C atoms and those of Stewart, Davidson and Simpson (1965) for the hydrogen atoms. The scattering factor for the  $\text{N}^+$  atom was calculated from the scattering factor of  $\text{N}^{+3}$  (Hurst and Matson, 1959) by using the relationship  $f(\text{N}^+) = [2f(\text{N}) + f(\text{N}^{+3})]/3$ . For the chlorine atom the anomalous dispersion corrections of Cromer (1965) were used. The function minimized in the least-squares refinements was  $R_2^2 = \sum \underline{w} (|F_o| - |F_c|)^2 / \sum \underline{w} |F_o|^2$ . In the early stages of refinement, the weights  $\underline{w}$  were set equal to 1.0, but in the later stages they were set to 0 when  $I = 0$  and to  $1/\sigma^2(F)$  otherwise;  $\sigma(F)$  was calculated from  $\sigma(\bar{I})$ :  $\sigma(F^2) = (Lp)^{-1} \sigma(\bar{I})$ ,  $\sigma(F) = [\sigma(F^2)]^{1/2}$  if  $I \leq \sigma(\bar{I})$  and  $\sigma(F) = F - [F^2 - \sigma(F^2)]^{1/2}$  if  $I > \sigma(\bar{I})$ . Johnson's ORTEP program (1965) was used for the stereoscopic pictures and as an aid in the thermal analysis.

### Structure Determination and Refinement

Because at the time we were not aware of Clastre's report (1964), the structure was solved independently. The chlorine-chlorine vectors were evident in a Patterson map, but their interpretation was ambiguous. The  $y$  coordinate of chlorine is near  $\frac{1}{4}$ ; therefore, the inversion vector  $(2x, 2y, 2z)$  and the screw axis vector  $(2x, \frac{1}{2}, 2(z+\frac{1}{4}))$  both appear in the Harker section at  $y = \frac{1}{2}$ . The ambiguity escaped notice, and by bad luck the wrong choice was made. As a result, the chlorine  $z$  coordinate was assigned a value which was  $\frac{1}{4}$  less than the correct one. A Fourier map phased by this chlorine atom indicated eight other atoms. These nine atoms, some of which were later noticed to be at unacceptable bond distances, gave  $R = \sum ||F_o| - |F_c|| / \sum |F_o| = 0.33$  for all the data but  $R = 0.09$  for reflections with both  $k$  and  $l$  even. This result suggested errors of  $\frac{1}{2}$  in some  $y$  or  $z$  coordinates. Addition of  $\frac{1}{2}$  to the  $y$  coordinates of three atoms gave more reasonable bond distances and decreased  $R$  to 0.31, but calculation of interatomic distances showed that molecules related by the inversion center were too close together, with some atoms less than 2 Å apart. Therefore, the entire molecule was moved one-fourth of the unit cell in the  $z$  direction, at which point  $R$  dropped to 0.10.

After the thermal motion of the chlorine atom was approximated by an ellipsoidal anisotropic model, a Fourier difference map revealed the positions of the twelve hydrogen atoms among the highest seventeen peaks. The hydrogen atoms were given individual

isotropic temperature factors and all other atoms were given anisotropic temperature factors. The R value dropped to 0.027. The values of  $|F_o|/|F_c|$  for the reflections of highest intensity were all less than 1.0. Therefore, an extinction correction of the form  $F_o' = F_o (1.0 + cI)$ , where  $c = 2 \times 10^{-8}$ , was applied to give a maximum correction of 5% for the strongest reflection, and R dropped to 0.026.

Up to this point, the atomic scattering factors of  $Cl^-$  and neutral N had been used. Two other possibilities were tried. The first, with  $N^+$  and  $Cl^-$ , gave an R value of 0.032, and the second, with both N and Cl neutral, gave an R value of 0.027; the largest shifts in the atomic positions and bond distances were all less than one third of the respective standard deviations. All further discussion will be for N neutral and  $Cl^-$  atoms. The final weighted  $R_2$  value was 0.034 and the standard deviation of an observation of unit weight was 1.33. The largest shift of any parameter in the final least squares refinement was less than one per cent of its standard deviation. There was no systematic trend in  $|F_o|/|F_c|$  as a function of either  $2\theta$  or the intensity. The highest peak on the final difference calculation was 0.11 electrons  $\text{\AA}^{-3}$ .

## Results and Discussion

A stereoscopic view of one molecule, which shows the numbering scheme of the atoms, is presented in Figure 1. The observed structure factor amplitudes  $|F_o|$  as well as the final calculated structure factors  $|F_c|$  are listed in Table 2. The final positional and thermal parameters for the hydrogen atoms are given in Table 3 while those for the non-hydrogen atoms are given in Table 4.

The atomic positions found in this investigation differed from those of Clastre (1964) by as little as 0.02 Å for the chlorine atom to as much as 0.16 Å for atom C(2). The mean difference was 0.07 Å, which is more than twenty times the estimated standard deviations in this investigation. Clastre made no statement concerning the precision of his results.

Selected intramolecular distances and angles are listed in Tables 5 and 6, respectively. Because of thermal motion, the observed bond distances tend to be less than the time-average distances between atoms. Our ignorance of the phase relations of thermal motion prevents an unambiguous correction for this effect, but some estimates have been made on the basis of a riding model. For bonds N-C(1), N-C(3), C(5)-O(1), and C(5)-O(2), for which this model seems reasonably consistent with the observed thermal parameters, the corrections fall in the range 0.010 to 0.018 Å.

The orientations of the methyl and methylene groups are very nearly staggered around each of the four C-N bonds, the departures

Figure 1. Stereoscopic view of one molecule of betaine hydrochloride.

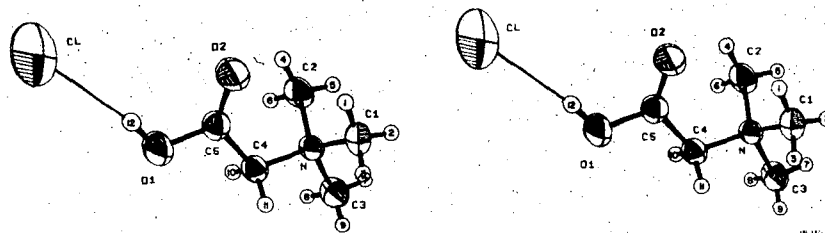






Table 3. Final Atomic Fractional Coordinates and Thermal Parameters with Their Standard Deviations for Hydrogen Atoms in Betaine Hydrochloride.

The numbers in parenthesis here and in succeeding tables are the standard deviations of the least significant digit(s). The thermal parameters are in units of square Angstroms. The temperature factor has the form:  $T = \exp[-B(\sin\theta/\lambda)^2]$

<u>Atom</u>	<u>X</u>	<u>Y</u>	<u>Z</u>	<u>B</u>
H(1)	.7362(26)	.1542(25)	.7369(18)	4.6(5)
H(2)	.8486(29)	.2080(21)	.6421(16)	3.3(4)
H(3)	.6466(32)	.2250(20)	.6230(20)	4.1(5)
H(4)	.8855(26)	.3019(24)	.8857(17)	4.0(4)
H(5)	1.0216(28)	.3508(20)	.7967(14)	3.7(4)
H(6)	.9188(27)	.4692(25)	.8622(16)	4.4(5)
H(7)	.9151(28)	.4549(20)	.6139(15)	3.9(4)
H(8)	.8157(26)	.5774(27)	.6754(16)	4.5(5)
H(9)	.7100(30)	.4784(24)	.5804(18)	4.8(5)
H(10)	.6136(25)	.5103(22)	.8037(16)	3.7(4)
H(11)	.5008(23)	.4191(17)	.7108(15)	2.7(4)
H(12)	.3407(27)	.3387(25)	.9524(18)	4.3(5)

Table 4. Final Atomic Fractional Coordinates and Thermal Parameters with Their Standard Deviations for Cl, C, N, and O Atoms in Betaine Hydrochloride.

The thermal parameters are in units of square Angstroms. The temperature factor has the form:

$T = \exp[-\frac{1}{2} \sum \sum B_{ij} h_i h_j / (b_i b_j)]$ , where  $h_i$  is the  $i$ th Miller index,  $b_i$  is the  $i$ th reciprocal axis length, and  $i$  and  $j$  are cycled 1 through 3.

Atom	X	Y	Z	$B_{11}$	$B_{22}$	$B_{33}$	$B_{12}$	$B_{13}$	$B_{23}$
Cl	.21472(6)	.24207(5)	1.09234(4)	3.34(3)	4.38(3)	3.59(3)	-.30(2)	1.17(2)	-.23(2)
O(1)	.37681(18)	.39010(16)	.90178(12)	3.60(7)	4.38(7)	3.99(7)	.52(6)	1.64(5)	.67(6)
O(2)	.58012(19)	.21083(15)	.89939(12)	4.37(7)	3.71(7)	3.95(7)	.59(6)	1.25(5)	.96(5)
N	.76178(16)	.37283(14)	.73148(11)	2.50(6)	2.77(8)	2.77(6)	.03(5)	.40(5)	.17(5)
C(1)	.74561(36)	.22378(24)	.67674(23)	3.48(11)	3.77(11)	3.56(11)	-.04(8)	.85(11)	-.70(9)
C(2)	.91492(28)	.37401(28)	.82812(20)	2.51(9)	4.45(12)	4.18(11)	.16(9)	-.06(8)	-.44(10)
C(3)	.80332(35)	.48153(27)	.64025(22)	3.84(11)	4.11(12)	4.74(12)	.05(9)	1.65(10)	.91(10)
C(4)	.58779(24)	.42035(22)	.77360(16)	2.45(8)	3.09(9)	3.13(9)	.09(7)	.31(7)	-.09(8)
C(5)	.51843(24)	.32588(23)	.86515(14)	2.63(9)	3.45(10)	2.65(9)	-.13(8)	.26(7)	-.30(7)

Table 5. Intramolecular Distances (in Å) in Betaine Hydrochloride

Standard deviations have been estimated by the method of least squares and are indicated in parenthesis.

<u>Atoms</u>	<u>Distance</u>	<u>Atoms</u>	<u>Distance</u>
N-C(1)	1.496(3)	C(3)-H(7)	0.95(2)
N-C(2)	1.498(3)	C(3)-H(8)	0.96(2)
N-C(3)	1.504(3)	C(3)-H(9)	0.92(2)
N-C(4)	1.497(2)	C(4)-H(10)	0.90(2)
C(4)-C(5)	1.500(3)	C(4)-H(11)	0.91(2)
C(5)-O(1)	1.316(2)	O(1)-H(12)	0.82(2)
C(5)-O(2)	1.193(2)	H(12)**Cl	2.15(2)
C(1)-H(1)	0.95(2)	O(1)**Cl	2.955(2)
C(1)-H(2)	0.92(2)	O(2)**N	2.893(2)
C(1)-H(3)	0.91(2)	O(2)**C(1)	2.979(3)
C(2)-H(4)	0.98(2)	O(2)**C(2)	3.090(3)
C(2)-H(5)	0.93(2)	O(2)**H(1)	2.38(2)
C(2)-H(6)	0.95(2)	O(2)**H(4)	2.44(2)

Table 6. Intramolecular Bond Angles (in Degrees) for Betaine Hydrochloride.

<u>Atom</u>	<u>Angles</u>
C(1)-N-C(2)	109.75(16)
C(1)-N-C(3)	108.31(16)
C(1)-N-C(4)	111.70(15)
C(2)-N-C(3)	108.50(15)
C(2)-N-C(4)	111.41(14)
C(3)-N-C(4)	107.04(15)
N-C(4)-C(5)	116.35(15)
C(4)-C(5)-O(1)	108.96(17)
C(4)-C(5)-O(2)	125.97(17)
O(1)-C(5)-O(2)	125.07(17)
C(5)-O(1)-H(12)	108.4(15)
O(1)-H(12) <sup>••</sup> Cl	168.4(21)

from an entirely staggered conformation being only  $9.4^\circ$  for N-C(1),  $4.3^\circ$  for N-C(2),  $1.6^\circ$  for N-C(3), and  $1.9^\circ$  for N-C(4). The plane of the carboxyl group is at an angle of  $6.7^\circ$  to that of atoms N, C(4), and C(5). The result is that the entire cation conforms within about  $0.1 \text{ \AA}$  to the symmetry of a non-crystallographic mirror plane. The mirror plane passes through (or near) atoms H(12), O(1), O(2), C(5), C(4), N, C(3), and H(7) and relates H(8) to H(9), H(10) to H(11), and the methyl groups C(1) to C(2). The carboxyl group is planar within experimental error.

The carboxyl group is twisted around bond C(4)-C(5) in such a way that atom O(2) is almost as close to and O(1) as far from the nitrogen atom in the same molecule as is possible. This results in an extended shape for the molecule in which the carboxyl hydrogen atom is remote from the positively charged ammonium group and thus can easily hydrogen bond to the chloride ion. The O-H...Cl angle is  $168 \pm 2^\circ$ , and the O...Cl distance of  $2.955 \pm .002 \text{ \AA}$  is much shorter than, for example, the O...Cl distance of  $3.03 \pm .02 \text{ \AA}$  distance in choline chloride (Senko and Templeton, 1960).

The molecular packing is shown in Figure 2, and the closest intermolecular approaches are listed in Table 7. For the bonded hydrogen atoms of this molecule, the center of gravity of the electron distribution as determined by x-ray diffraction is somewhat removed from the equilibrium nuclear position. Therefore, the intramolecular C-H and O-H distances listed in Table 5 are systematically shorter and the intermolecular packing distances in Table 7 involving hydrogen atoms are systematically longer by approximately 0.1 Å than the equilibrium internuclear separation as would be determined by neutron diffraction, for example.

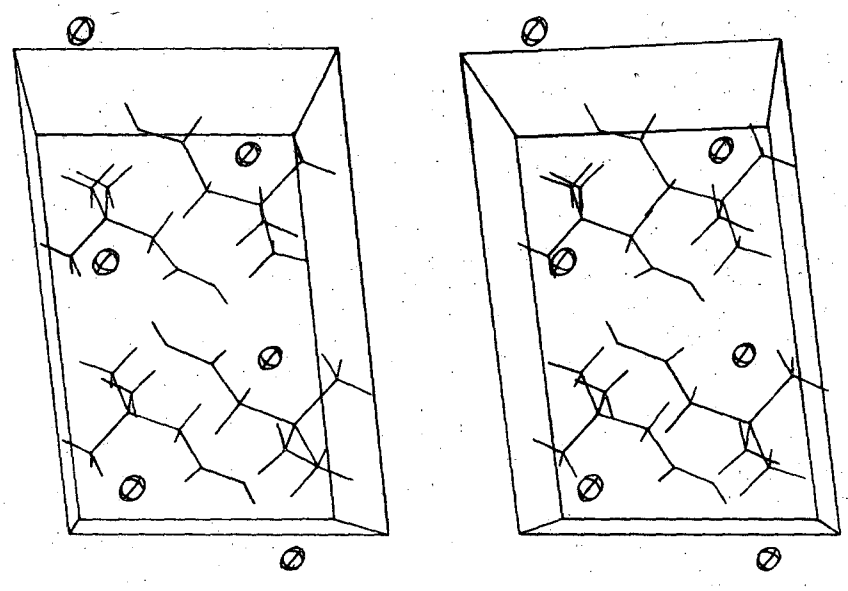
Table 7. Shortest Intermolecular Distances (in Å) for Crystals of  
Betaine Hydrochloride

The equivalent position numbers are 1 for  $x, y, z$ ; 2 for  $x, \frac{1}{2}-y, \frac{1}{2}+z$ ;  
 3 for  $-x, -y, -z$ ; and 4 for  $-x, \frac{1}{2}+y, \frac{1}{2}-z$ .

<u>Atom 1</u>	<u>Atom 2</u>	<u>Distance</u>	<u>Position Number</u> <u>of Atom 2</u>	<u>Atom 2: Translations in</u>		
				<u>x</u>	<u>y</u>	<u>z</u>
Cl	H(10)	2.79(2)	3	1	1	2
	H(11)	2.80(2)	2	0	0	0
	H(2)	2.88(2)	2	-1	0	0
	H(6)	2.88(2)	3	1	1	2
	H(7)	2.89(2)	2	-1	0	0
	H(5)	3.02(2)	2	-1	0	0
	H(8)	3.18(2)	3	1	1	2
	H(3)	3.20(2)	2	0	0	0
	H(9)	3.21(2)	4	1	-1	1
	H(4)	3.26(2)	1	-1	0	0
	H(8)	3.42(2)	4	1	-1	1
C(1)	O(1)	3.270(3)	4	1	-1	1
	O(2)	3.348(3)	2	0	0	-1
C(2)	O(1)	3.440(3)	1	1	0	0
C(4)	O(2)	3.459(3)	4	1	0	1
O(1)	O(1)	3.396(3)	3	1	1	2



Figure 2. Stereoscopic view of one unit cell of betaine hydrochloride.



XBL 697-254

### Choline Iodide

The choline iodide which we used in our structure determination had been recrystallized from a dimethyl formamide solution by the evaporation to dryness. A small fragment with maximum dimension 0.1 mm was sliced from an aggregate of crystals and was mounted on the b axis. This fragment was used for both the determination of cell dimensions and the collection of intensity data. The systematic absences ( $0k0$ ,  $k \neq 2n$ ) in Weissenberg photographs suggest that the space group is either  $P2_1$  or  $P2_1/m$ . The cell dimensions, which we determined from a least squares analysis of the positions of nineteen independent reflections, are  $a = 9.081 \pm 0.002 \text{ \AA}$ ,  $b = 8.176 \pm 0.002 \text{ \AA}$ ,  $c = 5.868 \pm 0.001 \text{ \AA}$  and  $\beta = 91.29 \pm 0.01^\circ$ . Intensity data were collected on a GE-XRD5 goniostat equipped with a scintillation counter, a Eulerian cradle goniostat and a Zr-filtered Mo x-ray source. The backgrounds were estimated from a plot of the background as a function of the Bragg scattering angle. Of the 818  $hkl$  and  $hk\bar{l}$  data collected by peak counting methods at a  $4^\circ$  takeoff angle and with  $2\theta \leq 50^\circ$ , 755 had net counts above the background. The intensities of four reflections at  $\chi = 90^\circ$  were each measured at several  $\varphi$  values. Since the spread in intensity for each reflection was less than 9%, we did not make an absorption correction. The crystal decay, measured by periodic measurements of two standard reflections, was negligible.

We used the atomic scattering factors of Cromer and Mann (1968) for the non-hydrogen atoms and those of Stewart, Davidson and Simpson

(1965) for the hydrogen atoms. The anomalous scattering factors of Cromer (1965) were used for the iodine ( $\Delta f' = -0.64 e$ ,  $\Delta f'' = 2.15 e$ ). Our least squares techniques, weighting scheme, and computer programs are identical to those described in previous chapters. Five percent of the intensity was included in the uncertainty of the intensity measurements.

### Solution and Refinement of the Structure

The structure was originally solved by Patterson techniques from a set of goniostat data obtained by W. G. Quarles in 1962. We found it necessary to discard approximately one fourth of the data set whose intensities differed from those on a set of films.

When we fixed the  $y$  coordinate of the iodine atom at  $y = \frac{1}{4}$ , the nitrogen atom and the carbon atom of one methyl group also had  $y$  coordinates of  $\frac{1}{4}$  within their standard deviations. In addition the other two methyl carbon atoms were related by a pseudo-mirror plane. The other three atoms heavier than hydrogen were off the pseudo-mirror plane by amounts of 0.2-0.5 Å which were far greater than the uncertainties in the  $y$ -coordinates. Thus we could exclude the possibility that the molecules crystallize in an ordered fashion in space group  $P2_1/m$ .

There are a number of other possibilities which must be considered in a final determination of the crystal structure. The molecules might be ordered on space group  $P2_1$ . More than one type of disorder must be considered. Twinning is a very real possibility since observations under the polarizing microscope indicated that most crystals were twinned. If the "single" crystal is twinned, the fraction in each of the two handednesses must be determined. Another possibility is that the single crystal is composed of many small domains of both handednesses, in which case it would be more appropriate to consider the molecule as being disordered in space group  $P2_1/m$ . In all of these cases, the atomic coordinates

of the atoms will be approximately the same. Thus the bond distances will be nearly the same in all cases.

The way to choose among these alternatives is to measure the amount of anomalous scattering. However, if the anomalous scattering is maximized, the absorption effects will also be maximized, and the large absorption will lead to an inaccurate structure. The two x-ray sources which we have used are copper whose  $\Delta f''$  is 6.68 e and absorption coefficient is  $292 \text{ cm}^{-1}$  and molybdenum whose  $\Delta f''$  is 2.15 e and absorption coefficient is  $37 \text{ cm}^{-1}$ .

In order to confirm the structure which we determined from the data of W. G. Quarles, we obtained a set of data using  $\text{CuK}\alpha$  radiation and peak counting methods. The molecular structure was the same, but the absorption effects were large enough to limit severely the accuracy of our structure determination. We measured a second set of data with  $\text{MoK}\alpha$  radiation. This set is described in the previous section. The third and last data set was taken at the USDA Western Region Laboratories with the help of Dr. K. Palmer. We used scanning techniques and  $\text{CuK}\alpha$  radiation to measure the intensities of all Bijvoet pairs of reflections out to  $2\theta \cong 145^\circ$ . We found it necessary to enclose the crystal in a capillary since the aged crystals were more hygroscopic. The x-ray absorption effects were severe enough to produce a factor of 2.8 in the ratio of the highest to lowest intensity of several reflections at  $\chi = 90^\circ$  as the  $\phi$  value was altered. During the two weeks which it took to collect

the data, the intensity of one standard decreased monotonically by fifteen per cent. The intensities of the other two standards increased by ten and twenty per cent in the first week and then began to decrease. We interpret this as both decay of the crystal and an increase in the mosaicity of the crystal which tends to increase intensity. The resultant data set contained intensities for Laue-symmetry related reflections which differed by as much as 30%.

Based on the structure derived from the second data set, we have calculated that the magnitude of the anomalous scattering effect will be at most two or three  $\sigma(F_0)$  if 5% of the intensity is included in  $\sigma(I)$ . Thus the errors in the third set of data precluded the possibility of obtaining not only an accurate structure but also a resolution of the space group problem. Since the second data set, which was obtained with  $\text{MoK}\alpha$  radiation, had both the smallest absorption effects and the most reliable intensity measurements, we used it in the subsequent analysis to obtain an approximate molecular structure and packing arrangement.

An R-value based on the positions and the anisotropic temperature factors of eight atoms heavier than hydrogen was 0.043. When we included the hydrogen atoms in the calculation but did not refine them, the discrepancy index dropped to 0.039 for the 755 non-zero data and to 0.047 for all 817 data. The weighted discrepancy index was 0.048 and the standard deviation of an observation of unit weight was 1.17. There was no systematic trend in  $w(\Delta F)^2$  as a function either of the intensity or Bragg scattering angle.

## Results and Discussion

The observed and calculated structure factor amplitudes are listed in Table 1, and the molecular numbering scheme for all atoms heavier than hydrogen is depicted in Figure 1. Hydrogen atoms H(1)-H(3) are attached to C(1), H(4)-H(6) to C(2), H(7)-H(9) to C(3), H(10) and H(11) to C(4), H(12) and H(13) to C(5) and H(14) to the oxygen atom. The final atomic coordinates for all the atoms are listed in Table 2, and the anisotropic temperature factors of all atoms heavier than hydrogen are given in Table 3. The temperature factors for all the hydrogen atoms were fixed at 5.0.

We present the intramolecular bond distances and angles in Table 4. They are listed merely as a matter of record since they undoubtedly suffer from the systematic errors which result from our ignorance of the amount of twinning and disorder. Slightly more plausible C-N distances are obtained if the nitrogen atom is on the other side of  $y = \frac{1}{4}$ , but when we tried refining the structure with this parameter changed, the  $y$ -coordinate of the nitrogen refined in one cycle back to its original position. The  $y$  coordinates of the atoms differ from  $y = \frac{1}{4}$  by the amounts (in Å):  $0.10 \pm 0.03$  for N,  $0.02 \pm 0.03$  for C(1),  $0.36 \pm 0.01$  for C(4),  $0.58 \pm 0.02$  for C(5) and  $0.16 \pm 0.05$  for O. If atom C(2) were to be reflected through the pseudo-mirror plane at  $y = \frac{1}{4}$ , it would be  $0.16 \pm 0.07$  Å away from atom C(3).





Table 2. Final Atomic Coordinates of All Atoms in the Asymmetric Unit of Crystals of Choline Iodide.

The positions of hydrogen atoms were not refined.

ATOM	X	Y	Z
I	-.27751(6)	1/4	1.1440(1)
O	.0734(8)	.269(5)	.929(1)
N	.2769(8)	.262(4)	.480(1)
C(1)	.371(1)	.248(3)	.691(2)
C(2)	.314(4)	.092(4)	.337(5)
C(3)	.306(2)	.390(4)	.345(3)
C(4)	.116(1)	.206(1)	.538(2)
C(5)	.047(1)	.321(2)	.704(2)
H(1)	.3646	.1430	.7905
H(2)	.3406	.3409	.7836
H(3)	.4743	.2669	.6545
H(4)	.2552	.0797	.1886
H(5)	.3126	-.0126	.4209
H(6)	.4157	.1088	.2907
H(7)	.2557	.4895	.4037
H(8)	.2640	.3584	.1943
H(9)	.4139	.4061	.3145
H(10)	.0694	.2050	.3838
H(11)	.1251	.0921	.5976
H(12)	.0841	.4324	.6651
H(13)	-.0600	.4128	.6631
H(14)	-.0291	.2722	.9909

Table 3. Anisotropic Thermal Parameters (in Å).

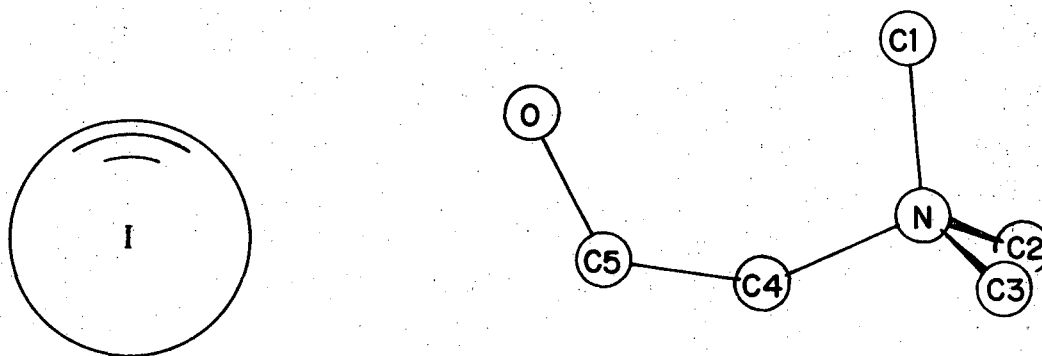
The form of the anisotropic thermal ellipsoids was the same as in previous chapters of this study.

ATOM	B11	B22	B33	B12	B13	B23
I	4.14(3)	4.13(3)	5.00(3)	.16(9)	.86(2)	-.3(1)
O	3.6(3)	11.9(14)	3.7(3)	-.2(8)	.6(2)	-.5(8)
N	3.9(3)	4.0(5)	3.0(3)	-.1(9)	.3(2)	-1.3(10)
C(1)	4.8(5)	6.1(7)	3.6(4)	3.7(9)	-.5(3)	-1.4(10)
C(2)	10.1(15)	3.1(7)	7.2(13)	-.6(7)	.8(10)	-2.0(7)
C(3)	3.9(8)	4.5(12)	3.0(9)	-.1(6)	.0(6)	-1.4(8)
C(4)	3.9(4)	3.8(7)	4.0(4)	-.5(3)	.3(4)	-.2(3)
C(5)	4.1(5)	6.1(7)	5.9(6)	1.3(5)	1.0(5)	.6(5)

Table 4. Selected Intramolecular Distances and Angles in  
Choline Iodide.

<u>Atoms</u>	<u>Distance (Å)</u>	<u>Atoms</u>	<u>Angle (Degrees)</u>
I...O	3.457(7)	C(1)-N-C(2)	104(2)
O-C(5)	1.40(2)	C(1)-N-C(3)	115(2)
N-C(1)	1.50(1)	C(1)-N-C(4)	108(1)
N-C(2)	1.66(4)	C(2)-N-C(3)	108(3)
N-C(3)	1.35(4)	C(2)-N-C(4)	94(2)
N-C(4)	1.58(2)	C(3)-N-C(4)	123(2)
C(4)-C(5)	1.50(2)	N-C(4)-C(5)	111(2)
O...N	3.26(1)	C(4)-C(5)-O	111(3)
O...C(1)	3.08(1)	C(5)-O...I	102(1)

Figure 1. Molecular numbering scheme for choline iodide.

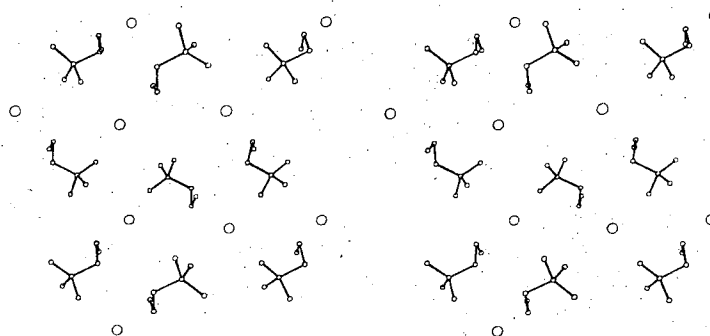


XBL 6911-6543

The molecular orientations of the choline cation in choline chloride and choline iodide are nearly identical. In both cases the oxygen atom is as far away as possible from the nitrogen atom and therefore extended towards the halide ion. The intramolecular distances from O to C(1) and to N in these two crystals are the same within experimental error (3.07 and 3.26 Å, respectively).

The packing in choline iodide is almost exclusively between iodide and choline ions. The only choline-choline heavy atom intermolecular distance less than 3.5 Å is the O...C(3) distance of  $3.34 \pm 0.02$  Å. The crystal packing of choline iodide is shown in Figure 2.

Figure 2. Stereoscopic view of the crystal packing of choline chloride. The view is down the  $c$  axis.



Choline Bromide

Because the crystals of choline bromide are very hygroscopic, we mounted single crystals in Lindemann or quartz capillaries under a nitrogen atmosphere in a dry box. From measurements on the goniostat of the d-spacings of the  $h00$ ,  $0k0$  and  $00l$  lines with Zr-filtered Mo radiation, we determined that the cell dimensions are  $a = 19.58 \pm 0.01$ ,  $b = 7.311 \pm 0.007$  and  $c = 5.682 \pm 0.004$ . These unit cell dimensions are within experimental error of those determined by Senko and Templeton (1960). We confirm that the probable space group is one of the orthorhombic pair  $Pna2_1$  or  $Pnam$ , depending on whether or not a center of symmetry is present.

A full set of intensity data was recorded on film with Ni-filtered Cu radiation. During the seventy hours that it took to record a lineup oscillation photograph and the  $h0l-h4l$  Weissenberg layers, we noticed that the shape of the spots became more diffuse and that extra spots appeared on the x-ray pattern. We present in the accompanying Figures reproductions of lineup pictures and zero layer Weissenberg pictures taken both at the beginning of the experiment and after seventy hours of x-ray exposure. The powder pattern lines and reflections which appear seem to be correlated with the molecular radiation damage. Since decomposition of choline bromide is slower than that of choline chloride, we tend to agree with the suggestion of Senko and Templeton (1960) that the structure of choline chloride which they determined is a time

average study of decomposed and undecomposed molecules. The structure of undecomposed choline chloride and bromide molecules could be determined only at room temperature with the use of many crystals or at low temperature.



Figure 1. Initial lineup and zero-layer Weissenberg photographs for choline bromide.

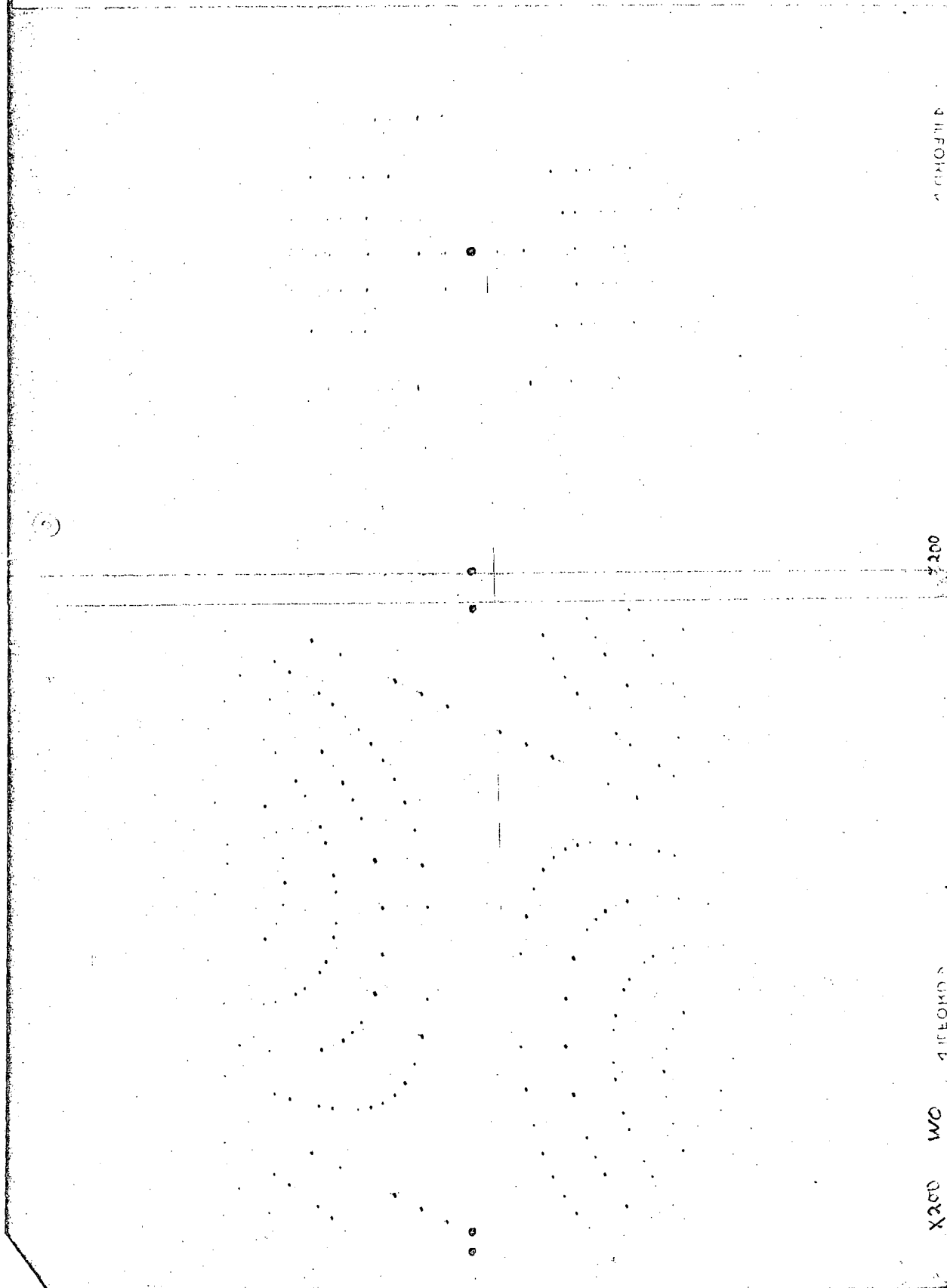
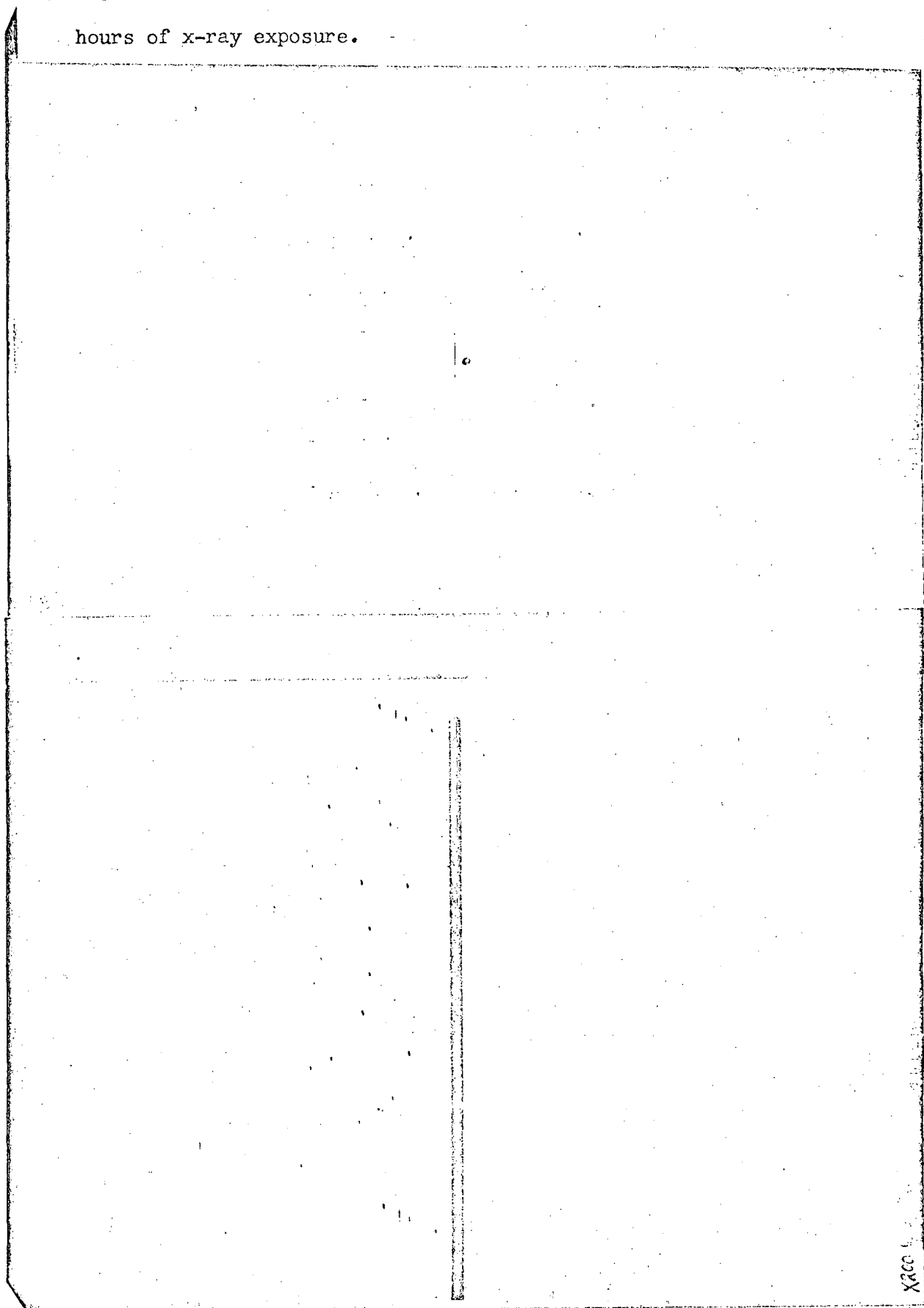


Figure 2. Photographs of choline bromide taken after seventy hours of x-ray exposure.



XACC

### Phosphonium Analogue

We have obtained a lineup picture as well as the hk0, hk1 and hk2 level Weissenberg pictures of the phosphonium analogue of choline chloride, i.e.  $[(\text{CH}_3)_3\text{PCH}_2\text{CH}_2\text{OH}]^+ \text{Cl}^-$ . The crystals were quite poor and were mounted in capillaries under a nitrogen atmosphere. Nevertheless, by using Ni-filtered  $\text{CuK}\alpha$  radiation, we have determined that the cell dimensions are  $a = 12.09 \pm 0.04$ ,  $b = 10.36 \pm 0.04$  and  $c = 6.90 \pm 0.04$  with four molecules in the unit cell. The probable space group is either  $\text{Pna}2_1$  or  $\text{Pnam}$ . Since choline chloride and its phosphonium analogue crystallize in different space groups, their packing arrangements must be different.

### Mechanism for the Decomposition of Choline Chloride

The amount of room available for atomic movement in the solid state is very small. A necessary condition for molecules in the solid state to be unstable to radiation is that there exist decomposition products which can be formed without a large amount of movement. In the absence of this condition, we would expect the converse. For betaine hydrochloride there do not exist stable products which would result from a cleavage, and crystals of betaine hydrochloride are stable to radiation. Although the molecule  $[(\text{CH}_3)_3\text{NCH}_2\text{CH}_2\text{CH}_2\text{OH}]^+ \text{Cl}^-$  could form the propanal and trimethylamine molecules, the extra methylene group of the parent compound probably prevents the migration of hydrogen atoms in the rearrangement to the stable products, and this molecule also is stable to radiation.

In order to be very radiation sensitive, the molecules must be arranged in a way which is conducive to a chain reaction. Of the four analogues of choline chloride which we have studied, none has the same space group symmetry and therefore packing arrangement as the choline chloride. A clue to the type of uniqueness of choline chloride came from radiation labeling studies of choline chloride, in which Lemmon and Smith (1963) found that almost all of the atomic migration involved only the hydrogen atoms of the  $-\text{CH}_2\text{CH}_2\text{OH}$  (Ac') group. We explored the possibility that those hydrogen atoms are involved in the chain mechanism.

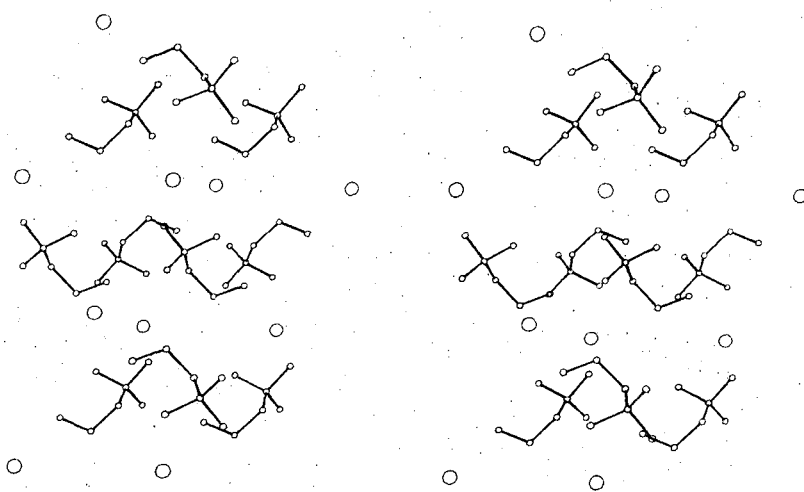
We have previously located and listed the atomic positions of the hydrogen atoms in betaine hydrochloride. We were able to calculate the probable locations of the five Ac' hydrogen atoms in choline chloride and iodide by using the conventional tetrahedral geometry for carbon atoms C(4) and C(5) and by assuming that the hydroxyl hydrogen atoms are hydrogen-bonded to the halide atoms.

The shortest C...H and O...H distances involving only the Ac' groups in these three molecules are: 2.72 Å for both C(4)...H(13) and O...H(10) in choline iodide, 2.98 Å for O(2)...H(11) in betaine hydrochloride, and 2.76 Å for O...H(11) and 2.51 Å for O...H(10) in choline chloride. The last-mentioned distance is interestingly shorter than the others, and the C(4) atom to which H(10) is attached is at a distance of 3.506 Å from the oxygen atom. Thus this hydrogen atom is pointed almost directly towards the oxygen atom. In fact the C-H...O angle is 172°. We are induced to suggest that these atoms are involved in the propagation steps of the chain reaction mechanism.

If the proton of H(10) jumps to the oxygen atom of the neighboring molecule in one of these chain propagating steps, a carbanion is left behind. The hydrogen atoms on Ac' could migrate until the negative charge rests on the oxygen atom of the Ac'. This negatively-charged oxygen atom could, in turn, induce another H(10) atom to migrate from the next adjoining molecule.

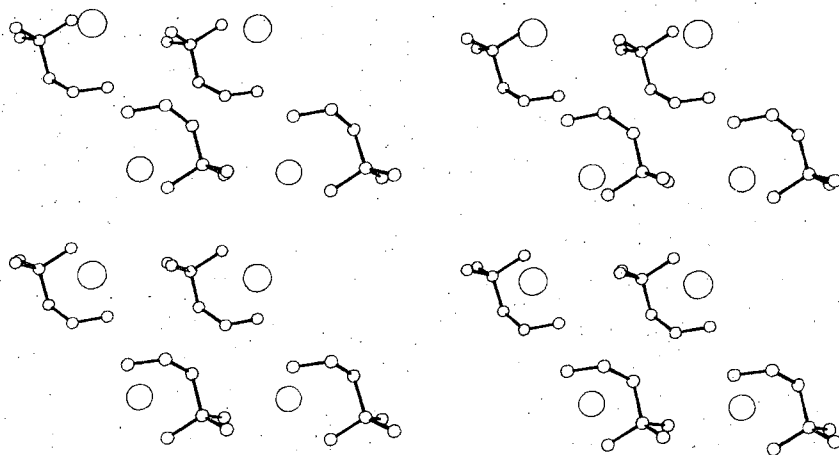
Two views of the crystal packing of choline chloride are presented in Figures 1 and 2.

Figure 1. Stereoscopic view of the crystal packing of choline chloride. The view is down the  $a$  axis.



163-091-170

Figure 2. Stereoscopic view of the crystal packing of choline iodide. The view is down the b axis.



XBL 6911-5544

Lindblom, Lemmon and Calvin (1961) have reported that the saturation damage in choline chloride is 17%. In our proposed mechanism, the proton is passed between molecules related by the  $2_1$  screw axis in the  $z$  direction. As the chain of molecules decomposes, the position of the molecules in adjacent chains may be altered enough to make them immune to further damage.

The normal behavior of the choline iodide results from a packing arrangement in which  $Ac^+$  groups are too far apart for protons to jump between the molecules. We predict that the choline bromide, which has a radiation sensitivity intermediate between the chloride and iodide, will have a  $H(10)\cdots O$  distance which is 2.55-2.65 Å. More x-ray crystallographic work on the choline bromide is necessary to check this prediction.



References

- S. Abrahamsson and I. Pascher, Acta Cryst., 21, 79 (1966).
- F. G. Canepa, P. Pauling and H. Sorum, Nature, 210, 907, (1966).
- J. Clastre, C. R. Acad. Sci., Paris, 259, 3267 (1964).
- R. L. Collin, J. Amer. Chem. Soc., 79, 6086 (1957).
- D. T. Cromer, Acta Cryst., 18, 17 (1965).
- D. T. Cromer and J. B. Mann, ibid., A24, 321 (1968).
- R. P. Hurst and F. A. Matsen, ibid., 12, 7 (1959).
- F. Jellinek, ibid., 10, 277 (1957).
- C. K. Johnson, ORTEP, A Fortran Thermal-Ellipsoidal Plot Program for Crystal-Structure Illustrations, ORNL-3794, revised.  
Oak Ridge, Tennessee.
- R. M. Lemmon, M. A. Parsons, D. M. Chin, J. Amer. Chem. Soc., 77,  
4139 (1955).
- R. M. Lemmon, P. K. Gordon, M. A. Parsons and F. Mazzetti, ibid.,  
80, 2730 (1958).
- R. M. Lemmon and M. A. Smith, ibid., 85, 1395 (1963).
- Y. Okaya, Abstracts American Crystallographic Association Annual  
Meeting, Bozeman, Montana, July 1964, p 54.
- M. E. Senko and D. H. Templeton, Acta Cryst., 13, 281 (1960).
- I. Serlin, Science, 126, 261 (1957).

R. F. Stewart, E. R. Davidson and W. T. Simpson, J. Chem. Phys., 42, 3175 (1965).

M. Sundaralingam and L. H. Jensen, Science, 150, 1035 (1965).

B. M. Tolbert, P. T. Adams, E. L. Bennett, A. M. Hughes, M. R. Kirk, R. M. Lemmon, R. M. Noller, R. Ostwald and M. Calvin, J. Amer. Chem. Soc., 75, 1867 (1953).

B. M. Tolbert and R. M. Lemmon, Radiat. Res., 3, 52 (1955).

OTHER BIO-ORGANIC COMPOUNDS

R. F. Stewart, E. R. Davidson and W. T. Simpson, J. Chem. Phys., 42,  
3175 (1965).

M. Sundaralingam and L. H. Jensen, Science, 150, 1035 (1965).

B. M. Tolbert, P. T. Adams, E. L. Bennett, A. M. Hughes, M. R. Kirk,  
R. M. Lemmon, R. M. Noller, R. Ostwald and M. Calvin, J. Amer.  
Chem. Soc., 75, 1867 (1953).

B. M. Tolbert and R. M. Lemmon, Radiat. Res., 3, 52 (1955).

Crystal and Molecular Structure of 7-Chloromercurinaphthalene-1-sulphonyl Fluoride, A Possible Protein Label

169

Fenselau et al (1967) have proposed that chloromercurinaphthalene-sulphonyl fluorides,  $C_{10}H_6HgClSO_2F$ , be employed as heavy atom labels for x-ray structural work on proteins. The sulphonyl fluoride, the reactive group of the label, has been demonstrated to react with the active site of the hydroxyl group of the serine residue of the protein chymotrypsin (Weiner and Koshland, 1965). The utility of these naphthalene derivatives as labels is derived from several factors. 1) Their selective reactivity necessitates determining the heavy atom positions for only a small number of sites. 2) Their covalent linkage ensures both an occupancy factor close to 1.0 and a relatively high contribution to the high-angle diffraction data. 3) Several isomers have been synthesized, e.g. the 4,1-, the 5,1-, the 7,1-, and the 5,2- derivatives (Fenselau et al, 1967), and any of these can be used as a label.

In the synthesis of several of the isomers, an amino group is converted to a diazonium salt and then replaced by the chloromercuric group through the mechanism of an  $S_N1$  reaction. It was possible, however, that the positive charge of the carbonium ion intermediate had migrated, resulting in an unexpected isomer. A single crystal x-ray analysis was undertaken to determine whether or not the actual isomer was the expected one. In addition, more detailed knowledge of the structure of these labeling compounds could be of use in the solution of labeled protein structures.

### Experimental

Samples of the 4,1- and 7,1- derivatives, both crystallized from dioxane, were obtained from Dr. D. Portsmouth and Prof. D. Koshland. The cell dimensions, determined from Weissenberg film data for the 4,1- derivative and from careful measurements of the  $h00$ ,  $0k0$ ,  $00l$ ,  $h0h$ , and  $\bar{h}0h$  reflections on a manual Eulerian cradle goniostat for the 7,1- derivative, are listed in Table 1. The probable space groups were determined from systematic absences on Weissenberg pictures. The densities were determined by flotation in mixtures of 1,2-dibromoethane and 1,1,2,2-tetrabromoethane.

The crystal of 7,1-chloromercurinaphthalene-1-sulfonyl fluoride, which was cut from a larger crystal and used for the data taking, was wedge-shaped. Its average height, width and thickness were 0.26, 0.14 and 0.065 mm, respectively. It was mounted on the reciprocal  $c$  axis. The integrated intensities of all data within half of a sphere in reciprocal space of radius  $d = 0.84 \text{ \AA}$  ( $2\theta \leq 50^\circ$ ) were obtained by a  $\theta$ - $2\theta$  scan technique using Zr filtered molybdenum radiation ( $\text{Mo K}\alpha_1$ ,  $\lambda = 0.70926$ ). A General Electric XRD-5 goniostat equipped with a DATEX card reader and a Eulerian cradle goniostat was employed to collect the intensity data. The decay of the crystal ( $\sim 10\%$  in the course of the data-taking) was monitored by periodic measurements of the intensities of three standard reflections. All data later were scaled up in order to keep the average intensity of these three reflections the same.

Table 1. Unit cell parameters for two chloromercurinaphthalene sulfonyl fluoride (CMNSF) derivatives.

	<u>7,1-CMNSF</u>	<u>4,1-CMNSF</u>
a	9.725 ± 0.003	17.50 ± 0.06
b	6.836 ± 0.002	4.92 ± 0.02
c	8.351 ± 0.003	13.13 ± 0.05
α	90.	90.
β	90.99 ± 0.03	104. ± 1.
	90.	90.
Z	2	4
d <sub>obs</sub>	2.64 ± 0.02	2.65 ± 0.02
d <sub>cal</sub>	2.66	2.63
Space Group	P2 <sub>1</sub> or P2 <sub>1</sub> /m	C2, Cm or C2/m

The crystal surfaces were approximated by the  $(100, \overline{11}, 1, 0)$ ,  $(051)$ ,  $(0\overline{2}1)$ ,  $(527)$ , and  $(4\overline{1}6)$  planes in the correction for absorption ( $\mu = 145.6 \text{ cm}^{-1}$  for Mo K $\alpha$  radiation). The crystal dimensions and face indices were first estimated from measurements made under a light microscope. The intensities of the 001, 002, and 007 reflections at  $\chi = 90^\circ$  were each measured at 24 different phi values. The crystal dimensions and face indices then were adjusted by small amounts until the spreads in intensities after the absorption correction for the three reflections were reduced from factors of 2.27, 2.32, and 2.27 to 1.17, 1.15, and 1.15, respectively.

The atomic scattering factors used in the analysis were those of Stewart, Davidson and Simpson (1965) for the hydrogen atoms and those of Cromer and Mann (1968) for the Hg, Cl, S, F, O, and C atoms. In addition, average scattering factors used to approximate the F and O atoms of a completely disordered sulfonyl fluoride group were calculated by using the relationship  $f(\text{OF}) = [ 2f(\text{O}) + f(\text{F}) ] / 3$ . For a partially disordered sulfonyl fluoride group, the scattering factors of the 1:1 fluorine-oxygen atoms were calculated:  $f(\text{FO}) = [ f(\text{F}) + f(\text{O}) ] / 2$ . The anomalous dispersion corrections of Cromer (1965) were used for the Hg, Cl, and S atoms.

The full-matrix least squares program used was our local unpublished version for the CDC 6600 computer. The function minimized was  $(R_2)^2 = \sum_w ( |kF_o| - |F_c| )^2 / \sum_w |kF_o|^2$ , where  $F_o$



and  $F_c$  are the observed and calculated structure factors and the weight  $w = 0$  if  $I = 0$ . If the intensity  $I > 0$ , the weights were calculated from the larger of the counting statistics and the difference between duplicate measurements (DeBoer, Zalkin and Templeton, 1968). Other programs used in this analysis include ORTEP (Johnson, 1965), a thermal ellipsoid plotting program, and HORSE, our modified version of Hamilton's absorption correction program.

### Structure Determination

The positions of all the atoms heavier than hydrogen were deduced from a three dimensional Patterson function which was based on the data uncorrected for absorption. The structure consists of the naphthalene ring and the Hg, S, and Cl atoms with equal or nearly equal  $y$  values. In addition, the sulfonyl fluoride is arranged in such a way that one atom is nearly or exactly in the plane of the naphthalene ring. The other two atoms of the sulfonyl fluoride have the same or nearly the same  $x$  and  $z$  coordinates, but they are (approximately or exactly) equidistant from the naphthalene plane and on opposite sides. The structure, then, corresponds to either the molecule located precisely on the mirror plane in space group  $P2_1/m$  with two atoms related by the mirror plane or the molecule located nearly on a pseudo-mirror plane in space group  $P2_1$ . The central crystallographic problem was to decide between these two alternatives. In order to choose between the two alternatives, we analyzed anomalous scattering, deviations from pseudosymmetry, thermal motion and the agreement between the observed and calculated data.

Six hydrogen atoms were included in all least squares refinements at fixed positions of 1.0 Å from their respective carbon atoms. They were initially assigned a group isotropic temperature factor which was fixed at 5.0 Å<sup>2</sup>. No distinction was made between the fluorine and oxygen atoms at this stage.

Three trial structures were refined in space group  $P2_1$ : the first had all atoms of the naphthalene ring and the chlorine atom on one side of the plane  $y = \frac{1}{4}$  (the  $y$  coordinate of the Hg atom was fixed at  $y = \frac{1}{4}$  for all refinements); the second trial structure had the chlorine atom and naphthalene ring on opposite sides of the plane; and the third trial structure had both the naphthalene and chlorine on the same side of the plane but the  $y$  coordinates switched for the two sulfonyl fluoride atoms related by the pseudo-mirror plane. Both the second and third trial structures refined in one cycle to the same molecular configuration as the first trial structure. This was achieved for the second trial structure by the shift of the  $y$  coordinate of the chlorine atom to the other side of the mirror plane and for the third trial structure by the adjustment of the  $x$  and  $z$  coordinates of the two sulfonyl fluoride atoms related by the pseudo-mirror plane. Thus it is sufficient to analyze the results of the refinement of the first trial structure in the discussion of space group  $P2_1$ .

The analysis of anomalous scattering for the molecular structure of space group  $P2_1$  indicates that the deviation from the centric space group  $P2_1/m$  is not meaningful. The rms difference between the calculated values of  $F(hk\ell)$  and  $F(h\bar{k}\ell)$  is  $0.465 \bar{\sigma}(F_0)$ , and the rms spread in the observed pairs of data between  $F(hk\ell)$  and  $F(h\bar{k}\ell)$  is  $1.459 \bar{\sigma}(F_0)$ , where  $\bar{\sigma}(F_0)$  is the averaged standard deviation for the pair of reflections. Thus the random and systematic errors

in the data are more than three times as much as the effect of the anomalous scattering. For the 28 pairs of reflections whose calculated values of  $|F(\underline{hkl}) - F(\underline{h\bar{k}l})|$  are greater than  $\bar{\sigma}(F_o)$ , the observed difference between pairs is of opposite sign for seven pairs and of smaller magnitude for fifteen of the remaining 21 pairs.

None of the refined atomic positions of space group  $P2_1$  differ from the centric symmetry of space group  $P2_1/m$  by much more than the standard deviations. The oxygen atoms differ from mirror symmetry by only 0.054 Å while the uncertainty in the position of each is 0.027 Å. For the thirteen atoms (excluding the Hg atom fixed at  $y = \frac{1}{4}$ ) nearly on the mirror plane, the rms distance from the plane at  $y = \frac{1}{4}$  is 0.042 Å. The largest distance for any of these atoms is 0.065 Å for atom C(2) but this is only 2.7 times the uncertainty in its  $y$  coordinate. These distances are small in comparison with the 0.264 Å amplitude of thermal motion for the thirteen atoms perpendicular to the  $ac$  plane. Thus the atoms are better described mathematically by a model of large anisotropic thermal motion perpendicular to the plane than by a model with disordered atoms.

The conventional R-value, defined as  $R = \Sigma || F_o | - |F_c || / \Sigma(F_o)$ , was calculated for the two structures in the two space groups and was based on two different data sets. For the centric space group  $P2_1/m$ , the  $\underline{hkl}$  and  $\underline{h\bar{k}l}$  data were averaged, but for the non-centric

space group  $P2_1$ , they were not. The group isotropic temperature factor for hydrogen atoms was refined to  $4.27 \text{ \AA}^2$  at which value it was held fixed in all subsequent refinements. The values of  $R_{\text{cen}}$  and  $R_{\text{non}}$ , where  $R_{\text{cen}}$  is the conventional R value for the centric structure using centric data and refined in space group  $P2_1/m$  and  $R_{\text{non}}$  is for the corresponding structure in space group  $P2_1$ , were 0.078 and 0.071, respectively. After the data were corrected for absorption,  $R_{\text{cen}} = 0.0267$  and  $R_{\text{non}} = 0.0296$ . Thus the agreement between observed and calculated data is not significantly better for the molecule refined in space group  $P2_1/m$ .

For the above reasons, we have decided that the 51 extra parameters needed to describe the molecule in space group  $P2_1$  rather than  $P2_1/m$  are not sufficiently worthwhile to justify their use. All subsequent description of the results and the discussion will be for the space group  $P2_1/m$ .

The atomic scattering factors used for the oxygen and fluorine atoms were the averaged ones calculated as mentioned above. The possibilities that the sulfonyl fluoride was completely ordered or only partially disordered were investigated. For the completely ordered sulfonyl fluoride, the scattering factors of fluorine were used for the atom on the mirror plane and those of oxygen for the other two mirror-related sulfonyl fluoride atoms. The result was an increase in the discrepancy index from 0.0266 to 0.0273. For the model with a partially disordered sulfonyl fluoride group, one

oxygen atom is ordered on the mirror plane but the other oxygen and the fluorine atoms are disordered at the other site. For the partial disorder model, the discrepancy index is 0.0269. For all three models, the molecular distances and angles are the same within the experimental precision. Since the data do not discriminate among the three models, we were forced to choose the partial disorder as the correct model on the basis of the interatomic bond distances (vide infra). All atomic coordinates and bond parameters mentioned below are for the description with the sulfonyl fluoride partially disordered.

The atomic coordinates were refined until the maximum shift was less than one per cent of its standard deviation. The final R-value is 0.0269 for the 1034 observed and 0.0281 for the 1055 zero and nonzero data. The  $R_2$  value is 0.031, and the standard deviation of an observation of unit weight is 1.04. There is no systematic trend in  $w(\Delta F)^2$  as a function of either the intensity or the Bragg scattering angle. On the difference Fourier map based on the final structure, the highest three peaks with electron density ranging from 0.75-1.05 e/Å<sup>3</sup> are due to anisotropies in the thermal motion of the mercury atom.

## Results and Discussion

The observed and calculated structure factors are listed in Table 2, and the numbering scheme used in this analysis is depicted in Figure 1. From the data we have derived the atomic fractional coordinates of all atoms in the asymmetric unit (Table 3) and the anisotropic thermal motion of all atoms heavier than hydrogen (Table 4). The bond distances and bond angles which we have derived from the atomic coordinates are listed in Tables 5 and 6, respectively.

We have confirmed that the crystal is composed of molecules of the 7,1-isomer of chloromercurinaphthalenesulfonyl fluoride as was originally expected. The molecule lies on the mirror<sup>plane</sup>, a special position of space group  $P2_1/m$ . The rms average magnitude of thermal motion is greatest for the chlorine, fluorine and oxygen atoms and least for the carbon atoms. The directions of the thermal motion of the fluorine and oxygen atoms suggest a small amount of libration of the sulfonyl fluoride group around bond S-C(1).

In order to determine the degree of order in the sulfonyl fluoride group, we analyzed its bond distances. Although, to our knowledge, the structure of no other sulfonyl fluoride has been determined in detail, the S-O and S-F distances can be estimated from the results of two other separate structure determinations. The two S-O bond lengths in a p-bromobenzenesulfonyl glucal molecule were found to be 1.38(2) and 1.42(2) Å (Camerman and Trotter, 1965).

Table 2. Observed and calculated structure factor amplitudes of 7-chloromercurinaphthalene-1-sulfonyl fluoride.

Asterisks indicate zero-weighted data.

TABLE OF OBSERVED AND CALCULATED STRUCTURE FACTORS FOR 7-CHLOROMERCURINAPHTHALENE-1-SULFONYL FLUORIDE.

Table with multiple columns containing numerical data for observed and calculated structure factor amplitudes, including indices like h, k, l and values for F\_obs and F\_calc.



Table 3. Final atomic fractional coordinates and their estimated standard deviations for all the atoms of 7-chloromercurinaphthalene-1-sulfonyl fluoride.

The numbers in parentheses here and in succeeding tables indicate the estimated standard deviations of the least significant digit(s).

ATOM	X	Y	Z
HG	.11872(3)	1/4	.05207(4)
CL	-.0216(2)	1/4	-.1729(3)
S	.7103(2)	1/4	.1918(3)
O	.8529(6)	1/4	.2227(8)
FO	.6641(5)	.0775(6)	.0998(5)
C(1)	.6216(7)	1/4	.3697(9)
C(2)	.6997(8)	1/4	.509(1)
C(3)	.6388(9)	1/4	.655(1)
C(4)	.4969(8)	1/4	.6656(9)
C(5)	.2690(8)	1/4	.536(1)
C(6)	.1875(7)	1/4	.4022(9)
C(7)	.2447(8)	1/4	.2490(9)
C(8)	.3869(7)	1/4	.2337(9)
C(9)	.4744(7)	1/4	.3714(8)
C(10)	.4129(7)	1/4	.5257(9)
H(2)	.8022	1/4	.5039
H(3)	.6973	1/4	.7543
H(4)	.4534	1/4	.7729
H(5)	.2258	1/4	.6437
H(6)	.0853	1/4	.4139
H(8)	.4281	1/4	.1248

Table 4. Anisotropic thermal parameters (in Å<sup>2</sup>) with their

estimated standard deviations for all atoms heavier than  
hydrogen in 7-chloromercurinaphthalene-1-sulfonyl fluoride.

The temperature factor has the form:  $T = \exp[ -\frac{1}{4} \sum \sum B_{ij} h_i h_j$   
 $/(b_i b_j) ]$ , where  $h_i$  is the Miller index,  $b_i$  is the  $i$ th

reciprocal axis length, and  $i$  and  $j$  are cycled 1 through 3.

ATOM	B11	B22	B33	B12	B13	B23
HG	2.21(2)	5.40(2)	3.95(2)	0	-.59(1)	0
CL	2.98(9)	10.6(2)	4.1(1)	0	-.99(8)	0
S	2.43(8)	6.9(1)	4.2(1)	0	.80(7)	0
O	2.6(3)	10.6(5)	5.4(2)	0	.9(3)	0
FO	5.2(2)	6.3(2)	5.8(2)	-.4(2)	1.4(2)	-1.7(2)
C(1)	1.8(3)	3.1(3)	3.3(3)	0	-.3(2)	0
C(2)	2.0(3)	3.2(3)	4.7(4)	0	-.9(3)	0
C(3)	3.7(4)	3.4(3)	3.5(3)	0	-1.4(3)	0
C(4)	3.1(3)	3.5(3)	3.2(3)	0	-.0(3)	0
C(5)	3.0(3)	4.2(3)	3.9(4)	0	.9(3)	0
C(6)	1.6(3)	4.3(3)	3.7(3)	0	.3(2)	0
C(7)	2.1(3)	3.3(3)	3.8(3)	0	-.5(3)	0
C(8)	2.1(3)	3.2(3)	3.0(3)	0	-.1(2)	0
C(9)	2.0(3)	2.9(3)	2.9(3)	0	-.0(2)	0
C(10)	2.8(3)	2.4(2)	3.2(3)	0	-.1(3)	0

Table 5. Intramolecular distances (in Å) in  
7-Chloromercurinaphthalene-1-sulfonyl Fluoride.

Standard deviations have been estimated by the  
 method of least squares and are indicated in  
 parentheses.

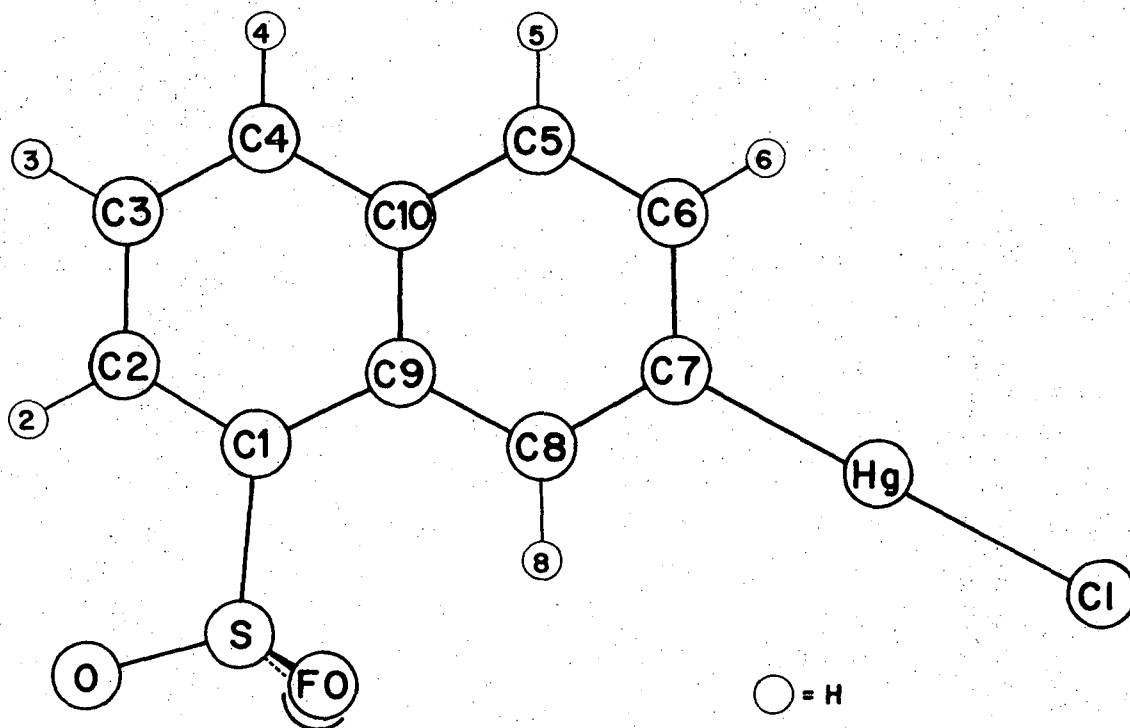
<u>Atoms</u>	<u>Distance</u>	<u>Atoms</u>	<u>Distance</u>
Hg-Cl	2.303(3)	C(5)-C(10)	1.403(11)
Hg-C(7)	2.033(8)	C(6)-C(7)	1.404(11)
S-O	1.406(7)	C(7)-C(8)	1.391(10)
S-FO	1.473(4)	C(8)-C(9)	1.419(10)
S-C(1)	1.731(7)	C(9)-C(10)	1.430(10)
C(1)-C(2)	1.377(11)	O...FO	2.399(7)
C(1)-C(9)	1.433(9)	O...C(1)	2.580(9)
C(2)-C(3)	1.363(12)	O...H(2)	2.41 <sup>a</sup>
C(3)-C(4)	1.384(12)	FO...FO	2.359(9)
C(4)-C(10)	1.41.(11)	FO...C(1)	2.583(7)
C(5)-C(6)	1.358(12)	FO...H(8)	2.59 <sup>a</sup>

<sup>a</sup> All hydrogen atoms held fixed.

Table 6. Intramolecular bond angles (in degrees) for7-Chloromercurinaphthalene-1-sulfonyl Fluoride.

<u>Atoms</u>	<u>Angles</u>	<u>Atoms</u>	<u>Angles</u>
Cl-Hg-C(7)	179.3(3)	C(5)-C(6)-C(7)	120.9(7)
O-S-FO	112.8(3)	Hg-C(7)-C(6)	119.6(4)
O-S-C(1)	110.3(5)	Hg-C(7)-C(8)	120.8(4)
FO-S-FO	106.3(2)	C(6)-C(7)-C(8)	119.6(7)
FO-S-C(1)	107.2(3)	C(7)-C(8)-C(9)	120.6(7)
S-C(1)-C(2)	116.7(4)	C(1)-C(9)-C(8)	125.3(7)
S-C(1)-C(9)	121.4(4)	C(1)-C(9)-C(10)	116.3(6)
C(2)-C(1)-C(9)	121.9(7)	C(8)-C(9)-C(10)	118.5(7)
C(1)-C(2)-C(3)	120.8(7)	C(4)-C(10)-C(5)	120.9(7)
C(2)-C(3)-C(4)	120.5(7)	C(4)-C(10)-C(9)	120.0(7)
C(3)-C(4)-C(10)	120.5(7)	C(5)-C(10)-C(9)	119.2(8)
C(6)-C(5)-C(10)	121.3(7)		

Figure 1. Numbering scheme for 7-chloromercurinaphthalene-  
-1-sulfonyl fluoride.



XBL 6910-5731

The S-F distance, determined by microwave spectroscopy, was found to be 1.585(1) Å in thionyl fluoride ( $\text{SF}_2\text{O}$ ) (Ferguson, 1954) and 1.57(1) Å in sulfuryl fluoride ( $\text{SF}_2\text{O}_2$ ) (Fristrom, 1952). The distance of  $1.406 \pm 0.007$  Å from the sulfur atom to the sulfonyl fluoride atom in the mirror plane in 7-chloromercurinaphthalene-1-sulfonyl fluoride is the same as S-O distances in the other structures. Moreover the distance of  $1.473 \pm 0.004$  Å from the sulfur atom to the  $\text{SO}_2\text{F}$  atom not in the molecular plane is the average of the S-F and S-O distances in the other molecules. It is on the basis of bond lengths that we have assigned the O and FO scattering factors to those atoms, since the data do not discriminate among the three possibilities. In the partially disordered model, which we feel corresponds most closely to the molecular orientation, the strongly electronegative fluorine atom is always near atom H(8).

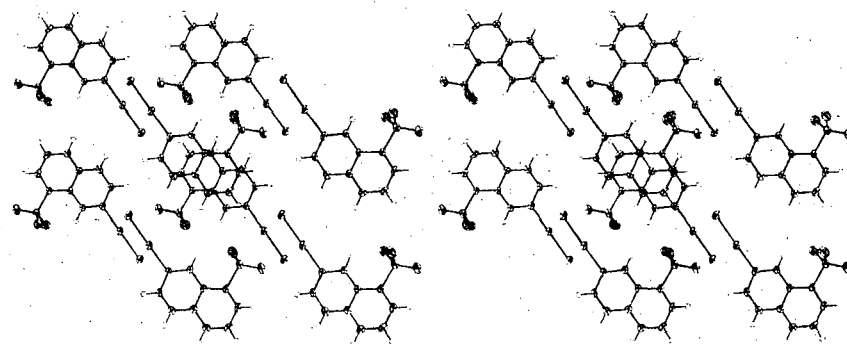
The partial disorder of the oxygen and fluorine atoms in the sulfonyl fluoride group may be due to a random mixture of two isomers of the molecule. In order for the sulfonyl fluoride to spin around the S-C(1) bond, the closest interatomic approach for the molecular geometry in this crystal would be 1.84 Å for atoms H(8) and an oxygen atom. This distance is 0.2 Å less than the sum of atomic "hard-shell" radii of the atoms (Bartell, 1960). Thus the barrier to rotation, at least in the solid state, is considerable. Even at the equilibrium position in the crystal, the repulsion between atom

H(8) and the sulfonyl fluoride group is sufficient to bend the sulfonyl fluoride group away from the hydrogen: the repulsion is manifested in the S-C(1)-C(9) angle of  $121.4 \pm 0.4^\circ$  which is larger than the  $116.7 \pm 0.4^\circ$  angle for atoms S-C(1)-C(2).

The molecules pack in sheets in the ac plane. The naphthalene rings in the sheets are related by centers of symmetry in such a way that there is almost complete overlap of rings in adjoining sheets (see Figure 2). The sheets are separated by a distance of  $\frac{1}{2} c$  or  $3.418 \pm .002 \text{ \AA}$ . There is just enough staggering of the overlapping naphthalene rings to increase the minimum intermolecular C-C distances to  $3.444 \pm 0.002 \text{ \AA}$  between atoms C(4) and C(9) and  $3.452 \pm 0.002 \text{ \AA}$  between atoms C(2) and C(5). All the other intermolecular carbon-carbon distances are greater than  $3.55 \text{ \AA}$ . In the projection down the b axis, the carbon atoms lie  $0.41 \text{ \AA}$  away from each other for the separation between C(4) and C(9),  $0.49 \text{ \AA}$  away for atoms C(2) and C(5), and greater than  $0.97 \text{ \AA}$  for the other atoms. Thus the large amounts of staggering result from the necessity to minimize intermolecular steric repulsion by slight increases of the intermolecular distances.

The forces holding the molecules together are the attractions between the electropositive mercury and hydrogen atoms and the electronegative chlorine, fluorine and oxygen atoms. Each mercury atom is adjacent to six neighboring molecules: two in the same sheet, two in the sheet above and two in the sheet below. Of the two molecules in the same sheet, only one molecule is close

Figure 2. Stereoscopic view of the packing of 7-chloromercuri-  
naphthalene-1-sulfonyl fluoride looking down the b axis.



NBL 690-5730



enough to be considered to be interacting and that contributes an O atom at a distance of  $2.973 \pm 0.006 \text{ \AA}$ . The other sheets each contribute a Cl and FO atom. The FO atom is  $0.35 \text{ \AA}$  closer to the Hg atom than the Cl atom and is out of the plane of the naphthalene rings towards the mercury atom. Each chlorine atom is adjacent to an H(3) atom in one molecule and an H(5) atom in another, all in the same sheet, and to two mercury atoms in adjacent sheets, one above and one below. These and other close intermolecular distances are listed in Table 7.

---

Table 7. Selected intermolecular distances (in Å) in crystals  
of 7-chloromercurinaphthalene-1-sulfonyl fluoride.

Carbon-carbon distances are for overlapping naphthalene rings.

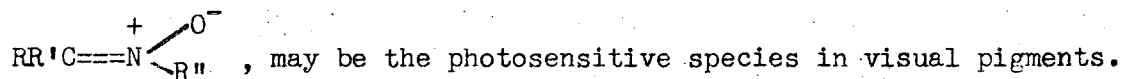
	<u>Atoms</u>	<u>Distance</u>
Hg	O	2.973(6)
	2 FO	3.343(4)
	2 Cl	3.691(2)
Cl	H(3)	2.79 <sup>a</sup>
	H(5)	2.88
	H(2)	3.17
O	H(6)	2.74
FO	H(4)	2.74
C(2)	2 C(5)	3.452(2)
	2 C(10)	3.599(2)
C(3)	2 C(8)	3.553(2)
	2 C(9)	3.596(4)
C(4)	2 C(9)	3.444(2)

References

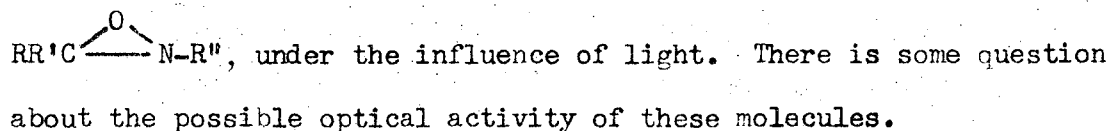
- Bartell, L. S. (1960). J. Chem. Phys. 32, 827.
- Camerman, A. and Trotter, J. (1965). Acta Cryst. 18, 197.
- Cromer, D. T. (1965). Acta Cryst. 18, 17.
- Cromer, D. T. and Mann, J. B. (1968). Acta Cryst. A24, 321.
- De Boer, B. G., Zalkin, A. and Templeton, D. H. (1968). Inorg. Chem. 11, 2288.
- Fenselau, A., Koenig, D., Koshland, D. E., Jr., Latham, H. G., Jr., and Weiner, H. (1967). Proc. Nat. Acad. Sci., U.S.A. 57, 1670.
- Ferguson, R. C. (1954). J. Amer. Chem. Soc. 76, 850.
- Fristrom, R. M. (1952). J. Chem. Phys. 20, 1.
- Johnson, C. K. (1965). ORTEP, A Fortran Thermal-Ellipsoidal Plot Program for Crystal-Structure Illustrations ORNEL - 3794, Revised. Oak Ridge, Tennessee.
- Roberts, J. D. and M. C. Caserio (1964). Basic Principles of Organic Chemistry. New York. W. A. Benjamin.
- Stewart, R. F., Davidson, E. R. and Simpson, W. T. (1965). J. Chem. Phys. 42, 3175.
- Weiner, H. and Koshland, D. E., Jr. (1965). J. Mol. Biol. 12, 881.

Unit Cell Data for Two Oxaziridines

It has been suggested (Wald and Brown, 1958) that a nitronium,



It is known that the nitroniums rearrange to form oxaziridines,



H. Ono has prepared and crystallized the stable triphenyl oxaziridine and a bromine derivative: N-(p-bromophenyl)-C,C-diphenyloxaziridine. The non-brominated compound forms stable yellow crystals. Its cell dimensions, obtained with CuK $\alpha$  radiation from an oscillation photograph and the  $h0l-h5l$  Weissenberg layers, are  $a = 17.55 \pm 0.03$ ,  $b = 18.27 \pm 0.03$ ,  $c = 9.44 \pm 0.02$ , and the probable space group is either  $Pca2_1$  or  $Pbcm$  (with the  $a$  and  $b$  axes switched). The probable number of molecules in the unit cell is 8. The para-bromo derivative forms tan colored crystals which turn dark brown if kept in the light at room temperature. We refrigerated the crystals to prevent their decomposition until we used them. Its cell dimensions, again determined from oscillation photographs and Weissenberg pictures, are  $a = 14.31 \pm 0.03$ ,  $b = 10.03 \pm 0.03$ ,  $c = 13.75 \pm 0.03$ , and  $\beta = 109 \pm 1^\circ$ . The probable space group is  $P2_1/n$ , and the number of molecules in the unit cell is four, if the densities of the two compounds are similar.

We conclude from the space group symmetry that there is no unique handedness for all molecules of the p-bromophenyl derivative, since the symmetry elements in the space group include a center of symmetry. The triphenyl oxaziridine may lie in a centric space group. A more detailed structural analysis would be necessary to answer this question.

G. Wald and P. K. Brown, Science, 127, 222 (1958)

Acknowledgements

I am particularly grateful to my chief mentors, Professors Melvin Calvin and David Templeton, for their continued interest in and support of this study. I want to thank Allan Zalkin, Richard Lemmon and Charles Weiss for their help and encouragement and Kenneth Palmer, Kenneth Raymond, Daniel Koshland, Kenneth Sauer, George Dantzig, Melvin Klein and Robert Plane for their assistance and suggestions. I would also like to thank my colleagues for their help: David St. Clair, Siddhartha Ray, Michael Drew, Helena Ruben, Frederick Hollander, William Quarles, Barry DeBoer, Gary Posner, Lucy Martin, Amar Nath, Howard Ono, and David Portsmouth. I am grateful to the Lawrence Radiation Laboratory and the U. S. Atomic Energy Commission under whose auspices this study was completed. And I want to thank my wife, Lucy, who helped with many aspects of the thesis.

APPENDIX

Glossary

absolute configuration. Handedness, usually determined from anomalous dispersion, in x-ray crystallography.

absorption.  $I_{\text{net}} = Ie^{-\mu t}$  where  $t$  = thickness,  $\mu$  = coefficient. The absorption coefficient,  $\mu$ , depends on the wavelength and the total number of electrons/unit thickness through which the x-ray beam must pass.

anisotropic thermal motion. Atomic vibrational motion which is represented by an ellipsoidal model.

anomalous dispersion. Phase shift due to the existence of any atom with an absorption edge on the long wave-length side of the radiation used for diffraction. It leads to a breakdown of Friedel's law for non-centric crystals and can be used to determine absolute configuration because of the handedness of the x-ray pattern. The atomic scattering factor,  $f = f_0 + \Delta f' + i\Delta f''$ , where  $\Delta f'$  and  $\Delta f''$  are the real and imaginary components due to anomalous scattering.

asymmetric unit. Some fraction  $1/n$  of the unit cell in which there is no crystallographic symmetry relating its components ( $n$  is an integer). The positions of the atoms of the asymmetric unit are determined in a crystal structure analysis. The other atoms in the unit cell are related by symmetry operations.



atomic scattering factor. Scattering power of an atom (in electrons).

It decreases with increasing Bragg diffraction angle because of destructive interference in the finite atomic volume. The a.s.f. of atoms with higher atomic numbers drops off more slowly as the Bragg angle increases than those with lower atomic number.

Bijvoet pairs of reflections. Pairs of reflections related by extra symmetry elements appearing in the diffraction pattern and due to the validity of Friedel's law.

block matrix least squares. See least squares refinement.

Bragg's Law.  $\lambda = 2d \sin\theta$ , fundamental diffraction law involving  $\lambda$  the x-ray wavelength,  $\theta$  the angle through which the x-ray beam is diffracted and  $d$  the spacings involved in the crystal.

cell dimensions. Set of three lengths and three angles which describe the shape of the unit cell.

center of symmetry. Symmetry element which, when present at the origin, relates a point at  $x, y, z$  to a point at  $-x, -y, -z$ .

centric. Possessing a center of symmetry.

collimator. Narrow tube used to produce a nearly parallel x-ray beam.

crystal. Three dimensional periodic arrangement of atoms.

crystal structure. Determination of the location of the electrons in a crystal by determining the symmetry of the unit cell and the contents of the asymmetric unit.

d-spacings.  $d_{hkl}$  = spacings between planes (having indices  $hkl$ ) through the crystal. The d-spacings depend on both  $hkl$  and the unit cell dimensions.

density calculation. Calculated from a knowledge of  $z$ , the number of molecules present, the molecular weight of each molecule and the volume of the unit cell. It is measured directly by adjusting the density of a solvent system until a crystal neither sinks nor rises in it.

diagonal least squares. See least squares refinement.

difference synthesis. See Fourier series.

diffraction. Interference of scattered electromagnetic radiation (often by a periodic array). In x-ray diffraction the x-rays are scattered by the electrons in the material. The spacings between diffraction maxima give information about the size and shape of the unit cell, and the intensities contain information about the arrangement of atoms.

diffractometer. Instrument equipped generally with a scintillation counter; the crystal can be oriented by adjusting three angles  $\chi$ ,  $\varphi$  and  $\theta$  in such a way that a single reflection is detected at a time by the counter placed at an angle  $2\theta$  with the incident x-ray beam.

discrepancy index. See R value.

E map. See Fourier series.

E value. See normalized structure factors.

electron density map. See Fourier series.

equivalent positions. Positions in the unit cell related by symmetry operations of the space group.

Eulerian cradle. Geometrical arrangement for orienting a crystal as a function of three angles, without imparting any translation to it.

extinction. Partial reduction of intensity due to destructive interference when a diffracted beam suffers subsequent rediffraction from the other side of the same array of planes. It is serious only for intense reflections and in perfect crystals but is negligible when the mosaicity of the crystal is considerable.

extinctions. See systematic absences.

filter. Thin piece of metal which selectively absorbs the  $K\beta$  x-ray.

Fourier series. Mathematical periodic function of form  $A = \sum K_n e^{2\pi i a \varphi_n}$ , where  $K_n$  = Fourier coefficient,  $\varphi_n$  = phase.

Type	$A$	$a$	$\frac{K_n}{n}$
electron density (Fourier map)	$\rho$	1	$F_o$ or $F_c$ , observed or calculated structure factor
difference Fourier	$\rho$	1	$  F_o  -  F_c  $
E-map	$\rho$	1	E, normalized structure factor
Patterson map	P	1	$F_o^2$
structure factor calculation	$F_c$	-1	f, atomic scattering factor

Fourier transform. See transform.

Friedel's law.  $I_{hkl} = I_{\bar{h}\bar{k}\bar{l}}$ , true in the absence of anomalous scattering. It results in a centric x-ray pattern and potential problems of space group identification.

full matrix least squares refinement. See least squares refinement.

goniometer head. Crystal holder with adjustable arcs used to orient a crystal in the x-ray beam.

goniostat. See diffractometer.

habit. General crystal shape which results from the development of sets of faces related by the point group symmetry.

heavy atom method. See Patterson technique.

indices. Three integers which describe the diffracting plane. Their reciprocals are in the ratio of the intercepts of the plane with the three coordinate axes of the unit cell. In the notation,  $\bar{h} = -h$ .

integrated intensity. All the x-ray photons diffracted from one plane. It is obtained either by peak scanning (while counting) or by having the counter aperture much larger than the diffracted spot.

intensity.  $I = kF^2$ , where the structure factor  $F$  depends on the structure and  $k$  is a constant. It is measured on a diffractometer with a scintillation counter or by estimates on film.

isotropic temperature factors. Atomic vibrational motion which is represented by a spherical model.

lattice. Periodic sequence of points (usually in three dimensions). It is used for a quantitative description of the periodic property (pure translational) of a repetitive pattern.

Laue symmetry. Point group symmetry plus an inversion center. Only Laue groups (rather than point groups) can be determined from x-ray data (in the absence of anomalous scattering).

least squares refinement. Systematic variations in the parameters used to describe a structure in such a way as to minimize the difference between the observed and calculated data. The set of linear equations used to determine shifts of parameters may be represented by a matrix. In a full matrix technique, all diagonal and off-diagonal terms are calculated and used. In diagonal least squares, only the diagonal elements are used. In block techniques, blocks of terms are used which include some or all diagonal elements but only some off-diagonal terms. Since the equations are non-linear, a least squares refinement of the parameters does not always refine to the correct structure.

Lorentz factor. Geometrical factor which affects the intensity of a reflection. It depends on the method by which the data is obtained.

Miller indices. Indices which do not have a common divisor.  
See also indices.

monoclinic. Crystal lattice which contains one twofold axis.

As a consequence, the unit cell dimensions are  $a \neq b \neq c$ ,  $\alpha = \gamma = 90^\circ$  and  $\beta \neq 90^\circ$ .

mosaic blocks. Mathematical conception of ideally imperfect crystal, composed of infinitesimally small perfect crystals.

noncentric. Not possessing a center of symmetry.

normalized structure factors, E. Structure factors put on an absolute scale and corrected for both the thermal motion of the vibrating atoms and the decrease of the atomic scattering factors with increasing Bragg scattering angle. The normalization increases the relative values of the higher angle data which are more sensitive to details of the structure than the low angle data.

optical goniometer. Device for measuring interfacial angles of a crystal, by precise observation of the orientation angles when faces are made to reflect a beam of light in a given direction. The results which may be obtained are the indices of the faces, the interaxial angles, the axial ratios and the point group symmetry (if a sufficient number of types of faces are present).

optical transform. See transform.

orthorhombic. Crystal lattice which contains three orthogonal twofold axes. As a consequence, the three interaxial angles of the unit cell each equal  $90^\circ$ .

packing. Crystalline intermolecular arrangement.

Patterson technique. Use of a Fourier map which has peaks at vector distances from an origin corresponding to interatomic vectors and whose heights are proportional to the product of electrons for each of the two atoms. It can be calculated without any knowledge of the structure, since the Fourier coefficients are  $F^2$ , which can be found directly from the intensity. In the special case of only one heavy atom present, the heavy atom can be located easily and its position used to generate a starting set of phases.

phase. Quantity associated with each structure factor value. The phase is a function of both the planar indices and the atomic position of all atoms in the unit cell. For centric space groups the phase  $\approx 0$  or  $\pi$ . For noncentric space groups the phase of a reflection may assume any value.

photographic methods. Technique for obtaining permanent records of data. A Weissenberg setup, which is one kind of moving crystal-moving film technique, often is employed.



point groups. Thirty-two combinations of three dimensional, repeating symmetry elements which do not involve translations. The faces of a crystal exhibit the point group (or higher symmetry).

polarization factor. Geometrical factor which affects the intensity of a reflection. It depends only on the Bragg scattering angle and is a result of the polarization of the diffracted x-ray beam.

powder pattern. X-Ray diffraction pattern of a powder, ie many small non-oriented crystals. It consists of lines (rather than discrete spots as in single crystal work). It is used for identifying crystals and occasionally for determining the structures of very small molecules.

R value. Measure of the discrepancy between the observed and calculated structure factor values.

reciprocal space. Mathematical abstraction which makes it convenient to deal with inverse quantities. A diffracting plane in real space is equivalent to a point in reciprocal space. This makes it convenient to consider diffracted spots as points in reciprocal space.

- reflections. Diffraction intensity data.
- scale factor. Proportionality constant used to put the observed and calculated structure factors on the same scale. It can be found by Wilson's method.
- scattering factor. See atomic scattering factor.
- scintillation counter. Quantum counting spectrometer which works by ionizing a NaI crystal. It is used to measure intensities to precisions of ~5% (Film methods: ~20%).
- screening aperture. Collimator at the receiving end of Eulerian-cradle goniostat used to eliminate stray, non-diffracted radiation.
- screw axis. Symmetry element composed of both a rotation axis and a translation. A  $2_1$  screw axis in the  $y$  direction relates a point at  $x, y, z$  to a point at  $-x, \frac{1}{2}y, -z$ .
- size of crystal. Must be less than the x-ray beam size which is ~0.5 mm but have enough electrons to produce an observable x-ray pattern, ie weigh about 1  $\mu$ g.
- space group. One of the 230 self-consistent combinations of symmetry elements possible in an infinite repetitive pattern in three dimensions.

special position. Point which is unchanged by the operations of one or more symmetry elements of a space group.

standard deviation of an observation of unit weight.  $\sum_i w_i \Delta_i^2 / (n-p)$   
 where  $w_i$  = weight,  $\Delta_i = ||F_o| - |F_c||_i$ ,  $n$  is the number of data and  $p$  is the number of parameters. It is used as a measure of correctness of weighting scheme.

statistical methods. Probability techniques for determining phases of reflections.

structure factor. Quantity proportional to the square root of the intensity. For calculated value, see Fourier series.

systematic absences. Utter extinction of the intensities of certain reflections due to the destructive interference of scattering from molecules related by symmetry elements involving translation.

takeoff angle. Inclination of the incident beam to the surface of the target.

temperature parameters. Numbers used to describe the magnitude of an atom's thermal motion. See also isotropic and anisotropic thermal motion.

thermal motion. Atomic motion which lessens the x-ray scattering.

transform. In the Fourier series, the data (structure factors) and structure (electron density) are transforms of each other, ie when the phases of the reflections are known, one can be calculated from the other. The optical transform method is a technique for generating a periodic group of spots (analogous to data) from a model of the structure.

trial and error solution. Technique for systematically varying the position of a model and choosing the best model on the basis of the agreement between the observed data and the data calculated on the basis of it.

trial structure. Set of proposed atomic positions which can be used to calculate structure factors. The trial structure is often refined to a structure in better agreement with the data by the technique of least squares.

twinning. Existence of two different orientations of a lattice in one (apparent) crystal.

unit cell. Portion of a structure enclosed in the parallelepiped described by the three unit vectors of the lattice.

weight of a reflection. Inverse of the square of the uncertainty of the structure factor. The uncertainty depends on the counting statistics and the spread in duplicate measurements.

Weissenberg technique. See photographic methods.

Wilson's method. Plot of the decrease of diffracted intensity as a function of the Bragg scattering angle. It is used to determine the overall scale factor and temperature factor.

x-ray. High energy photon which has been produced by bombardment of a piece of metal, eg Cu, Mo, Fe or Cr, in a vacuum. A K electron of the metal is knocked out by a high energy electron, and an electron from a higher orbital takes its place, emitting an x-ray as it does so.

LEGAL NOTICE

*This report was prepared as an account of Government sponsored work. Neither the United States, nor the Commission, nor any person acting on behalf of the Commission:*

- A. Makes any warranty or representation, expressed or implied, with respect to the accuracy, completeness, or usefulness of the information contained in this report, or that the use of any information, apparatus, method, or process disclosed in this report may not infringe privately owned rights; or*
- B. Assumes any liabilities with respect to the use of, or for damages resulting from the use of any information, apparatus, method, or process disclosed in this report.*

*As used in the above, "person acting on behalf of the Commission" includes any employee or contractor of the Commission, or employee of such contractor, to the extent that such employee or contractor of the Commission, or employee of such contractor prepares, disseminates, or provides access to, any information pursuant to his employment or contract with the Commission, or his employment with such contractor.*

TECHNICAL INFORMATION DIVISION  
LAWRENCE RADIATION LABORATORY  
UNIVERSITY OF CALIFORNIA  
BERKELEY, CALIFORNIA 94720